2008

Dividing the Preplate: Characterization of Neuronal Subpopulations in the Early Murine Cerebral Cortex

Hilleary Botts Osheroff

DIVIDING THE PREPLATE: CHARACTERIZATION OF NEURONAL SUBPOPULATIONS IN THE EARLY MURINE CEREBRAL CORTEX

A Thesis Presented to the Faculty of

The Rockefeller University

in Partial Fulfillment of the Requirements for

the degree of Doctor of Philosophy

by

Hilleary Botts Osheroff

June 2008

DIVIDING THE PREPLATE: CHARACTERIZATION OF NEURONAL SUBPOPULATIONS IN THE EARLY MURINE CEREBRAL CORTEX

Hilleary Botts Osheroff, Ph.D.
The Rockefeller University 2008

The preplate is a transient layer of the developing cerebral cortex which is comprised of the earliest generated cortical neurons. Preplate neurons are a heterogenous population of future Cajal-Retzius neurons and future subplate neurons, which are derived from multiple sources of progenitors. During the formation of the cortical layers, the preplate is split into an upper marginal zone and the lower subplate layer by the radial migration of projection neurons from the cortical ventricular zone. Cajal-Retzius and subplate neurons have important developmental functions in regulating radial migration and in pioneering corticofugal projections. The genetic mechanisms of preplate neuron specification are not well understood, and few markers exist to identify subpopulations of the preplate. The aim of this thesis is to functionally and molecularly characterize neuronal subpopulations of the mouse preplate. Using transgenic mice expressing EGFP in distinct preplate subpopulations, I applied birthdating analyses and live imaging to describe the proliferative and migratory characteristics of subpopulations of Cajal-Retzius and subplate neurons. Purified subpopulations were used in a gene expression array analysis to define mRNAs differentially expressed between subpopulations. New markers for a subpopulation of Cajal-Retzius neurons were identified, as well as novel markers for future subplate neurons, which will be of use in the study of these cells. These

data may yield insight into genetic and cellular mechanisms of preplate differentiation and development, and identify novel genes with potential roles in preplate neuron functions.

ACKNOWLEDGEMENTS

I would like to thank my advisor, Mary Beth Hatten, committee members Nat Heintz and Cori Bargmann, for their encouragement, Hatten lab members Stephanie Schneider, Emili Cid, and David Solecki for their help and support, and my collaborators Sergei Tevosian, Antonio Iavarone, and Anna Lasorella for providing transgenic mice. And my husband Chris, for putting up with me.

TABLE OF CONTENTS

LIST OF FIGURES

LIST OF TABLES

Chapter 1

Introduction

The development of the mammalian neocortex is characterized by the formation of a series of transient layers, resulting from waves of radial and tangential migrations of neuronal precursors from their germinal zones. The earliest transient layers direct the formation of succeeding layers to establish the architecture and synaptic connectivity of the adult neocortex.

The neocortex contains two major types of neurons: projection neurons and interneurons. Projection neurons, also known as excitatory or pyramidal neurons, principally use glutamate as their neurotransmitter and are derived from the neocortical anlage (Sidman and Rakic 1973). Inhibitory interneurons are GABAergic and are derived from outside of the neocortex in proliferative zones in the basal forebrain (Anderson, Eisenstat et al. 1997). Both types of cortical neurons undergo extensive migration from their birthplaces to form the distinctive cortical layers (Fig 1.1a). Projection neurons migrate from their birthplace in the proliferative cortical ventricular zone, using glial fibers that stretch radially across the developing cortex as their substrate and guide (Sidman and Rakic 1973; Hatten 1999). In contrast, interneurons undergo tangential migration from the ventricular zone of the ganglionic eminence, through the striatum into the

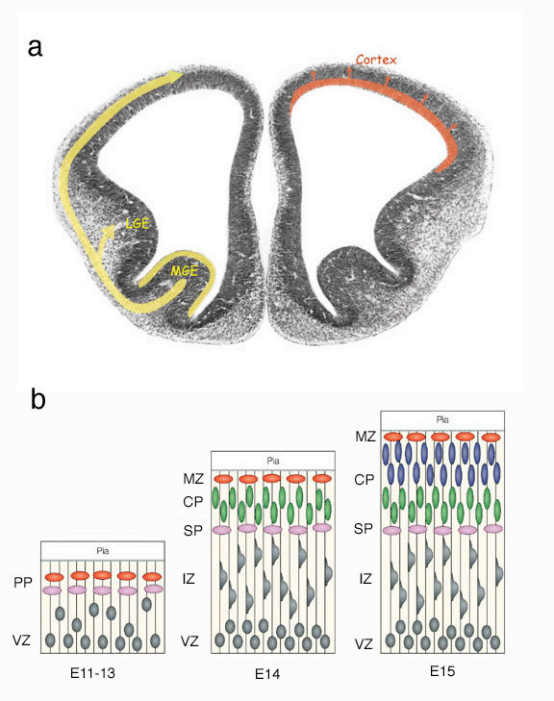

Figure 1.1. Neuronal migration during preplate splitting and cortical development. (a) Neurons of the cortex undergo both tangential (yellow) and radial (red) migration to reach their final destination. GABAergic interneurons are born in the medial ganglionic eminence (MGE) and migrate tangentially into the cortex, while glutamatergic projection neurons are born in the cortical ventricular zone and migrate into post-mitotic regions radially. (Image from Goffinet, 2006) (b) Preplate splitting and the formation of the cortical plate. At the preplate stage (E11-13), there are two distinct layers of the neocortical epithelium: preplate neurons (red and pink cells) and proliferating ventricular zone precursors (gray cells). The cortical plate (green cells) forms by the radial migration of neurons from the ventricular zone, separating the marginal zone cells (red) and the subplate cells (pink). Each successive layer forms on top of the older layers (blue cells). (Adapted from Tissir & Goffinet, 2003)

neocortex, where they migrate perpendicular to the radial glia (Fig 1.1a) (Nadarajah and Parnavelas 2002). In the mouse, neurons are born between embryonic days 10 and 17 (E10-E17), and neuronal migration continues to occur until the first postnatal week.

The specification of projection neurons in the developing cortex is determined largely by neuronal birthdate (McConnell 1989). Cohorts of neurons destined for particular layers are born during the same time frame, and layers may be identified by the birthdate of the neurons within it. The neocortex is laminated from the inside-out with respect to neuronal birthdate: the earliest born cells occupy the deepest layer, closest to the ventricular zone, while the latest born cells occupy the most superficial layer (Angevine and Sidman 1961). Neurons migrate from the ventricular zone where they are born to settle in the most superficial layer; thus, later-born neurons must migrate through the early-born neurons to reach their final destination.

Transient layer formation during cortical development. During development of the neocortex, a series of transient neuronal and plexiform layers are formed. The preplate is the earliest of these layers, comprised of a heterogeneous population of differentiated neurons born in the dorsal forebrain between E10 and E12 in mouse (E12-13 in rat) (Bayer and Altman 1990; Wood, Martin et al. 1992; Hevner, Daza et al. 2003). Preplate neurons reside in a layer in the outermost

aspect of the developing cortex, situated between the ventricular zone and the pia mater (Fig 1.1b). Beginning around E13, newly-born future projection neurons migrate radially out of the ventricular zone to settle in the middle of the preplate, dividing the preplate neurons into upper and lower layers in a process known as preplate splitting (Fig 1.1b). The new layer formed in the middle of the preplate is termed the cortical plate, a transient structure that gradually develops into the major cell-dense cortical layers II-VI.

The major neuronal populations of the preplate are Cajal-Retzius neurons and subplate neurons. During preplate splitting, these populations segregate into the upper and lower layers of the split preplate (Fig 1b). Cajal-Retzius neurons remain subpial in the most superficial layer, the cortical marginal zone, while subplate neurons descend into a deeper layer below thecortical plate neurons. During the waves of radial migration that form the cortical plate, each layer of newly born cortical neurons migrates through the subplate layer and past the earlier-generated cells to stop beneath the Cajal-Retzius layer.

The Cajal-Retzius cell-containing marginal zone corresponds to the future layer I of the adult cortex. In the mouse, the majority of Cajal-Retzius cells disappear after neuronal migration has completed in the first postnatal weeks, leaving layer I a cell-poor plexiform layer containing axons and dendrites of cortical plate cells (Derer and Derer 1990). While the majority of subplate neurons are also lost postnatally, a small population of subplate neurons remains in the deepest layer of the adult cortex in cat and rat, termed layer VIb or VII

(Chun and Shatz 1989; Reep 2000; Torres-Reveron and Friedlander 2007), though there is disagreement as to whether they constitute a distinguishable neuronal layer of their own.

Characteristics of preplate subpopulations. Originally described independently by Santiago Ramon y Cajal and Gustaf Retzius in the late 1800s, Cajal-Retzius neurons display extreme variability in morphology between species (Meyer, Goffinet et al. 1999). In human fetal brain, Cajal-Retzius neurons extend parallel axons through the lower marginal zone and numerous radial dendrites towards the pial surface. In lower mammals such as rabbit and rodent, these neurons are much less elaborate, with decreased numbers of dendritic processes. In the mouse, Cajal-Retzius neurons are horizontal bipolar neurons which reside in the middle of the marginal zone in the early postnatal period. This morphological variability complicated the identification of Cajal-Retzius neurons. More recently, a reliable marker for Cajal-Retzius neurons of all species was identified: reelin protein. In the embryonic neocortex, only Cajal-Retzius neurons express reelin (Ogawa, Miyata et al. 1995; Schiffmann, Bernier et al. 1997). The calcium binding protein calretinin is also often used as a marker for Cajal-Retzius neurons (del Rio, Martinez et al. 1995), though not all reelin-expressing cells coexpress calretinin (Hevner, Neogi et al. 2003). In this thesis, I will use the term Cajal-Retzius neuron to describe reelin-expressing neurons in the embryonic preplate or marginal zone (Meyer, Goffinet et al. 1999).

Subplate neurons are less distinctive morphologically than the Cajal-Retzius neurons, and few molecules are known to be specific to subplate in the embryonic cortex. In early stages of preplate splitting the subplate layer can be easily visualized separating from the marginal zone by immunostaining for markers of neuronal differentiation such as MAP2 (Soriano, Del Rio et al. 1994). The sole marker used specifically for subplate neurons is the golli-lacZ transgene, which is expressed only in the subplate after preplate splitting, but is not specific to future subplate neurons at the preplate stage (Landry, Pribyl et al. 1998).

Birthdating experiments have demonstrated that Cajal-Retzius neurons and subplate neurons are partially co-generated (Bayer and Altman 1990; Wood, Martin et al. 1992), although the peak of production of each type is distinct (Hevner, Daza et al. 2003; Hevner, Neogi et al. 2003). Cajal-Retzius neurogenesis peaks at E10.5 in the mouse, while subplate neurogenesis peaks approximately a day later at E11.5. Birthdates of subplate neurons also overlap with those of neurons destined for layers V and VI (Takahashi, Goto et al. 1999; Hevner, Daza et al. 2003).

Other neuronal components of the preplate – interneurons and the subpial granular layer. GABAergic interneurons migrating tangentially from their birthplace in the basal forebrain are found in the marginal zone prior to their eventual radial migration into the cortical plate, and comprise the other major

component of the preplate and marginal zone (Wichterle, Turnbull et al. 2001; Hevner, Daza et al. 2004). Based on immunohistochemical staining for the calcium-binding proteins calretinin and calbindin, as well as GABA and reelin, Meyer et al (1998) proposed the existence of a rodent subpial granular layer (SGL), a heterogeneous population of small cells in the preplate and marginal zone expressing variously reelin, calbindin, calretinin, and GABA, which was hypothesized to be comprised of Cajal-Retzius cell precursors which undergo subpial tangential migration from the retrobulbar cortex in the anterior forebrain. The rodent SGL corresponds to the SGL described in human fetal cortex, where the SGL exists as a population of small calretinin-positive neurons located in the outermost marginal zone, which are proposed to differentiate into Cajal-Retzius neurons throughout fetal development (Meyer and Goffinet 1998). An alternate view is that the rodent SGL described on the basis of marker gene expression at static time points in fact corresponds to migratory interneurons derived from the ganglionic eminence (Wichterle, Turnbull et al. 2001; Jimenez, Rivera et al. 2003). As the markers used to describe this subpopulation are expressed by interneurons (calbindin, GABA), this classification is likely to be correct.

Functions of Cajal-Retzius neurons in cortical development. The most well-studied genetic model of cortical development is the *reeler* mouse, in which the formation of the cortical plate is profoundly disrupted. The product of the gene deleted in *reeler* is reelin protein (D'Arcangelo, Miao et al. 1995), an extracellular

matrix molecule expressed by Cajal-Retzius neurons. As Cajal-Retzius neurons are the only reelin-expressing neurons in the embryonic wild-type neocortex, they are thought to play an important role in cortical plate development. Postnatally, a subset of GABAergic cortical interneurons express reelin, after reelin expression has been downregulated in layer I (Alcantara, Ruiz et al. 1998).

Two major developmental defects are seen in the *reeler* cortex. First, the cortical plate does not form in between the marginal zone and subplate layers. Cortical plate neurons fail to migrate past subplate neurons and stop beneath the preplate, resulting in an ectopic preplate sometimes referred to as the superplate (Sheppard and Pearlman 1997). Second, the ectopic cortical plate is inverted, with an outside-in rather than an inside-out pattern of lamination. Whereas in the wild-type cortical plate, the earliest-born cortical neurons are located in the deepest layers, with each successive layer of younger neurons more superficial to the older neurons, in the *reeler* cortical plate the oldest neurons are the most superficial, located underneath the superplate, while each successive layer accumulates beneath the last rather than on top of it (Caviness and Sidman 1973).

Reelin acts as a ligand for the receptors ApoER2 and Vldlr (Hiesberger, Trommsdorff et al. 1999; Benhayon, Magdaleno et al. 2003), which are expressed both by neurons of the cortical plate (Trommsdorff, Gotthardt et al. 1999) and by radial glia (Luque, Morante-Oria et al. 2003). Binding of these receptors by reelin leads to phosphorylation of Dab1, which interacts with the

cytoplasmic tails of both receptors (Hiesberger, Trommsdorff et al. 1999; Benhayon, Magdaleno et al. 2003). Loss of function mutants of both receptors or Dab1 phenocopy the unsplit preplate and inverted cortical plate seen in the *reeler* mutant (Sheldon, Rice et al. 1997; Trommsdorff, Gotthardt et al. 1999), and therefore these molecules are assumed to be required for reelin signaling. Reelin also binds and signals through $\alpha 1\beta 3$ integrin, which affects neuronal migration *in vitro* and may modulate neuron-glia interactions (Dulabon, Olson et al. 2000) as well as Dab1 signaling (Schmid, Jo et al. 2005). The reelin signaling pathway may be modulated by other genes known to be involved in cortical migration, such as Cdk5, which can phosphorylate Dab1 independent of reelin signaling (Keshvara, Magdaleno et al. 2002). Loss of function of Cdk5 and/or its regulator p35 results in cortical lamination defects with similarities to, but not identical with, the *reeler* phenotype (Kwon and Tsai 1998; Rakic, Davis et al. 2006). In Cdk5 or p35 knockouts the preplate splits (although imperfectly) and the migration of early-born cortical neurons is normal, but later-born neurons have migration defects reminiscent of *reeler*, failing to migrate past the earlier-born neurons.

Biochemical and genetic experiments concerning reelin signaling and its effects on cortical development have not clarified the cellular mechanisms underlying *reeler* and associated phenotypes. Multiple hypotheses have been put forward to explain the effects of reelin signaling. Reelin has been proposed to act as a “stop” signal for migrating neurons (Dulabon, Olson et al. 2000; Hack, Hellwig et al. 2007), or a detachment signal required for migrating neurons to

detach from their radial glial guides upon reaching the top of the cortical plate (Dulabon, Olson et al. 2000; Hack, Bancila et al. 2002). These models of reelin function assume that reelin acts as a positional signal to migrating neurons. An alternate model is that reelin acts as a permissive signal for cortical plate formation. Supporting this model, partial rescue of the *reeler* phenotype was achieved by ectopic expression of reelin in the ventricular zone, resulting in preplate splitting but disorganized cortical lamination (Magdaleno, Keshvara et al. 2002). This suggests that reelin has effects which are not dependent on specific expression of reelin by marginal zone neurons.

A third hypothesis is that reelin may act to maintain the radial glial scaffold necessary for proper neuronal migration. Radial glial phenotypes are disrupted in the *reeler* cortex (Hartfuss, Forster et al. 2003) as well as in postnatal cortex in which the marginal zone/layer I has been chemically ablated (Super, Del Rio et al. 2000). In the absence of reelin or Cajal-Retzius neurons, fewer radial glia display long processes which contact the pia. In the *reeler* cortex, there is a decrease in the number of “immature”, BLBP-positive radial glia (Hartfuss, Forster et al. 2003), while in layer I-ablated brain there is a corresponding increase in “mature,” GFAP-positive astrocytes (Super, Del Rio et al. 2000). It is likely that reelin plays multiple necessary roles during cortical plate formation, signaling to both migrating neurons and glial cells.

The majority of studies on the role of Cajal-Retzius neurons in cortical development have focused on reelin signaling. The question of whether these

cells have reelin-independent functions in cortical development has not been addressed. Cajal-Retzius neurons are known to participate in early embryonic networks of neural activity, which may be important for the establishment of cortical connectivity or activity-dependent neuronal survival. They develop far-ranging axonal networks in the tangential plane, which form synaptic contacts with the apical dendrites of cortical plate neurons (Radnikow, Feldmeyer et al. 2002). They receive both GABAergic and glutamatergic synaptic inputs from underlying cortical plate neurons (Radnikow, Feldmeyer et al. 2002; Kirmse, Dvorzhak et al. 2007), and during late embryogenesis receive inputs from serotonergic neurons (Janusonis, Gluncic et al. 2004). The functional significance of these transient neuronal connections has not yet been established.

Functions of the subplate in cortical development. In contrast to the major functions of Cajal-Retzius neurons in guiding cell body position within the cortex, subplate neurons are thought to pioneer corticofugal axonal tracts, and to guide thalamocortical axons to their layer IV targets (Allendoerfer and Shatz 1994). Thalamic projections comprise the major subcortical input to cortex, and reciprocal cortical projections project to the thalamus. Corticothalamic and thalamocortical connections are established during embryonic development, and subplate neurons are required for both of these processes to occur properly. Directly after settling in the preplate, subplate neurons begin extending axons through the intermediate zone that will ultimately make synaptic contact with the

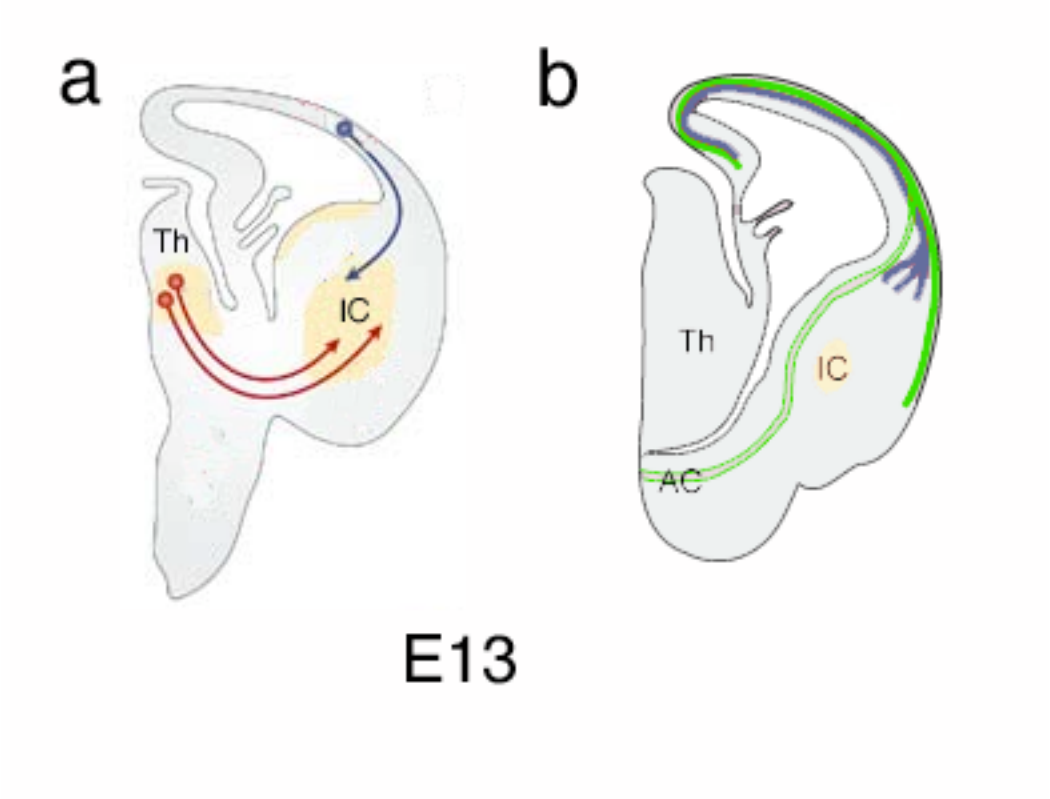

Figure 1.2. Early corticofugal projections from the preplate/subplate. (a) At E13, corticothalamic (blue) and thalamocortical (red) projections reach the internal capsule. (b) Preplate/subplate neurons project corticothalamic axons (blue) to the internal capsule and contralateral axons (green) to the anterior commissure. Abbreviations: anterior commissure (AC), internal capsule (IC), thalamus (Th).

thalamic nuclei (Fig 1.2a) (McConnell, Ghosh et al. 1989). Subplate cells are also thought to pioneer projections to the contralateral cortex, including the corpus callosum and anterior commissure (Jacobs, Campagnoni et al. 2007), and these projections are formed concurrently with the corticothalamic tract (Fig 1.2b). In the rat, corticothalamic projections originating in the subplate layer reach the internal capsule by E15 (comparable to E13.5 in mouse) and reach the thalamus one day later (De Carlos and O'Leary 1992). As layer V and VI neurons arrive in the cortical plate, they extend axons following the path laid down by subplate axons through the internal capsule. Layer V neurons project to various subcortical targets, while layer VI axons follow the subplate axons to the thalamus.

In rodents, thalamic axons extend towards their cortical targets simultaneously with subplate axon extension, meeting in the internal capsule in the ventral forebrain (Fig 1.2a). Thalamocortical and corticothalamic axons reach the internal capsule at approximately the same time (De Carlos and O'Leary 1992), an observation which led to the “handshake hypothesis” of axon guidance, which proposes that cortical afferents and efferents meet in the internal capsule, and the established tracts guide the reciprocal projections to their final target (Molnar and Blakemore 1995). Calling this model into question, thalamocortical and corticothalamic targeting appear to be dissociable to some extent. Mutations in Ephrin A signaling pathways affect corticothalamic targeting, while

thalamocortical targeting is unchanged (Torii and Levitt 2005), and therefore the formation of these fiber tracts are not strictly dependent upon one another.

There are several lines of evidence to support the idea that the subplate layer does participate in thalamocortical targeting within the cortex. Upon reaching the cortex, thalamocortical projections travel over the subplate layer itself, making contact with the chondroitan sulfate proteoglycan (CSPG)-rich layer of subplate cell bodies, rather than the deeper intermediate zone through which subplate and layer V/VI axons extend (Bicknese, Sheppard et al. 1994). These afferent projections "wait" in the subplate for a period of several days before ascending into the cortical plate to form synaptic contacts within layer IV, their final target. Chemical ablation of subplate neurons during this waiting period prevents thalamocortical axons from innervating the cortical plate (Ghosh, Antonini et al. 1990). In the *reeler* mutant, thalamocortical projections course across the ectopic subplate neurons of the superplate, where they also undergo a waiting period, then descend to the ectopic cortical plate to innervate the inverted layer IV (Caviness and Frost 1983; Molnar, Adams et al. 1998). It has been observed that in *reeler,* thalamocortical axons preferentially follow ectopic cells with subplate birthdates that express the CSPG neurocan in both the cortical plate and superplate (Li, Oohira et al. 2005), which suggests that these projections are attracted by subplate-specific guidance molecules. Finally, in the COUP-TFI knockout mouse the subplate layer fails to differentiate normally, and thalamocortical targeting to layer IV is impaired (Zhou, Qiu et al. 1999).

Specific ablation of subplate neurons prior to axon extension by layer V and VI neurons has not been possible, and therefore it has not been determined whether subplate pioneer projections are required for guidance of corticofugal projections from these layers. Chemical ablation of the subplate has been carried out only after the subplate neurons have sent projections to thalamus (Ghosh, Antonini et al. 1990), and due to the lack of specificity of known subplate markers, genetic ablations have resulted in the loss of the entire preplate, including Cajal-Retzius neurons (Xie, Skinner et al. 2002). Specific ablation of subplate neurons early in development will be necessary to fully understand the role of pioneering subplate axons in corticothalamic, thalamocortical and corticocortical targeting.

Developmental history of preplate neurons. Considering the crucial role of preplate neurons in cortical development, relatively little has been known about the birthplace and specification of these neurons. In the classical view of cortical development, all cortical neurons were thought to arise from the neocortical ventricular zone (VZ), and that the multilayered mature cortex developed exclusively by radial migration of neuronal progenitors out of the VZ. The discovery that GABAergic interneurons, one of the two major classes of cortical neurons, originate from progenitors in the basal forebrain (Anderson, Eisenstat et al. 1997), challenged this view. Recently, fate-mapping studies of Cajal-Retzius neurons in embryonic cortex have yielded the surprising result that Cajal-Retzius

precursors are born in restricted compartments of the neocortical VZ, and undergo tangential migration to form the preplate layer in a process analogous to interneuron migration. The other major cellular component of the preplate, the subplate neurons, are presumed to derive from the VZ and translocate radially to the preplate layer, although there is little data which supports this hypothesis directly. In the following section, I will review what is known regarding the developmental history of preplate subpopulations.

Cajal-Retzius subpopulations: multiple origins of the earliest-born cortical neurons. The study of gene expression in Cajal-Retzius neurons has supported the theory that these cells have their origins in the dorsal telencephalon (pallium) as opposed to basal telencephalon (subpallium). Cajal-Retzius neurons have gene expression patterns characteristic of pallium-derived projection neurons: they express transcription factors such as Tbr1 and Emx2, are glutamatergic rather than GABAergic like interneurons, and do not express transcription factors characteristic of subpallium-derived interneurons (Hevner, Shi et al. 2001; Shinozaki, Miyagi et al. 2002; Hevner, Neogi et al. 2003). Recent work has confirmed three independent sites of origin of Cajal-Retzius neurons at the borders of the dorsal cortex: the cortical hem (Yoshida, Assimacopoulos et al. 2006), the pallial-subpallial boundary (PSB), and the septum (Bielle, Griveau et al. 2005) (Fig 1.3).

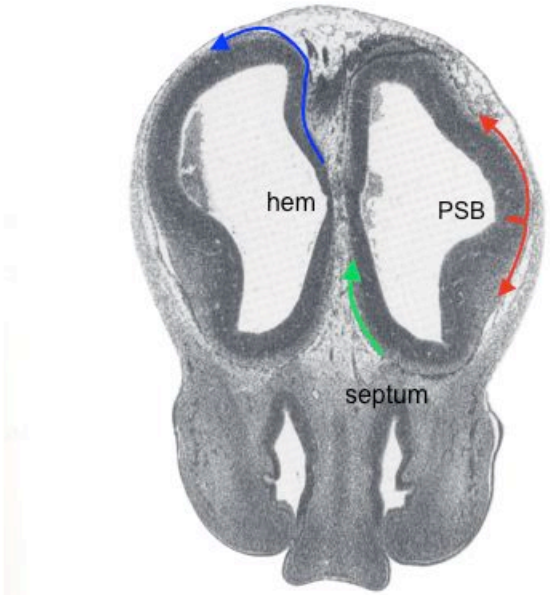

Figure 1.3. Migratory routes of Cajal-Retzius neurons. Cajal-Retzius neurons migrate tangentially through the preplate from sources in the cortical hem (blue), pallial-subpallial boundary (PSB) (red) and the septum (green).

The cortical hem, a signaling center in the dorsalmost region of the telencephalon adjacent to the cortex, was identified as a major source of Cajal-Retzius neurons by Cre recombinase-mediated fate-mapping of Wnt3a-expressing cells in the telencephalon (Yoshida, Assimacopoulos et al. 2006). Embryonically, Wnt3a-Cre is expressed specifically in the hem, and not in the neocortex proper. Fate-mapping of Wnt3a-expressing cells revealed reelin-positive cells migrating out of the cortical hem and into the adjacent preplate beginning at E10.5 (Yoshida, Assimacopoulos et al. 2006), the peak time of production of Cajal-Retzius neurons (Hevner, Neogi et al. 2003). Ablation of the cortical hem resulted in loss of the majority of reelin-positive marginal zone neurons. These results confirmed the hypothesis originally proposed on the basis of gene expression analysis (Meyer, Cabrera Socorro et al. 2004) and *in utero* electroporation experiments (Takiguchi-Hayashi, Sekiguchi et al. 2004).

Additionally, Cre-based fate mapping has revealed sources of Cajal-Retzius neurons at the borders between the pallium and subpallium – the PSB in the lateral forebrain, and the septum in the medial forebrain (Bielle, Griveau et al. 2005). The transcription factor Dbx1 is transiently expressed in these restricted regions of neuroepithelium during embryonic development. Fate-mapping the Dbx1-expressing cells with a transgenic Dbx1-Cre line revealed tangential migrations of reelin-positive cells from these regions into the preplate layer. Thus, there are at least three verified sources of Cajal-Retzius neurons in the embryonic forebrain.

Considerable intermingling of the different subpopulations might be expected, as cells migrate large distances across the cortex regardless of their source. Hem-derived cells migrate to cover the entire dorsal forebrain, but rostrally do not migrate much below the future rhinal sulcus, located roughly at the dorsal-ventral forebrain boundary (Yoshida, Assimacopoulos et al. 2006). Caudally, hem-derived cells cover the ventral forebrain as well. PSB-derived cells spread across the surface of both dorsal and ventrolateral cortex (Bielle, Griveau et al. 2005). The existence of gradients or concentrations of subpopulations in the tangential plane of the cortex is inferred from these migratory pathways. As well, it is not clear whether migrating cells from different sources follow specific guidance cues. The migration of hem-derived cells has been reported to be guided by an attractive response towards the pia via SDF-1/CXCR4 signaling, which serves to keep migrating cells in a subpial position, but no guidance cues directing migration in the dorsoventral or rostrocaudal axes were found to be expressed in the subpial environment (Borrell and Marin 2006). Rather, contact inhibition between migrating preplate neurons was proposed to be responsible for the rapid spreading of Cajal-Retzius cells to cover the cortex.

Functional significance of Cajal-Retzius subpopulations. Subtypes of Cajal-Retzius neurons may have non-overlapping functions, perhaps in areal patterning and the specification of underlying cortical regions. Alternatively, the multiple and distantly spaced sites of origin of Cajal-Retzius neurons may simply provide a

mechanism for the rapid formation of the reelin-positive layer, and there are no functional differences between differentially derived cells.

Although ablation of subsets of Cajal-Retzius neurons does not result in gross defects in preplate splitting or cortical lamination, some region-specific effects are observed (Meyer, Cabrera Socorro et al. 2004; Bielle, Griveau et al. 2005; Yoshida, Assimacopoulos et al. 2006). In hem-ablated cortex, the hippocampus fails to develop but lamination of the rest of cortex is normal (Yoshida, Assimacopoulos et al. 2006). This phenotype may not be specific to loss of hem-derived Cajal-Retzius cells, but rather to the loss of Wnt and BMP signaling upon hem ablation, as these signals participate in hippocampal specification (Shimogori, Banuchi et al. 2004). However, in the p73 null mouse, Cajal-Retzius cells derived from the cortical hem are specifically lost, although the hem itself was presumably present (Meyer, Cabrera Socorro et al. 2004), and loss of p73 resulted in region-specific cortical malformations. Caudal but not rostral cortical regions were reduced in size, and the hippocampus, though present, was malformed. While both hem ablation and p73 deletion resulted in massive loss of Cajal-Retzius neurons, reelin expression was not entirely abolished and preplate splitting nonetheless occurred. These data suggest that the hem-derived subpopulation of Cajal-Retzius neurons indeed participates in region-specific patterning.

Ablation of Dbx1-positive progenitors in the septum and PSB also resulted in a region-specific effect, as mild defects in the thickness of the lateral cortex

were observed (Bielle, Griveau et al. 2005). Even in the absence of Dbx1+ progenitors, a complete reelin-positive cell layer formed, presumably derived from the cortical hem, and in both hem-ablated and p73 null cortex, low levels of cortical reelin expression were still observed. It therefore makes sense that the gross defects associated with total loss of reelin (failure of preplate splitting and layer inversion) were not observed, and suggests that a high level of reelin expression is not necessary for cortical plate formation. Confirming this observation, the reduced levels of reelin expression seen in the *reeler* heterozygous cortex do not appear to affect either preplate splitting or lamination, although *reeler* heterozygotes do display other phenotypic and behavioral deficits (Tueting, Costa et al. 1999).

Region-specific patterning defects associated with the loss of specific Cajal-Retzius subpopulations but without the total loss of reelin signaling might be explained by a reelin-independent, subtype-specific role in cortical patterning. An alternative hypothesis is that high local reelin levels might be required for regionalization, and thus act as a permissive cue. Yoshida et al (2005) suggest a scenario in which several interacting signaling pathways emanating from Cajal-Retzius neurons partially control the guidance of radial migration and layer formation. In this model, deletion of the *reelin* gene in the *reeler* mouse allows other signals from Cajal-Retzius cells to act unopposed, resulting in the *reeler* phenotype, whereas upon ablation of entire subtypes of Cajal-Retzius neurons layer formation proceeds but patterning is affected.

The question of whether subpopulations of Cajal-Retzius neurons derived from different sources have different molecular properties remains open. Bielle et al (2005) reported that while PSB-derived cells express calretinin, a marker generally thought to be characteristic of most Cajal-Retzius cells, septum-derived cells do not. It has been suggested that cells derived from the hem express the Cajal-Retzius marker p73 whereas those from the PSB do not (Hanashima, Fernandes et al. 2007). As well, a gene array analysis of the total Cajal-Retzius population found several genes expressed only in dorsal preplate or lateral marginal zone at E13, suggesting subpopulation-specific expression (Yamazaki, Sekiguchi et al. 2004). If subtypes of Cajal-Retzius neurons have subtype-specific functions, these functions must be associated with subtype-specific patterns of gene expression. A more complete picture of subtype-specific gene expression will be instrumental in uncovering potential roles of Cajal-Retzius neurons in cortical patterning.

Gene expression in subplate neurons. Subplate neurons have multiple pathways of axonal projections, and therefore the molecular and morphological heterogeneity observed within this layer is to be expected. Subsets of neurons in the embryonic subplate express calretinin, calbindin, GABA, CCK, and neuropeptide Y, and these neurons display distinct morphologies (Del Rio, Martinez et al. 2000). It is not clear whether all of these neurons are derived from

the preplate, or whether cells expressing genes characteristic of interneurons (GABA, calbindin) are actually interneurons migrating through the subplate.

A difficulty in studying subplate development is the lack of specific markers to distinguish subplate neurons from other early-born cortical neurons. Many of the markers used to characterize subplate neurons, such as Map2 or Tuj1, are simply markers of neuronal differentiation expressed in all post-mitotic cortical neurons (including Cajal-Retzius neurons). Subplate neurons are thus generally identified by birthdate, morphology, and their position in the cortex. One of the few specific markers used for subplate is the expression of transgenes driven by the golli promoter (Landry, Pribyl et al. 1998). The golli transgene has the disadvantage of being transiently expressed by some Cajal-Retzius neurons prior to preplate splitting, and thus is not entirely specific to subplate.

Loss of several transcription factors expressed in multiple types of projection neurons are essential for the production of subplate neurons. Tbr1 and Emx1/2 are required for both subplate and Cajal-Retzius neuron specification (Hevner, Shi et al. 2001; Shinozaki, Miyagi et al. 2002). These transcription factors are broadly expressed in the developing cortex. Sox5 is another transcription factor required for proper subplate specification. In addition to being expressed by subplate cells, Sox5 is also expressed by early-born neurons of the cortical plate (layers VI and V) whose production overlaps with that of subplate neurons and that, like subplate neurons, project to subcortical and contralateral cortical regions (Lai, Jabaudon et al. 2008). Loss of Sox5 results in loss of

distinction between these early-born neuronal subtypes, suggesting that these sequentially generated populations share common progenitors in the neocortical VZ.

Little direct evidence is available to support the long-held contention that subplate neurons arise from the local cortical VZ and translocate radially into the preplate layer. Time-lapse imaging of VZ cells labeled with DiI in cultured cortical explants of early rat telencephalon, labeled prior to preplate formation, revealed cells translocating radially from the VZ to the preplate in a columnar fashion (O'Leary and Borngasser 2006), although the ultimate fate of these cells could not be determined in the culture system used. Many future subplate neurons are likely to be born in the local ventricular zone, but the possibility that a subpopulation arises from another region cannot be excluded.

Aims of this work. Progress towards understanding the genetic and cellular mechanisms of preplate cell development and function has been hampered by the lack of markers and tools to identify and manipulate specific preplate subpopulations. The aim of this thesis is to more fully describe gene expression and migration in preplate subpopulations, using the resource of transgenic mice created by the GENSAT Project at Rockefeller University.

BAC transgenic mice as tools in the study of CNS development. *In vivo* expression of transgenes in specific cellular populations of the central nervous

system is a valuable tool that can be used to trace the movements of populations of cells at both static time points and in real time, to purify specific populations for the analysis of gene expression or *in vitro* assays, and to manipulate gene expression or perform cellular ablations in *in vivo* mouse models. The libraries of EGFP and Cre recombinase transgenic mice generated by the GENSAT Project at Rockefeller University (Gong, Zheng et al. 2003; Gong, Doughty et al. 2007) are valuable resources for the study of central nervous system development. Transgenic mice produced by GENSAT use bacterial artificial chromosome (BAC) technology to drive expression of transgenes under the control of the native locus.

The GENSAT database can be used to identify new markers of specific CNS subpopulations. A primary aim of this thesis was to identify and characterize BAC transgenic lines from the database that express EGFP in specific populations of preplate neurons. The subpopulations of cells marked by EGFP expression in the lines identified were characterized by analysis of marker gene expression and birthdating, and these mice were used to investigate the migration and gene expression patterns of preplate subpopulations.

Defining subpopulations of Cajal-Retzius neurons by gene array analysis. As discussed above, previous studies indicate that Cajal-Retzius neurons may be heterogenous with respect not only to birthplace but to gene expression (Yamazaki, Sekiguchi et al. 2004; Bielle, Griveau et al. 2005; Hanashima,

Fernandes et al. 2007). To further understand molecular heterogeneity of Cajal-Retzius neurons, I have taken a direct approach to identifying subpopulation-specific patterns of gene expression in Cajal-Retzius neurons by using gene expression array analysis in an attempt to generate a complete catalog of genes differentially regulated between subpopulations.

With the identification of subpopulation-specific genes, we could begin to answer the outstanding questions of how and why the Cajal-Retzius layer forms from discretely derived subpopulations. First, what attractive or repulsive environmental cues control the migration of each subpopulation through the preplate layer? Different birthplaces imply different migratory pathways, but does this necessarily imply the existence of different guidance receptor systems for neurons derived from different birthplaces? It is possible that the subpial milieu simply stimulates non-directional motility, and that cells spread across the surface of the forebrain more or less randomly. Alternatively, specific migratory pathways might be taken by specific subpopulations, which would be expected to be controlled by distinct signaling molecules and their associated receptors. As well, newly born neurons presumably must migrate radially from the ventricular germinal zones to the subpial region before undergoing tangential migration, which must also employ some sort of directional guidance. A catalogue of the cell-surface receptors with potential roles in guidance that are either specifically enriched in Cajal-Retzius subpopulations or common to Cajal-Retzius subpopulations is a starting point from which to address these questions. An

additional advantage of the EGFP-BAC lines I have identified is that live imaging could be performed to directly observe the migration of subpopulations, tracing the migratory routes taken by subpially migrating neurons.

Finally, understanding which signaling molecules are expressed in specific subpopulations of Cajal-Retzius neurons will be crucial for the development of hypotheses concerning the potential roles of subpopulations in region-specific patterning.

Molecular characterization of future subplate neurons. I carried out a parallel gene array analysis to identify genes specifically expressed in the future subplate component of the preplate, and verified several genes expressed only in future subplate prior to preplate splitting. An immediate benefit of these verified subplate-specific genes is to identify convenient markers for future subplate with commercially available antibodies. Currently, there are no antibodies known that specifically identify the subplate component of the preplate. The new markers I have identified for future subplate neurons will be useful in studying preplate development and the interactions of preplate neurons with the cells of the developing cortical plate. Furthermore, the markers I have identified should allow the generation of transgenic lines to specifically target these cells for ablation, genetic manipulations, or visualization. New tools for the study of subplate neurons should advance our understanding of the source, specification, behavior, and role of these cells in cortical development.

Chapter 2

Identification and characterization of BAC transgenic mouse lines expressing EGFP in preplate subpopulations in the developing cortex

To identify BAC-EGFP transgenic lines appropriate for the study of preplate subpopulations, I screened the GENSAT database (www.gensat.org) for lines expressing EGFP in the marginal zone, or future layer I, at E15.5. At E15.5, the majority of cells in the marginal zone are either Cajal-Retzius neurons, identified by their expression of reelin protein, or migratory interneurons, identified by their expression of calbindin. Five lines were identified and examined at E12 and E15 by immunostaining for these marginal zone markers (data not shown), and three lines which co-expressed EGFP in reelin-positive, calbindin-negative cells were selected for further characterization: Phosphodiesterase 1C-EGFP, Girk4-EGFP, and Wnt3a-EGFP.

Phosphodiesterase 1C-EGFP is expressed in reelin-positive Cajal-Retzius neurons and, transiently, in future subplate neurons. Immunohistochemistry for EGFP and reelin was performed on cryostat sections of E12, E15, and P7 brains (Fig 2.1). At the embryonic time points examined, the Pde1C-EGFP transgene was expressed by the majority of reelin-positive cells in the marginal zone (Fig 2.1, a-f). A number of reelin-negative, Pde1C-EGFP-positive cells were also observed at these stages. At E12, reelin-positive cells were localized

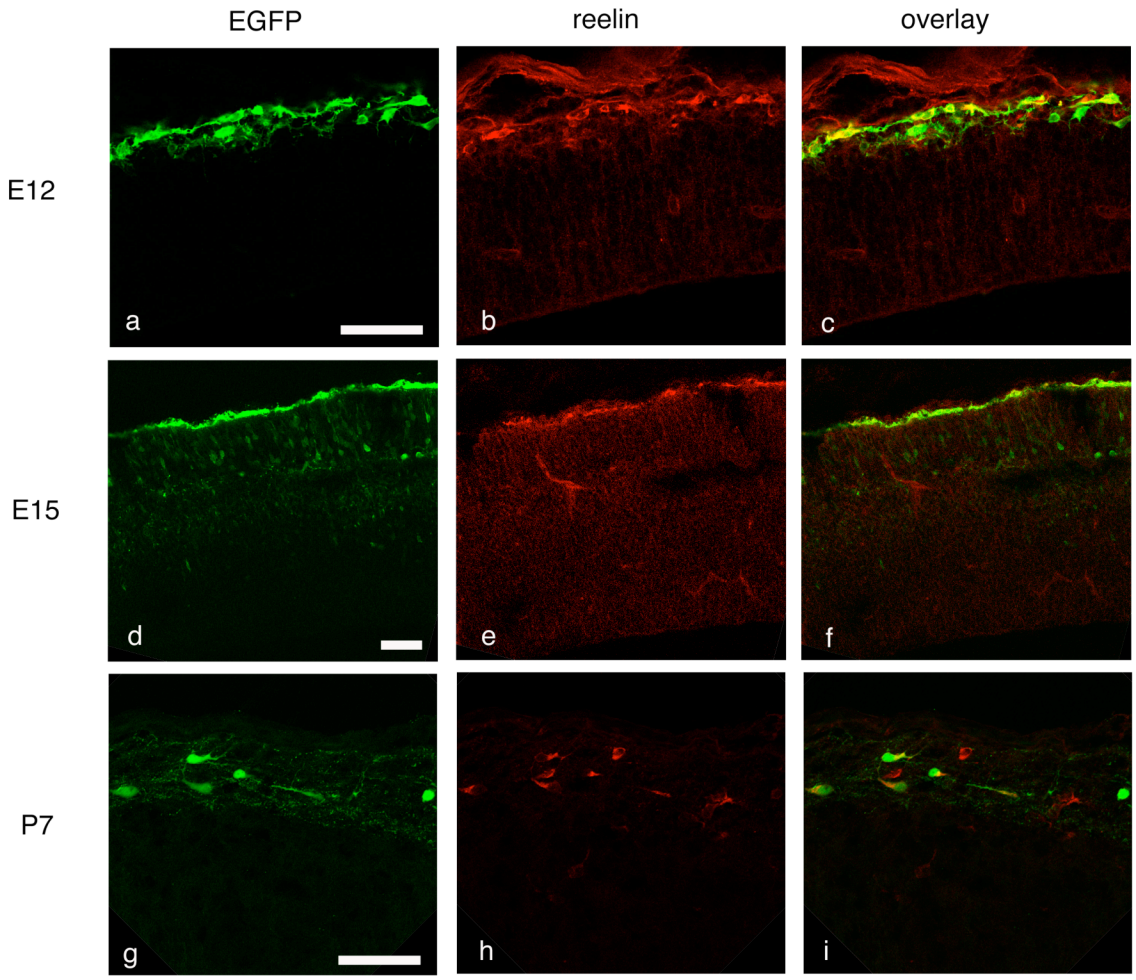

Figure 2.1. Pde1C-EGFP is co-expressed with reelin in the embryonic preplate/marginal zone and early postnatal layer I. Immunostaining in sagittal cryostat sections of E12 (a-c), E15 (d-f), and P7 (g-i) brains for EGFP (green, a, d, g) and reelin (red, b, e, h). The overlays (c, f, i) show a partial colocalization of Pde1C-EGFP and reelin. Scale bars = 50 μm.

beneath the pia in the most superficial aspect of the neuroepithelium, while the reelin-negative, Pde1C-EGFP-positive cells were usually located just beneath the reelin-positive population (Fig 2.1, a-c). Reelin-positive cells displayed the bipolar morphology and horizontal orientation typical of Cajal-Retzius neurons, while the reelin-negative population tended to have more rounded cell bodies and were not necessarily oriented parallel to the pial surface.

At E15, after the onset of cortical plate formation and preplate splitting, reelin-negative cells expressing low levels of Pde1C-EGFP were observed in deeper cortical layers (Fig 2.1, d-f). Pde1C-EGFP expression was maintained in some reelin-positive layer I neurons in the P7 cortex (Fig 2.1, g-i). No expression of Pde1C-EGFP was seen outside of layer I in the P7 cortex.

Some Pde1C-EGFP-expressing cells in the preplate also express calretinin (Fig 2.2), a calcium-binding protein that is expressed by most Cajal-Retzius neurons (del Rio, Martinez et al. 1995). Triple staining E12 cortex for EGFP, reelin, and calretinin showed that nearly all reelin- and/or calretinin-positive cells in the preplate coexpressed Pde1C-EGFP (Fig 2.2). However, a significant proportion of Pde1C-EGFP-positive cells express neither reelin nor calretinin, and therefore are not Cajal-Retzius neurons. These data indicate that Pde1C-EGFP is expressed in the vast majority of Cajal-Retzius neurons, but is not specific to Cajal-Retzius neurons at the preplate stage.

Because not all Pde1C-EGFP-expressing preplate/marginal zone cells could be identified as Cajal-Retzius neurons, I examined the expression of the

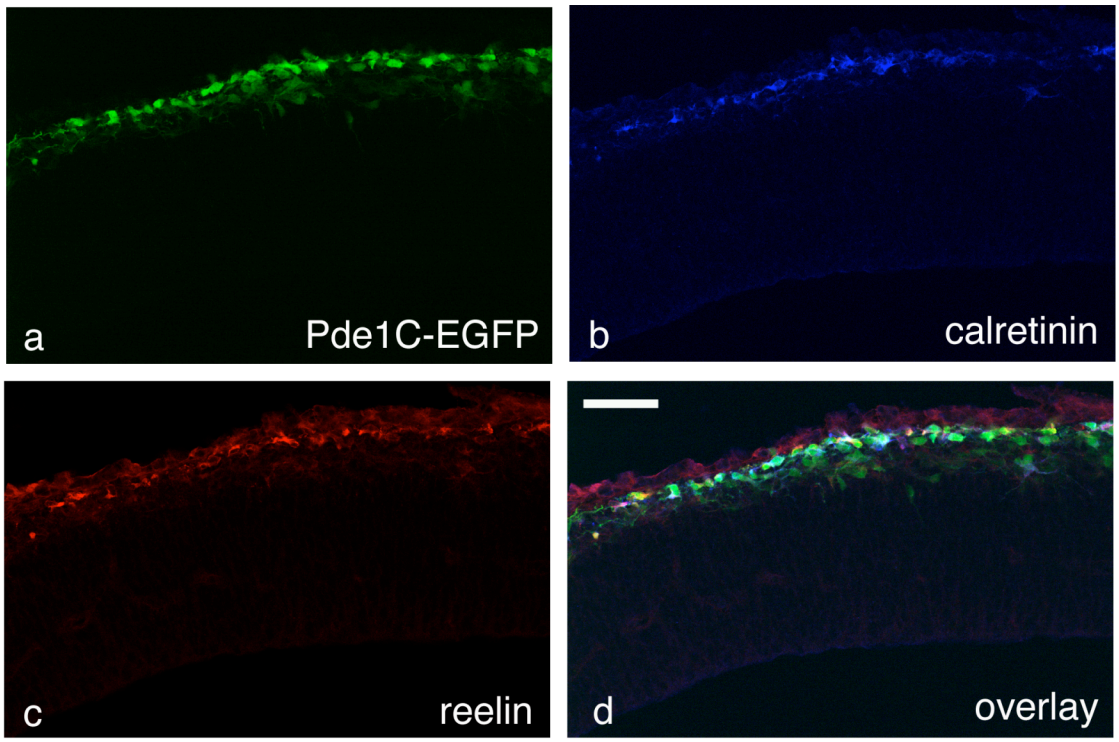

Figure 2.2. Pde1C-EGFP is expressed in all Cajal-Retzius neurons, as well as in a non-Cajal-Retzius population of the preplate. Immunostaining in coronal cryostat sections of E12 Pde1C-EGFP cortex for EGFP (green, a), calretinin (blue, b), and reelin (red, c). Pde1C-EGFP is expressed in all subpial calretinin- and/or reelin-positive cells, but a substantial number Pde1C-EGFP-positive cells do not co-express either marker. Scale bar in (d) = 50 μm.

interneuron marker calbindin in E13 brains. Calbindin is expressed in the majority of interneurons which migrate tangentially from the ganglionic eminence into the neocortex (Anderson, Eisenstat et al. 1997). Almost no calbindin-positive interneurons can be observed in neocortex at E12 (data not shown), so I examined calbindin expression by immunohistochemistry at E13, when calbindin-positive interneurons are migrating through the preplate of the lateral neocortex. At E13, although the calbindin-expressing and Pde1C-EGFP-expressing cells were of comparable size, had similar bipolar morphologies and were intermingled in the preplate, there was no colocalization of calbindin and Pde1C-EGFP (Fig 2.3), indicating that the reelin-negative, Pde1C-EGFP-positive neurons observed at embryonic time points are probably not interneurons.

Several lines of evidence indicated that the reelin-negative, Pde1C-EGFP-positive cells are future subplate neurons. The pattern of distribution of the reelin-negative, Pde1C-EGFP-positive cells followed the lateral-to-dorsal and anterior-to-posterior gradient of corticogenesis described by Takahashi et al. (1999). At any given point in embryonic development, lateral cortex is more “mature” than dorsomedial cortex – production of cortical plate neurons, radial migration, and preplate splitting begin in lateral cortex, and proceed in a gradient towards dorsal cortex. In dorsal cortex at E13, preplate splitting has not yet occurred. In E13 dorsal cortex, there were few reelin-negative, Pde1C-EGFP-positive cells. Those present at this stage were localized just below the reelin-positive cells (Fig 2.4 a-c), as at E12. In contrast, in E13 lateral cortex preplate splitting is initiating, and

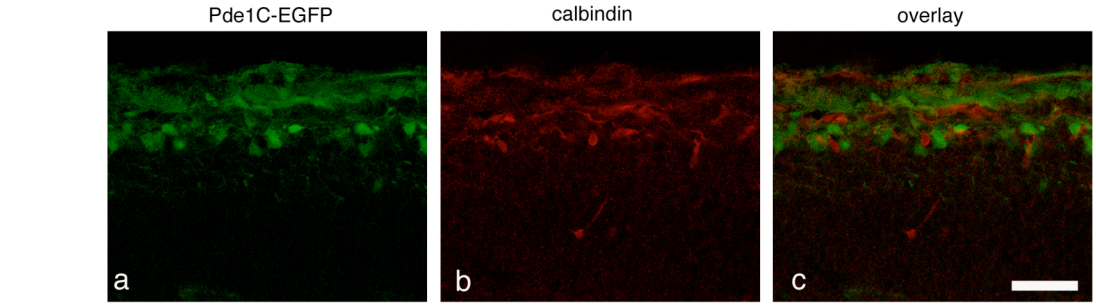

Figure 2.3. Pde1C-EGFP does not colocalize with the interneuron marker calbindin in the embryonic preplate/marginal zone. Immunostaining in coronal cryostat sections of E13 Pde1C-EGFP brain for EGFP (green, a) and calbindin (red, b). The overlay (c) shows no colocalization of the two markers. Scale bar = 50 μm.

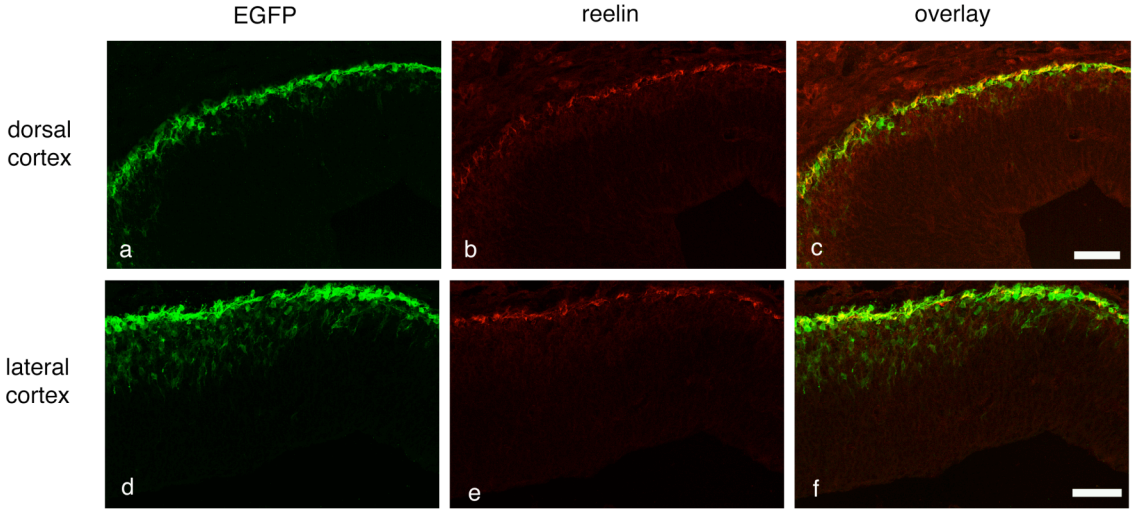

Figure 2.4. Reelin-negative, Pde1C-EGFP-positive cells are differentially localized in lateral and dorsal cortex. Immunostaining in coronal cryostat sections of E13 Pde1C-EGFP cortex for EGFP (green, a, d) and reelin (red, b, e). Reelin-negative cells are subpial in dorsal cortex (a-c), and deeper in lateral cortex (d-f). Scale bars in (c), (f) = 50 μm.

Pde1C-EGFP-positive, reelin-negative cells were numerous. These cells were localized in deeper layers and some were oriented radially (Fig 2.4, d-f). This expression pattern is consistent with the position of future subplate neurons, which appear in a lateral-to-dorsal gradient beginning at E11, reside subpially in the preplate prior to cortical plate formation, and descend from their subpial location to a deeper layer of cortex during cortical plate formation and preplate splitting.

While reelin-negative cells in the dorsal preplate expressed similar levels of Pde1C-EGFP as the Cajal-Retzius neurons (Fig 2.4,c), expression of Pde1C-EGFP was reduced in reelin-negative cells that were located deep to the preplate in lateral neocortex and piriform cortex (Fig 2.4, f). Weak EGFP expression was also visible in early corticofugal pioneer axons, presumably extended from subplate neurons, which at E13 had not yet exited the cortex (Fig 2.5, arrows). These weakly expressing cells and fibers could only be visualized by antibody staining and slight overexposure of the image. In contrast, very strong expression of Pde1C-EGFP wa apparent in the lateral olfactory tract and the anterior commissural projections (Fig 2.5a). The anterior commissure is made up of projections from both neocortical neurons and the olfactory bulb, and I attribute the strong expression in the anterior commissure to the high levels of Pde1C-EGFP expressed in the olfactory bulb (Fig 2.5b), as the projections from cortical neurons did not display this level of expression.

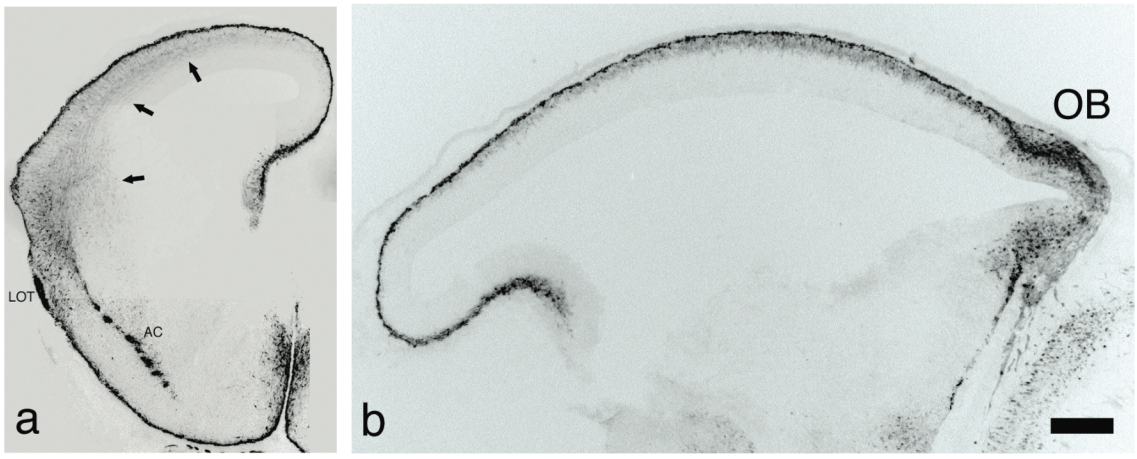

Figure 2.5. Pde1C-EGFP is expressed in neocortex and olfactory tracts. Composite photographs of immunostaining for EGFP in coronal (a) and saggital (b) cryostat sections of E13 Pde1C-EGFP cortex. Pde1C-EGFP is highly expressed in the superficial preplate, (future marginal zone) anterior commissure, lateral olfactory tract, and olfactory bulb, and is expressed at lower levels in deeper preplate neurons and early cortical projections. Abbreviations: lateral olfactory tract (LOT), anterior commissure (AC), olfactory bulb (OB). Fluorescent grayscale images were inverted and levels adjusted with Photoshop to produce the images shown. Scale bar = 200 μm.

Fate mapping of Pde1C-expressing cortical cells. By E15, the Pde1C-EGFP-positive, reelin-negative cells expressed only very low levels of EGFP (Fig 2.1), and no expression aside from in reelin-positive cells was seen postnatally (Fig 2.1). At E15, the weakly-expressing cells appeared to be coalescing in a deep layer corresponding to subplate. The weak stain meant that EGFP could not be used as a marker to determine the final destination of the reelin-negative cells. Fate-mapping of Pde1C-expressing cells was done using a Pde1C-Cre recombinase BAC transgenic line generated by GENSAT (Gong, Doughty et al. 2007). Three Pde1C-Cre transgenic lines were mated to the reporter line ROSA26R, and embryos were examined at E13 to select a line with an expression pattern that most closely matched the expression pattern of Pde1C-EGFP. None of the Cre transgenic lines examined had beta-galactosidase expression in the ventral superficial cortex to match the Pde1C-EGFP expression at this stage (see Fig 2.5). However, as beta-galactosidase expression in dorsal and lateral cortex in the IT-150 line closely matched the expression pattern of Pde1C-EGFP in these regions (Fig 2.6a,b), this line was chosen for further study. At E13, scattered radial columns of beta-galactosidase-positive cells were observed throughout the cortex.

Pde1C-Cre IT-150 animals were mated to the reporter line ROSA26R and embryos were collected at E16, well after EGFP expression in the Pde1C-EGFP line has disappeared in non-Cajal-Retzius cells. At E16, beta-galactosidase

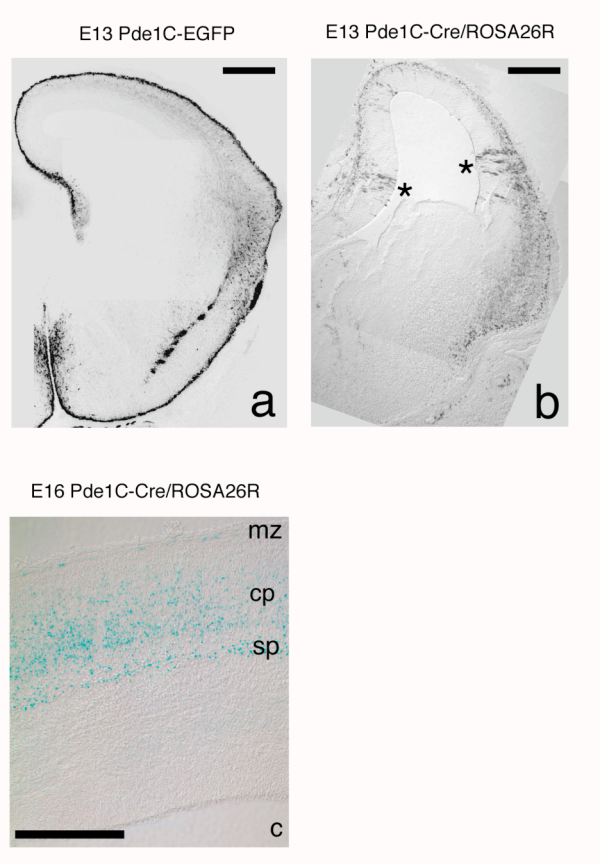

Figure 2.6. Pde1C-Cre BAC transgenic reproduces the expression pattern of Pde1C-EGFP BAC transgenic in E13 neocortex, and Pde1C-Cre is expressed in subplate neurons. (a) Immunostaining for EGFP in coronal cryostat section of Pde1C-EGFP E13 brain. Pde1C-EGFP is strongly expressed in the preplate/lateral zone, and more weakly expressed in deeper cortical layers, corticofugal projections, and lateral cortex. (b) X-gal staining in coronal cryostat section of Pde1C-Cre$^{+/-}$/ROSA26R$^{+/-}$ E13 brain. Beta-gal is expressed by cells in the preplate/marginal zone and lateral cortex. Radially oriented beta-gal expressing cells are occasionally observed in the ventricular zone/intermediate zone of the cortical hem and neocortex (asterisks). (c) X-gal staining in coronal cryostat section of Pde1C-Cre$^{+/-}$/ROSA26R$^{+/-}$ E16 brain. Beta-gal is expressed in scattered cells in the marginal zone and in the subplate, as well as in cells of the lower cortical plate. Scale bar in a,b = 400 μm, c = 200 μm. Abbreviations: marginal zone (mz), cortical plate (cp), subplate (sp).

expression was seen in few marginal zone cells, in the subplate, and in the lower cortical plate (Fig 2.6c). This suggests that Pde1C is transiently expressed in early, deep layer cortical plate neurons as well as in Cajal-Retzius and future subplate neurons, and that the cells expressing weak levels of the Pde1C-EGFP transgene at E15 may be a mixture of subplate and cortical plate neurons. The low number of labeled cells in the Pde1C-Cre marginal zone may indicate that the Cre transgene either does not express as highly in Cajal-Retzius neurons as the EGFP transgene, or that the EGFP protein is more stable than Cre recombinase.

Taken together, these data indicate that Pde1C transgenes are expressed transiently in preplate cells destined for the subplate and marginal zone, as well in neurons destined for the cortical plate. Pde1C-EGFP is strongly expressed in both Cajal-Retzius neurons and future subplate neurons at E12, but expression of this marker subsequently decreases in future subplate neurons, while it is maintained in Cajal-Retzius neurons.

Pde1C-EGFP expression in subplate neurons. Subplate neurons are heterogenous with respect to both the expression of marker proteins and the targeting of their projections (Del Rio, Martinez et al. 2000). Whether Pde1C-EGFP marks all future subplate neurons or only a subset is not clear from these data. However, there is evidence to support the hypothesis that Pde1C-EGFP is

transiently expressed in multiple subpopulations of subplate neurons, at least with respect to axon targeting. The two major axonal tracts pioneered by subplate neurons at E13.5 are the corticothalamic tracts and the anterior commissure (Jacobs, Campagnoni et al. 2007). These tracts can be molecularly distinguished by the expression of TAG1, which is expressed by corticothalamic projections but not by the corticofugal limb of the anterior commissure (Denaxa, Chan et al. 2001). The axonal glycoprotein L1, in contrast, is expressed in all corticofugal fibers in the developing cortex (Fukuda, Kawano et al. 1997; Jones, Lopez-Bendito et al. 2002). I examined the colocalization of TAG1 with Pde1C-EGFP in the weakly-expressing fibers of the intermediate zone (see Fig 2.5). In E13 cortex, a mixture of TAG1-positive (Fig 2.7, filled arrowheads) and TAG1-negative (Fig 2.7, open arrowheads) Pde1C-EGFP-positive fibers were observed in the intermediate zone, which suggests that Pde1C-EGFP is expressed in populations of subplate cells sending out both early corticothalamic projections as well as other corticofugal projections not destined for the thalamus.

Girk4-EGFP and Wnt3a-EGFP are expressed exclusively in Cajal-Retzius neurons. Immunostaining for reelin and EGFP was performed on cryostat sections of E12 brains from Girk4-EGFP and Wnt3a-EGFP transgenics. Both Girk4-EGFP and Wnt3a-EGFP were co-expressed in reelin-positive cells at E12 (Fig 2.8, a-f). In both lines, the vast majority of EGFP-positive cells co-expressed reelin. In both lines, some of reelin-positive, EGFP-negative cells were observed

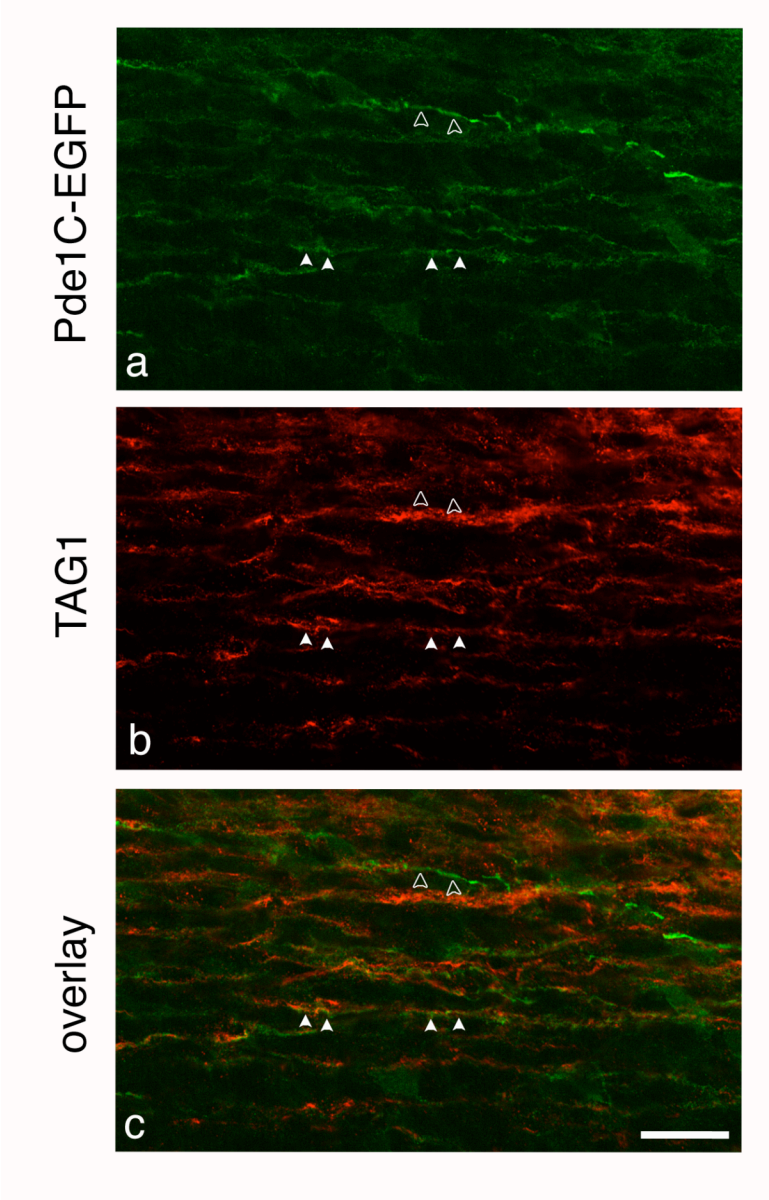

Figure 2.7. Pde1C-EGFP is expressed in both TAG1-positive and TAG1-negative subsets of subplate pioneer axons. High-power confocal images of Pde1C-EGFP E13 cortex stained for EGFP (a) and TAG1 (b). Overlay is shown in (c). Some Pde1C-positive intermediate zone fibers coexpress TAG1 (filled arrowheads), while some are TAG1-negative (open arrowheads). Scale bar = 20 μm.

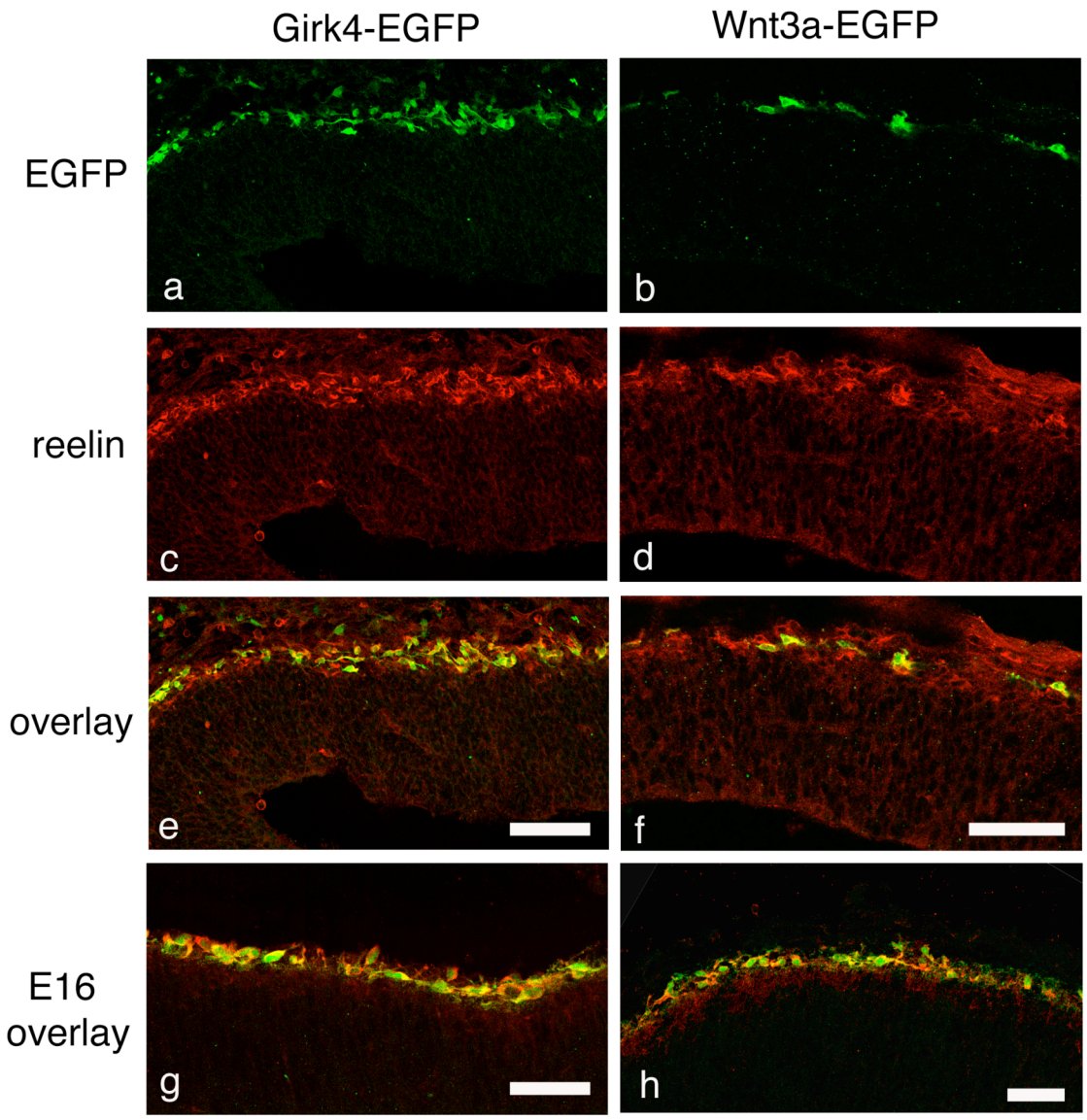

Figure 2.8. Girk4-EGFP and Wnt3a-EGFP are expressed exclusively in Cajal-Retzius neurons. Immunostaining in cryostat sections of E12 (a-f) and E16 (g-h) cortex for EGFP (green, a,b) and reelin (red, c,d) in Girk4-EGFP transgenic embryos (a, c, e) and Wnt3a-EGFP transgenic embryos (b,d,f). In g-h, secondaries used were the same as for a-f. Scale bars = 50 μm.

at E12 – neither Girk4-EGFP nor Wnt3a-EFGP were expressed in all reelin-positive neurons. Expression of EGFP in reelin-positive cells was maintained in both lines at E16 (Fig 2.8, g-h). Examination of postnatal expression patterns in each line in the GENSAT database showed that Girk4-EGFP expression was weakly maintained in layer I of P7 cortex, but Wnt3a-EGFP was not expressed in the postnatal cortex. Thus, both the Girk4-EGFP and Wnt3a-EGFP transgenes are expressed by Cajal-Retzius neurons during embryogenesis.

Girk4-EGFP and Wnt3a-EGFP are expressed in distinct but overlapping populations of Cajal-Retzius neurons. Expression of both the Girk4-EGFP and Wnt3a-EGFP transgenes was first apparent at E11.5 by immunostaining for EGFP (Fig 2.9, a-d). This spatiotemporal expression pattern is consistent with the timing of generation of Cajal-Retzius neurons, the majority of Cajal-Retzius neurons being generated between E10.5 - E11.5 (Hevner, Neogi et al. 2003). At E11.5, the distribution of EGFP-positive cells within the cortex differed significantly between the two lines. Wnt3a-EGFP was highly expressed in the cortical hem, the dorsalmost region of the neuroepithelium (Fig 2.9c). Wnt3a-EGFP-positive cells were observed in hem-adjacent dorsal preplate caudally (Fig 2.9c) and the dorsal/medial preplate rostrally (Fig 2.9a). At the same stage, Girk4-EGFP-positive cells were found in both dorsal and lateral preplate, distributed evenly across the cortex (Fig 2.9b,d). In rostral cortex, Girk4-EGFP

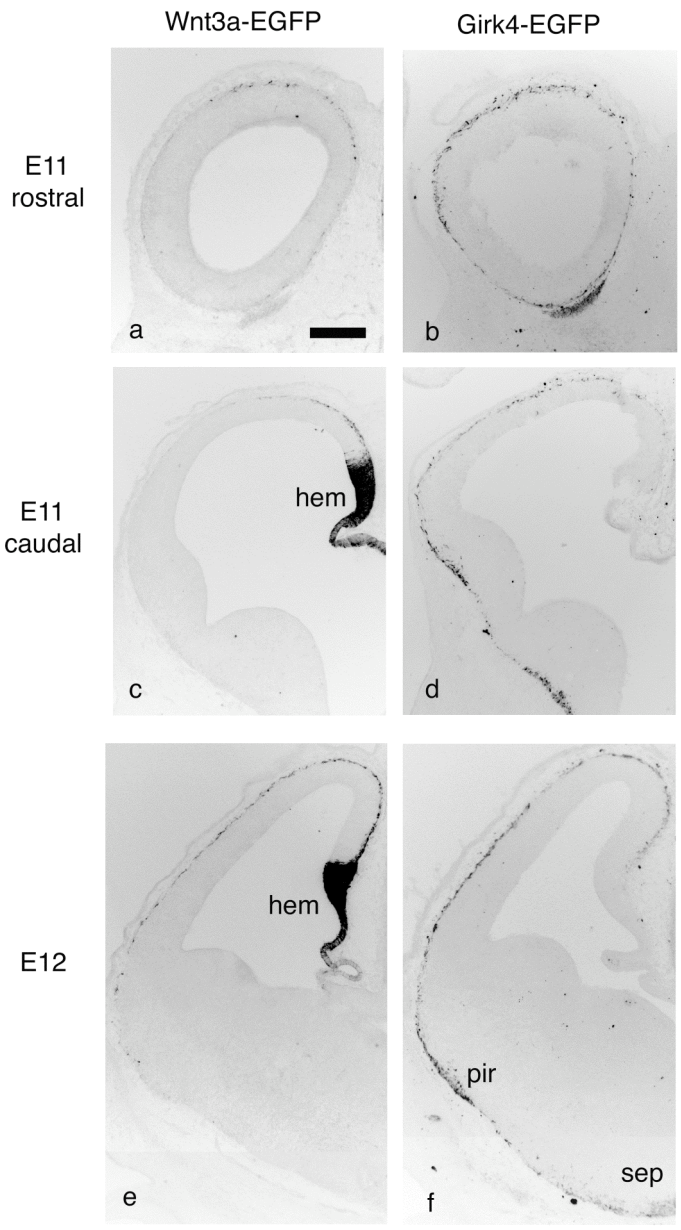

Figure 2.9. Comparison of expression profiles of Girk3-EGFP and Wnt3a-EGFP in early embryonic cortex. Immunostaining for EGFP in cryostat sections of E11 (a-d) and E12 (e,f) cortex from Wnt3a-EGFP BAC transgenic embryos (a,c,e) and Girk4-EGFP BAC transgenic embryos (b,d,f). Fluorescent grayscale images were inverted and levels adjusted with Photoshop to produce the images shown. Abbreviations: septum (sep), piriform cortex (pir). Scale bar = 200 μm.

completely covered the cortex (Fig 2.9b). Caudally, a cluster of Girk4-EGFP-expressing cells was observed in the ventral forebrain, close to the midline (Fig 2.9d). Because this lateral and ventral expression was not seen in Wnt3a-EGFP embryos, Girk4-EGFP-positive cells in these regions probably represent a distinct population of Cajal-Retzius neurons from those marked by the expression of Wnt3a-EGFP.

By E12.5, Wnt3a-EGFP-positive preplate cells extended from the dorsal-most cortex to the lateral cortex (Fig 2.9e). Girk4-EGFP-positive cells at the same developmental stage covered the entire cortex, with aggregations of EGFP-expressing cells close to the septum (ventral midline) and in the preplate surrounding the piriform cortex (2.9f). The EGFP-expressing preplate layer in Girk4-EGFP E12 cortex was somewhat thicker and more dense than that observed in the Wnt3a-EGFP E12 cortex, suggesting that the Girk4-EGFP-positive Cajal-Retzius neurons represent a larger population than the Wnt3a-EGFP-positive Cajal-Retzius neurons. Based on its spatiotemporal expression pattern, the Wnt3a-EGFP transgene likely marks a subpopulation of Cajal-Retzius neurons derived from the cortical hem (Yoshida, Assimacopoulos et al. 2006).

Comparing the distribution of EGFP-positive cells at E11.5 suggested that there might be overlap between the populations of Cajal-Retzius neurons identified by EGFP reporter gene expression in each line. Both Girk4-EGFP and Wnt3a-EGFP were expressed by cells adjacent to the cortical hem (Fig 2.9a-d).

To determine whether these populations overlap, I examined the expression of endogenous Girk4 mRNA in each population. If Wnt3a-EGFP-expressing cells are a subset of Girk4-EGFP-positive cells, then expression of Girk4 mRNA should be detectable in Wnt3a-EGFP-positive cells.

Girk4 mRNA levels were measured by quantitative real-time PCR (qPCR) in purified populations of EGFP-positive cells from each line. Single-cell suspensions were prepared from E12 cortices, and EGFP-positive cells were purified by fluorescence activated cell sorting (FACS) (for details, see Chapter 4). Total RNA from sorted cells was extracted and amplified for use in the qPCR assay. GAPDH was amplified as the internal standard to determine relative expression levels.

By qPCR, Girk4 mRNA was found to be highly upregulated in both Girk4-EGFP and Wnt3a-EGFP-positive cells, compared to expression in unpurified whole cortex (Fig 2.10). Girk4 mRNA was present at nearly undetectable levels in unpurified cortex, while high levels of Girk4 mRNA were present both in Girk4-EGFP-positive cells and Wnt3a-EGFP-positive cells. Wnt3a-EGFP-positive cells therefore express Girk4 at a level not significantly different from that observed in Girk4-EGFP-positive cells ($p=0.92$ by t-test). Therefore, it is probable that the Wnt3a-EGFP-positive population is a subset of the Girk4-EGFP-positive Cajal-Retzius neurons. Girk4-EGFP likely labels a broad population of Cajal-Retzius neurons derived from multiple sources, including the cortical hem.

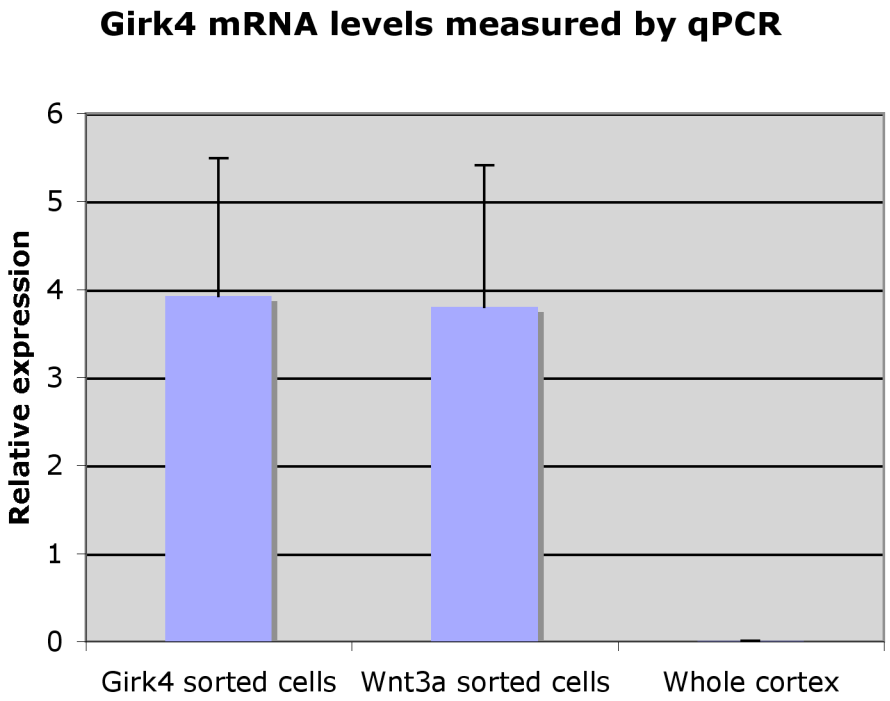

Figure 2.10. Girk4 mRNA is expressed by Wnt3a-EGFP-positive cells at E12. Levels of Girk4 mRNA in FACS-purified EGFP+ cells from Girk4-EGFP+ and Wnt3a-EGFP+ transgenic E12 cortices. GAPDH was amplified as an internal standard. Error bars represent standard deviation.

In summary, these experiments identified three BAC transgenic lines that express EGFP in subpopulations of the preplate. The Wnt3a-EGFP transgeneis expressed in a subpopulation of reelin-positive Cajal-Retzius cells that are likely derived from the cortical hem. The Girk4-EGFP transgene is expressed in a broader population of Cajal-Retzius neurons, as it expresses EGFP in nearly all reelin-positive cells, and is expressed by cells in more lateral regions than is the Wnt3a-EGFP transgene. These populations of Cajal-Retzius cells overlap, as each expresses comparable levels of Girk4 mRNA. The Pde1C-EGFP transgene is expressed in all Cajal-Retzius neurons as well as future subplate neurons. Expression of Pde1C-EGFP in the future subplate neurons is transient and decreases after preplate splitting initiates.

Chapter 3

Migratory behavior and proliferative characteristics of preplate subpopulations

Birthplaces of Girk4-EGFP and Wnt3a-EGFP-expressing Cajal-Retzius neurons. Recent studies have shown that Cajal-Retzius neurons, while sharing the general characteristics of pallium-derived excitatory cortical neurons (as opposed to subpallium-derived interneurons), are generated in discrete proliferative compartments of the neocortical ventricular zone (Bielle, Griveau et al. 2005; Yoshida, Assimacopoulos et al. 2006), and must migrate tangentially through the preplate to cover the surface of the cortex. Thus, although Cajal-Retzius neurons express neurotransmitters and transcription factors characteristic of projection neurons, they have migratory properties characteristic of interneurons. It should nonetheless be noted that the entire cortical ventricular zone cannot be ruled out as a source of an additional subpopulation of Cajal-Retzius neurons.

To define the site of origin and the migratory pathways of preplate subpopulations, I examined the expression of mitotic markers, performed BrdU birthdating, and used live imaging to track the tangential migration of EGFP-positive preplate neurons in the BAC transgenic lines identified in the previous chapter.

Live imaging of Cajal-Retzius subpopulations. As Cajal-Retzius cells are thought to be derived from restricted regions of the neuroepithelium, it has been proposed that they undergo subpial tangential migration to form the preplate layer across the entire surface of developing forebrain. This migration has been inferred from fate-mapping and *in vitro* slice manipulations, but has not previously been directly imaged. To investigate the migratory capacity of preplate neurons and to attempt to identify migratory pathways specific to subpopulations of preplate neurons, I used live imaging to examine subpial tangential migration of EGFP-positive cells in whole-mounted cortices.

Tangential migration of Wnt3a-EGFP Cajal-Retzius neurons. The two major sources of Cajal-Retzius neurons identified by fate mapping using Cre transgenic mice are the cortical hem, the dorsomedial-most region of the forebrain, and the pallial-subpallial boundary (PSB). The cortical hem is marked by the expression of Wnt3a (Grove, Tole et al. 1998), among other signaling molecules, and it therefore was probable that the Wnt3a-EGFP-positive Cajal-Retzius cells represented a hem-derived population.

To confirm that Wnt3a-EGFP-positive Cajal-Retzius neurons migrate tangentially within the preplate, I performed time-lapse imaging of Wnt3a-EGFP cells in cultured whole-mounted E12 cortex. Hemisectioned cortices of Wnt3a-EGFP transgenic embryos were embedded in Matrigel on movie dishes, pial membrane intact and oriented against the coverslip. EGFP-positive cells were

imaged over several hours by spinning disk confocal microscopy. Imaging was done either immediately after embedding or 12-24 hours later. By morphological criteria, survival of EGFP-positive cells in whole-mounted cortices was unaffected by being kept in culture for up to one day. Wnt3a-EGFP-positive cells were imaged in the tangential plane of cortex, away from the edges of the tissue. Due to variability in the morphology of embedded it was not possible to perfectly replicate the regions of the cortex imaged. Migrating cells were imaged in the region of the rostral cortex, dorsal to the subpallium and dorsal and caudal to the olfactory bulb. Movies made in four independent experiments revealed large numbers of highly motile, tangentially migrating Wnt3a-EGFP-positive neurons (Fig 3.1a,b). In the tangential view, these cells generally displayed a bipolar morphology, often with elaborate growth cones at the leading process. Migrating cells frequently displayed a mode of migration wherein the leading process thickened towards the cell body, and the cell body then moved into the thickened process.

In order to determine directional patterns of tangential migration, the trajectories of individual cells were tracked either manually or automatically using MetaMorph 6.3 software. Each cell's movements were plotted on a line graph in which the origin represents the starting position of each cell. Two examples of the migratory pathways of Wnt3a-EGFP cells traced from individual movies are shown in Fig 3.1c and d. Notably, most Wnt3a-EGFP cells migrated exclusively from dorsal regions towards ventral regions, and never from ventral towards

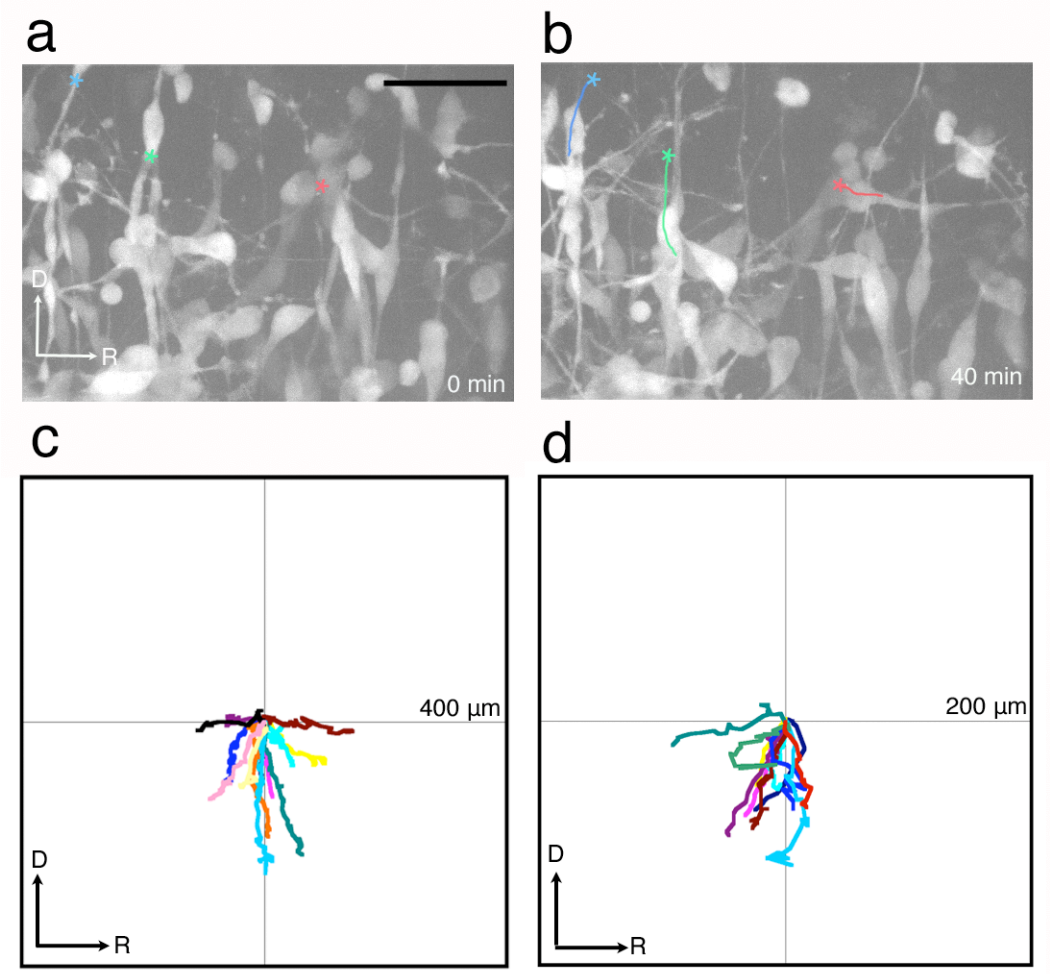

Figure 3.1. Wnt3a-EGFP Cajal-Retzius neurons migrate tangentially within the preplate from dorsal to ventral. Live imaging by spinning-disk confocal of Wnt3a-EGFP in whole-mounted E12 cortex revealed multiple tangentially migrating neurons (a,b). Asterisks in a and b mark the starting point (at 0 min) of the leading edge of the cell body of migrating neurons. Colored lines in (b) trace the path of the leading edge of migrating cells over the 40 minutes of imaging. Arrows indicate orientation (D = dorsal, R = rostral). Panels c and d plot the migration of individual cells in two movies of Wnt3a-EGFP cells. The origin marks the starting point of each migrating cell, and each cell is represented by a different color line. The cells tracked in (c) were imaged over 215 minutes; the cells tracked in (d) were imaged over 130 minutes. Scale bar in a = 20 µm.

dorsal. Cells also migrated both rostrally and caudally. The entirely ventrally-directed migration observed is consistant with the proposed origin of these cells in the cortical hem, the dorsalmost region of the forebrain.

Tangential migration of Girk4-EGFP Cajal-Retzius neurons. To investigate the migratory trajectories of Girk4-EGFP neurons, I used time-lapse imaging of living Girk4-EGFP-positive neurons in E12 whole-mounted cortices, precisely as described above. In five independent experiments, multiple motile, tangentially migrating Girk4-EGFP-positive cells were observed within the preplate (Fig 3.2a,b). Cell tracking showed that Girk4-EGFP-positive cells migrated towards both dorsal and ventral regions, in contrast to the Wnt3a-EGFP population (Fig 3.2c-e). This strongly supports the hypothesis that subpopulations of Girk4-EGFP-positive Cajal-Retzius cells are derived from a lateral region of forebrain such as the PSB, from which they migrate dorsally.

In the rostrocaudal axis, Girk4-EGFP cells were observed migrating both caudally and rostrally, depending upon the region imaged. In more rostral regions, the majority of cells migrated caudal-ventrally (Fig 3.2d), whereas in more caudal regions they migrated rostrally (Fig 3.2c, e). It is likely that that these cells are derived from the anterior hem. Cells imaged in more caudal regions probably represent a mixed population of hem-derived cells migrating ventrally, and another, more laterally derived population migrating dorsally. The large number of rostrally migrating cells seen in caudal regions are consistent with the

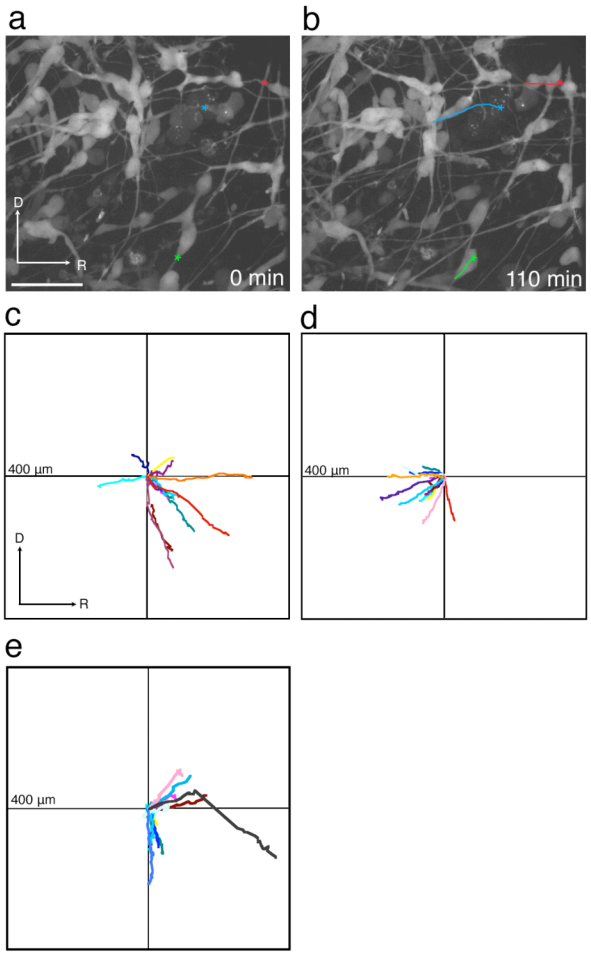

Figure 3.2. Girk4-EGFP Cajal-Retzius neurons migrate tangentially within the preplate. Live imaging by spinning-disk confocal microscopy of Girk4-EGFP in whole-mounted E12 cortex. a) Starting frame of movie; asterisks mark the starting point of the leading edge of the cell body. Colored lines in (b) trace the path of the leading edge over 110 minutes of imaging. Arrows indicate orientation (D = dorsal, R = rostral). Panels c-e plot the migration of individual cells in two sample movies of Girk4-EGFP cells. Movies tracked in c and e were imaged in caudal cortex, while the movie tracked in d was imaged in rostral cortex. The origin marks the starting point of each cell, and each cell is represented by a different color line. Cells tracked in panel c were imaged for 215 minutes, cells tracked in panel d were imaged for 170 minutes, and cells tracked in panel e were imaged for 225 minutes. Scale bar in (a) = 20 μm.

migratory pathway of PSB-derived Cajal-Retzius cells proposed by Bielle et al (2005).

Tangential migration of Pde1C-EGFP preplate neurons. In the Pde1C-EGFP cortex, live imaging revealed large numbers of tangentially migrating Pde1C-EGFP-positive cells, migrating in multiple directions (Fig 3.3). In rostral cortex, there were large numbers of rostrally migrating cells as well as some caudally migrating cells (Fig 3.3d). The majority were migrating from ventral to dorsal, with a few cells migrating in the opposite direction. In more caudal cortex, cells were observed migrating largely from dorsal to ventral, and in both directions along the rostrocaudal axis (Fig 3.3c). It is probable that the majority of Pde1C-EGFP-positive migratory cells observed were Cajal-Retzius neurons, although it is possible that some subplate neurons might also migrate tangentially within the preplate.

Preplate subpopulations are not actively proliferating. The formation of the Cajal-Retzius layer by tangential migration from a focal birthplace is a process reminiscent of the formation of the cerebellar external granular layer (EGL) (Hatten 1999). Cerebellar granule neuron precursors migrate tangentially from their birthplace in the rhombic lip to cover the surface of the cerebellar anlage, forming a secondary germinal zone where precursors continue

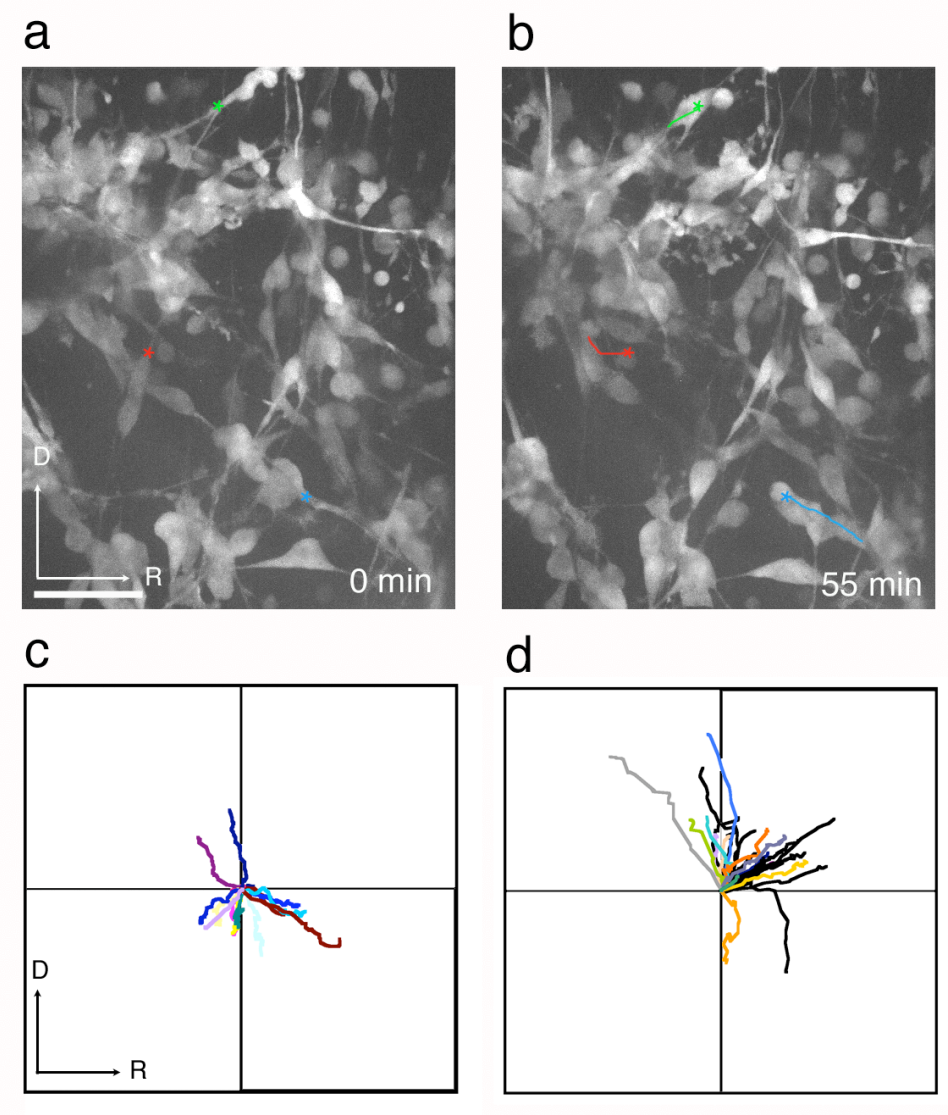

Figure 3.3. Pde1C-EGFP Cajal-Retzius neurons migrate tangentially within the preplate. Live imaging by spinning-disk confocal microscopy of Pde1C-EGFP in whole-mounted E12 cortex. a) Starting frame of movie; asterisks mark the starting point of the leading edge of the cell body. Colored lines in (b) trace the path of the leading edge over 55 minutes of imaging. Arrows indicate orientation (D = dorsal, R = rostral). Panels c,d plot the migration of individual cells in two sample movies of Pde1C-EGFP cells. The origin marks the starting point of each cell, and each cell is represented by a different color line. Cells tracked in panel c were imaged for 175 minutes, and cells tracked in panel d were imaged for 160 minutes. Scale bar in (a) = 20 μm.

proliferation before their terminal differentiation. The similarities between EGL and preplate formation prompted me to examine the proliferative characteristics of EGFP-positive preplate populations. Although the classical models of cortical development hold that proliferation of neuronal precursors occurs only in the germinal ventricular zone, and that neurons forming the preplate are entirely postmitotic, actively proliferating cells are occasionally observed within the preplate (Valverde, De Carlos et al. 1995; Costa, Kessaris et al. 2007), although it is not clear what cell types these mitoses give rise to.

To determine whether any of the preplate subpopulations expressing EGFP transgenes were actively proliferating, or whether they represented purely postmitotic differentiated neurons, I performed double immunostaining for EGFP and the M phase marker ser-10 phosphorylated histone H3 (Fig 3.4) and Ki67 (data not shown), which is expressed during all phases of mitosis. At E11, the majority of phospho-histone H3 or Ki67-positive cells were located along the ventricular surface or in the pial membrane covering the neuroepithelium (Fig 3.4). Very few mitotic cells were observed intermingled with the EGFP-positive preplate neurons (Fig 3.4a,b, arrowheads), and mitotic markers were never coexpressed in the preplate with EGFP in any of the lines examined. In the case of the Wnt3a-EGFP line, EGFP is expressed not only in the preplate, but also in the cortical hem (Fig 3.4e). Phospho-histone H3 is expressed by Wnt3a-EGFP-positive cells on the ventricular surface of the cortical hem (Fig 3.4d, arrowheads), although not all proliferating cells in the hem are EGFP-positive.

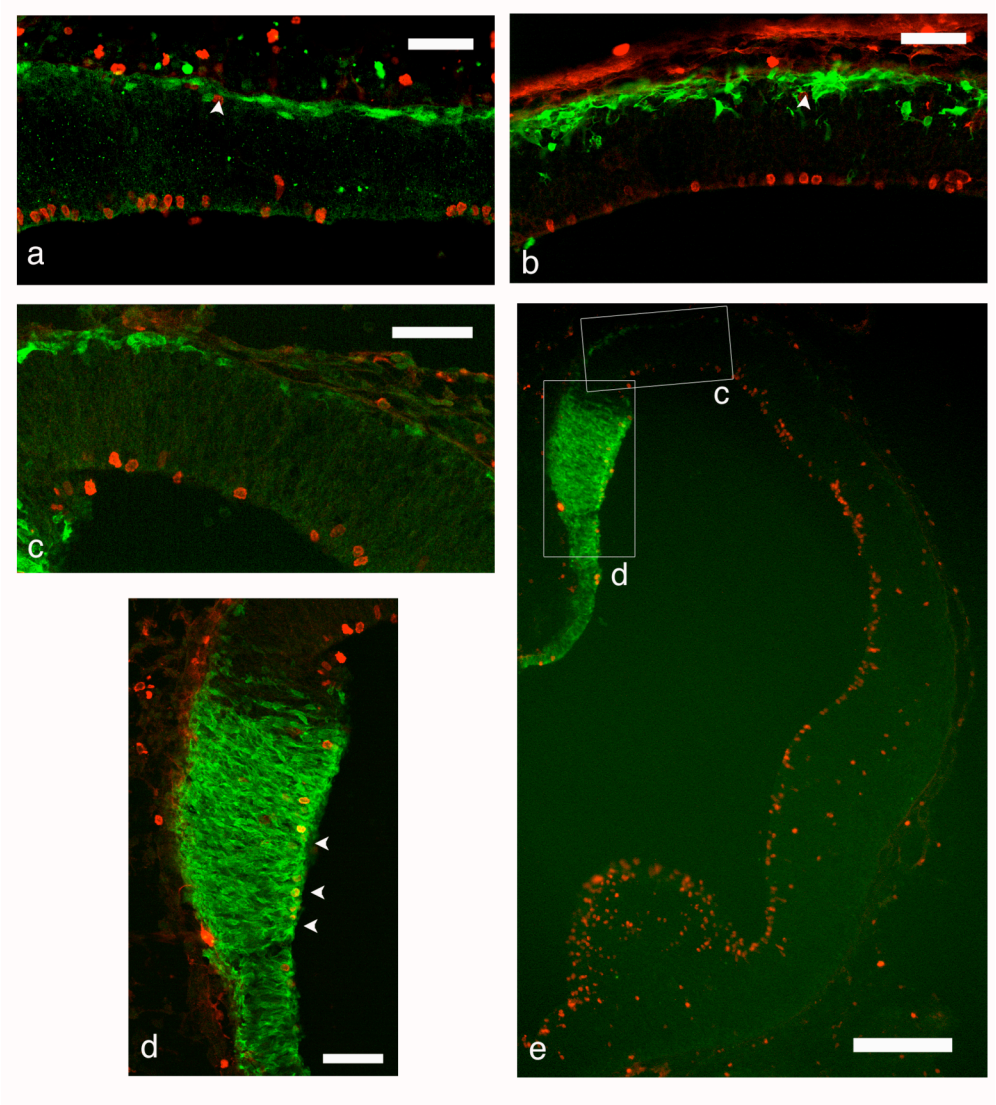

Figure 3.4. EGFP is expressed in post-mitotic preplate cells in all EGFP-BAC lines examined. Double immunofluorescent staining in E11 cryostat sections for EGFP (green) and phospho-histone H3 (red). Confocal images of Girk4-EGFP (a), Pde1C-EGFP (b), and Wnt3a-EGFP (c-d) show no colocalization of EGFP with the M phase marker phospho-histone H3 in preplate cells (a-c). Arrowheads in a, b indicate mitotic cells intermingled with preplate cells. Some Wnt3a-EGFP-positive cells in proliferative ventricular zone of the cortical hem express phospho-histone H3 (d, arrowheads). Epifluorescent image of Wnt3a-EGFP E11 cortex (e) shows the location of higher power images in (c) and (d). Scale bars: a-d = 50 μm, e = 200 μm.

However, no Wnt3a-EGFP-positive cells in the preplate coexpressed phospho-histone H3 (Fig 3.4c). Therefore, all of the lines studied appear to display EGFP-expression exclusively in post-mitotic preplate cell populations, and likely do not label an extra-ventricular source of cortical progenitors.

Gradients of newly-born preplate neurons identified with short-term BrdU birthdating. Because preplate cells are not actively proliferating at levels detectable by mitotic markers, neurons within the preplate must have undergone migration from a birthplace outside the preplate. To attempt to identify the birthplaces of preplate subpopulations, I performed short-term bromodeoxyuridine (BrdU) labeling and examined the distribution of recently-born neurons across the cortical anlage. BrdU was injected at E10.5, the peak of production of Cajal-Retzius neurons, embryos were collected 24 hours later, and the distribution of BrdU-labeled EGFP-positive preplate cells was examined. Distinct sites of origin should produce distinct distributions of BrdU-labeled cells in the developing cortex. If a preplate subpopulation is generated in a single focal site of origin (such as the cortical hem), newly-born cells should be found only adjacent to that site. If a subpopulation is generated in multiple focal sites, newly-born cells should be found adjacent to both sites. At E11, the developing cortex is small and intermingling between cells derived from distinct sites might also be expected. Finally, if a subpopulation is generated in the cortical ventricular zone, more newly-born cells should be found laterally and rostrally than dorsally and

caudally, following the gradient of neurogenesis described by Takahashi et al (1999).

Wnt3a-EGFP cells are born in the cortical hem. Short-term BrdU birthdating in the Wnt3a-EGFP line revealed a pattern of newly-born Wnt3a-EGFP-positive preplate neurons consistent with these cells being born in the cortical hem and migrating tangentially into the preplate layer. In E11.5 cortex, Wnt3a-EGFP cells strongly labeled with BrdU injected at E10.5 were found in and adjacent to the hem (Fig 3.5, filled arrowheads), while Wnt3a-EGFP cells further from the hem were BrdU-negative (Fig 3.5, open arrowheads).

Gradients of newly-born Girk4-EGFP Cajal-Retzius neurons in E11.5 cortex. I repeated the BrdU birthdating analysis for Girk4-EGFP-positive Cajal-Retzius population. Because Girk4-EGFP cells form a complete layer across the cortex at this stage, I analyzed the distribution of BrdU/Girk4-EGFP-positive and Girk4-EGFP-positive cells along both the dorsoventral and rostrocaudal axes. To examine the distribution of cells in the dorsoventral axis, cells were counted in four equal zones of the cortex between the hem and the PSB (Fig 3.6a). The number of EGFP+ and EGFP+/BrdU+ cells in each zone were counted, and the percentage of labeled cells in each zone of the total number of labeled cells in each section was calculated. Zone 1 was the most dorsal region, and zone 4 was

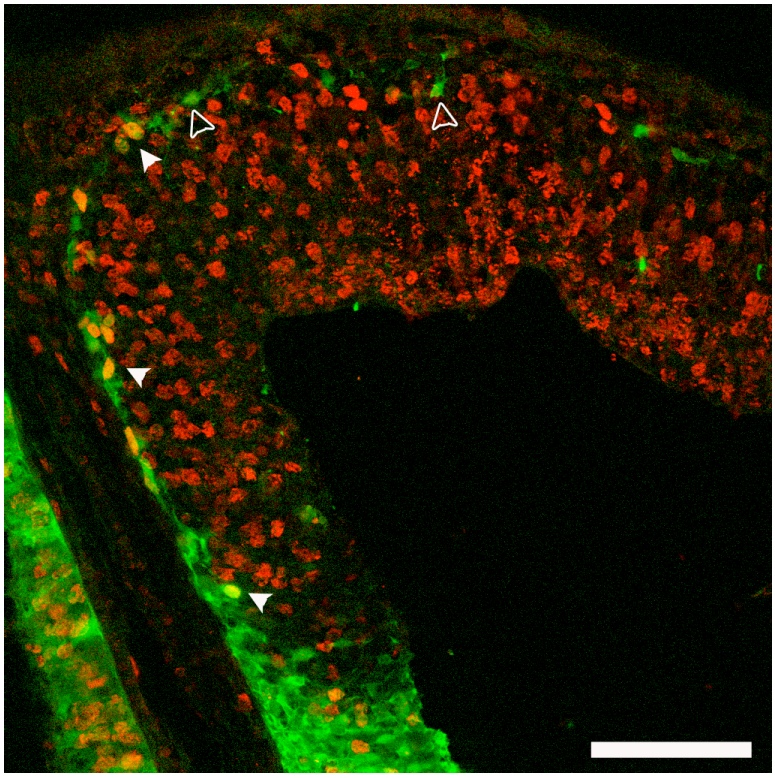

Figure 3.5. Short-term birthdating of Wnt3a-EGFP-positive Cajal-Retzius neurons. Coronal cryostat section of Wnt3a-EGFP E11.5 embryo, injected with BrdU at E10.5, was stained for EGFP (green) and BrdU (red). Wnt3a-EGFP-positive cells labeled with BrdU at E10.5 are located either in or just adjacent to the cortical hem (filled arrowheads). Cells further from the hem are negative for BrdU (open arrowheads), and presumably were born prior to injection. Scale bar = 100 μm.

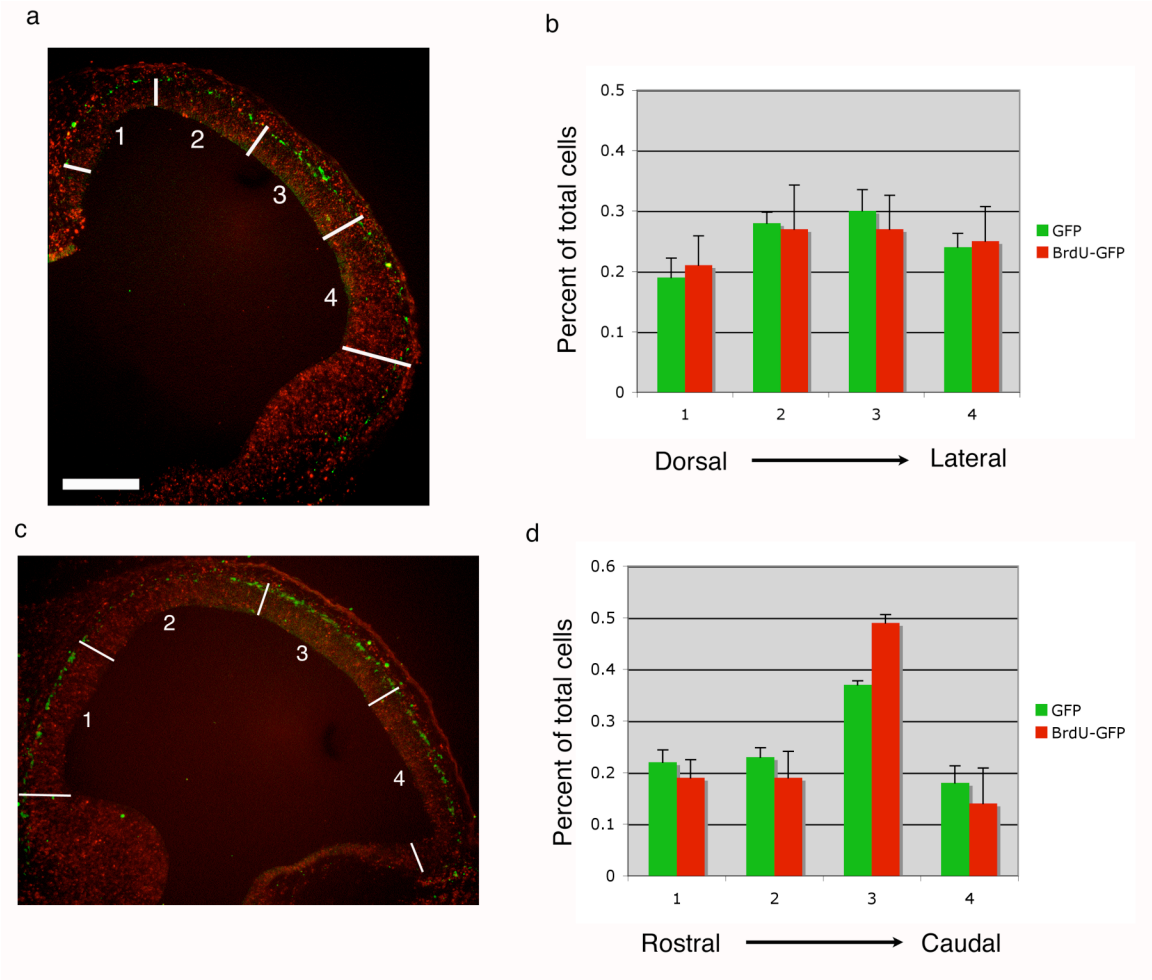

Figure 3.6. Girk4-EGFP cells born at E10.5 are evenly distributed across neocortex at E11.5. BrdU injections were given at E10.5 and embryos collected 24 hours later. Sections were immunostained for EGFP (green) and BrdU (red). For localization in the dorsoventral axis, coronal sections were divided into four equal bins between the cortical hem and the pallial-subpallial boundary (a). Bin 1 was most dorsal, bin 4 most lateral. BrdU/Girk4-EGFP-double positive cells follow a similar distribution across the cortex as total Girk4-EGFP-positive cells (b), revealing no gradient of cells born at E10.5. For localization in the rostrocaudal axis, sagittal sections were divided into four equal bins between the anterior pole of the telencephalon and the cortical hem (c). Bin 1 was most rostral, bin 4 most caudal. (d) Girk4-EGFP and BrdU/Girk4-EGFP-double positive cells are concentrated in bin 3, or slightly caudal cortex. Scale bar = 200 μm.

the most lateral. Two sections from each of four individual embryos were counted for the analysis. Only sections at the level of the developing ganglionic eminence were used, so that the PSB could be distinguished; thus, rostralmost and caudalmost sections were omitted from this analysis. Overall, 20% of Girk4-EGFP-positive cells were labeled with BrdU. In coronal sections, Girk4-EGFP-positive cells were distributed fairly evenly across the cortex, with slightly more cells in lateral regions than in dorsal (Fig 3.6b). The distribution of BrdU/EGFP double-positive cells followed this pattern very closely, and there was no distinct gradient of BrdU-labeled cells that would indicate either a single focal site of origin or the neurogenic gradient seen for cells derived from the ventricular zone. Therefore, these data suggest multiple focal sources of Girk4-EGFP-positive Cajal-Retzius neurons, likely to be located both dorsally and laterally.

To examine the distribution of cells in the rostrocaudal axis, sagittal sections of E11.5 embryos were analyzed in a similar manner. Sagittal sections (two per embryo, n=4 embryos total) were divided into four equal zones from the caudal cortical hem to the rostral-most point of the telencephalon (Fig 3.6c), and EGFP+ and EGFP+/BrdU+ cells were counted as for coronal sections (Fig 3.6d). Zone 1 was the most rostral, and zone 4 was the most caudal (Fig 3.6c). Sections from extremely medial and extremely lateral cortex were not used for this analysis. Similar numbers of EGFP+ and EGFP+/BrdU+ cells were found in zones 1-2 and 4, corresponding to the rostral half of the cortex and the caudalmost pole of the cortex, respectively. A significantly higher percentage of total EGFP+ and

EGFP+/BrdU+ cells was found in zone 3, or slightly caudal cortex, compared to the others. This gradient might correspond to cells derived from the PSB or cortical hem.

Gradients of newly-born Pde1C-EGFP preplate neurons. I carried out short-term birthdating of Pde1C-EGFP-positive preplate neurons precisely as described for Girk4-EGFP-positive cells. Approximately 15% of Pde1C-EGFP-positive cells in E11.5 cortex were labeled by BrdU injection at E10.5. Distribution of Pde1C-EGFP+ and EGFP+/BrdU+ cells across the dorsoventral axis showed a gradient of EGFP+ and BrdU/EGFP+ cells concentrated towards the lateral cortex (Fig 3.7a). More EGFP+ cells were found in zones 2-4 than in zone 1, the dorsalmost zone. Compared to the EGFP-single-positive cells, more BrdU/EGFP+ cells were found in zones 3 and 4, the most lateral zones, than in the dorsal zones 1 and 2. In the rostrocaudal axis, the distribution of cells in the Pde1C-EGFP cortex (Fig 3.7b) was similar to that seen in the Girk4-EGFP cortex (Fig 3.6d). Relatively few EGFP+ and BrdU+/EGFP+ cells were seen at the rostral-most and caudal-most regions (zones 1 and 4, respectively), and relatively more cells were seen in the central regions (zones 2 and 3), with the highest concentration in zone 3, as in the Girk4-EGFP cortex. Because of this similarity, it is probable that this observed gradient is due to Cajal-Retzius neurons, as in the Girk4-EGFP cortex, rather than future subplate neurons.

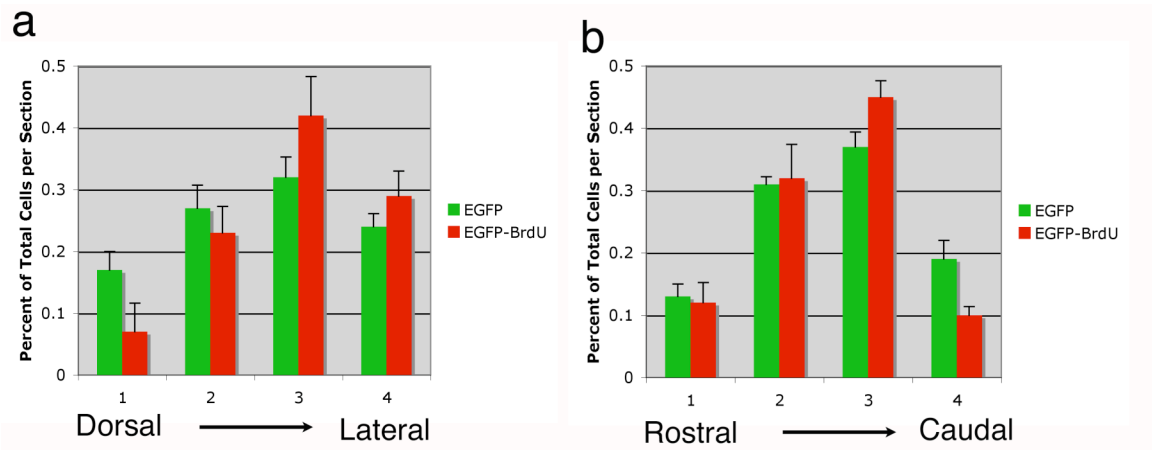

Figure 3.7. Distribution of Pde1C-EGFP cells born at E10.5. Quantification of 24-hour BrdU birthdating in Pde1C-EGFP embryos. BrdU was injected at E10.5 and embryos were collected at E11.5. (a) Distribution of Pde1C-EGFP-positive cells in the dorsoventral axis, labeled or unlabeled with BrdU. More EGFP and BrdU positive cells are found in lateral cortex compared to dorsal cortex. (b) Distribution of Pde1C-EGFP-positive cells in the rostrocaudal axis, labeled or unlabeled with BrdU. Fewer EGFP and BrdU-positive cells are found in rostral and caudal cortex than in the middle region.

In summary, these experiments showed that proliferating cells were not present in the preplate subpopulations. BrdU injected at E10.5 labeled EGFP-positive cells concentrated adjacent to the cortical hem in the Wnt3a-EGFP cortex, and live imaging of Wnt3a-EGFP cells revealed a dorsal-to-ventral tangential migratory pathway. In the Girk4-EGFP cortex, BrdU injected at E10.5 labeled cells evenly distributed across the dorsoventral axis of cortex, while in the rostrocaudal axis BrdU-labeled EGFP cells accumulated in somewhat caudal regions. Live imaging of Girk4-EGFP cells showed multiple migratory pathways, with cells migrating towards dorsal, ventral, rostral, and caudal. Both BrdU birthdating and imaging data obtained for Pde1C-EGFP cells were similar to those obtained for Girk4-EGFP cells.

Chapter 4

Gene array expression analysis of preplate subpopulations

Having characterized the subpopulations of preplate neurons represented by the Pde1C-EGFP, Girk4-EGFP and Wnt3a-EGFP BAC mouse lines, I went on to analyze gene expression in each subpopulation. In order to identify subpopulation-specific genes, purified cells from each line were used in a gene expression array analysis, and samples were directly compared to one another.

Purification and array analysis of EGFP-positive preplate neurons. To purify EGFP-positive cells from whole cortex, E12.5 cortices from each line were dissected away from subcortical regions, briefly digested with papain, and triturated to a single-cell suspension (Fig 4.1b). In the case of the Wnt3a-EGFP line, the cortical hem was also removed, in an attempt to separate the proliferating progenitors from differentiated preplate neurons. The cell suspension was presorted by size to remove debris and clumps of cells (Fig 4.1a). For sorting based on EGFP fluorescence, gates were set by sorting a cell suspension prepared from wild-type littermates as a EGFP-negative baseline (Fig 4.1c).

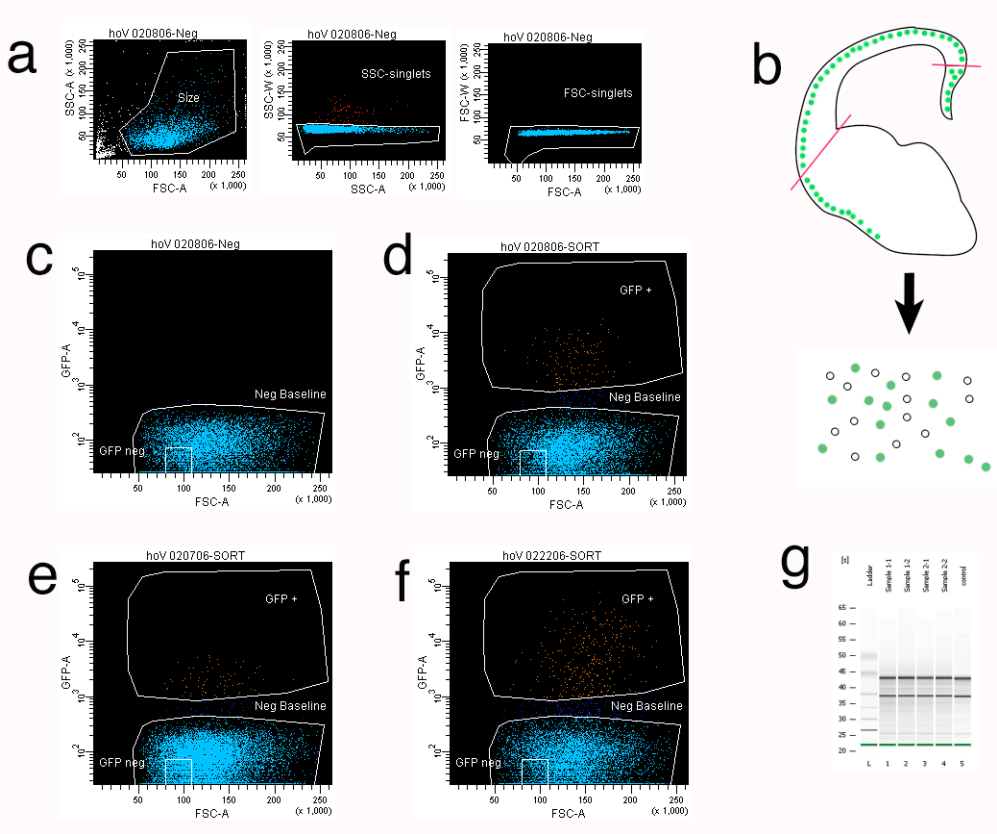

Figure 4.1. Schematic of purification of EGFP+ cells from E12 BAC transgenic embryos. Transgenic cortices from E12 embryos were dissected and a single-cell suspension prepared as shown in (b). Ventral forebrain and cortical hem were removed, and cortices were then triturated to form a cell suspension of mixed EGFP+ and EGFP- cells. Cells were sorted for size by forward and side scatter (example shown in panel a) to remove debris and clumps of multiple cells. Cells outside the boundary line are excluded from the sort. The lower gate for EGFP fluorescence was set by applying a cell suspension of EGFP-negative cells (panel c, EGFP fluorescence on y axis, forward scatter on x axis). Panels d-f show scatter plots of representative sorts from each line: Girk4-EGFP (d), Wnt3a-EGFP (e), and Pde1C-EGFP (f). EGFP+ gates are indicated. Total RNA was prepared from each sort, and RNA integrity was checked by analyzing with a Agilent 2100 Bioanalyzer PicoChip (g, ladder ranges from 6000 to 200 nt).

EGFP+ cells were collected based on these gates (sample scatter plots from each line are shown in Fig 4.1d-f) and total RNA was extracted from the purified populations (Fig 4.1g). In a successful purification, between 40,000-100,000 EGFP+ cells were obtained from each litter, depending on the line – a typical preparation of Wnt3a-EGFP cells yielded approximately 40,000 cells, while a typical preparation of Pde1C-EGFP cells could yield more than 100,000 cells. Labeled cRNA was produced from total RNA using the Affymetrix Two-Cycle amplification kit and used to probe Affymetrix Mouse 240A 2.0 gene arrays. These arrays contain 22,626 gene-specific probe sets. Some genes are represented by multiple probe sets, while some are represented by only one probe set. Each litter of embryos yielded enough RNA for one hybridization. Three replicates for each line were carried out, along with three replicates of control unpurified cortical cells.

Array data analysis and quality control. All analyses of array data were carried out using Genespring 7.3 (Agilent Technologies). Data for all samples were imported together into Genespring as CEL files and normalized by GC-RMA. To determine the quality and reproducibility of the data, several approaches were taken. First, hierarchical clustering in Genespring was used to construct a condition tree grouping related samples together (Fig 4.2a). Replicate experiments from each line clustered together on the condition tree, indicating that the biological replicates yielded highly related expression patterns. Second,

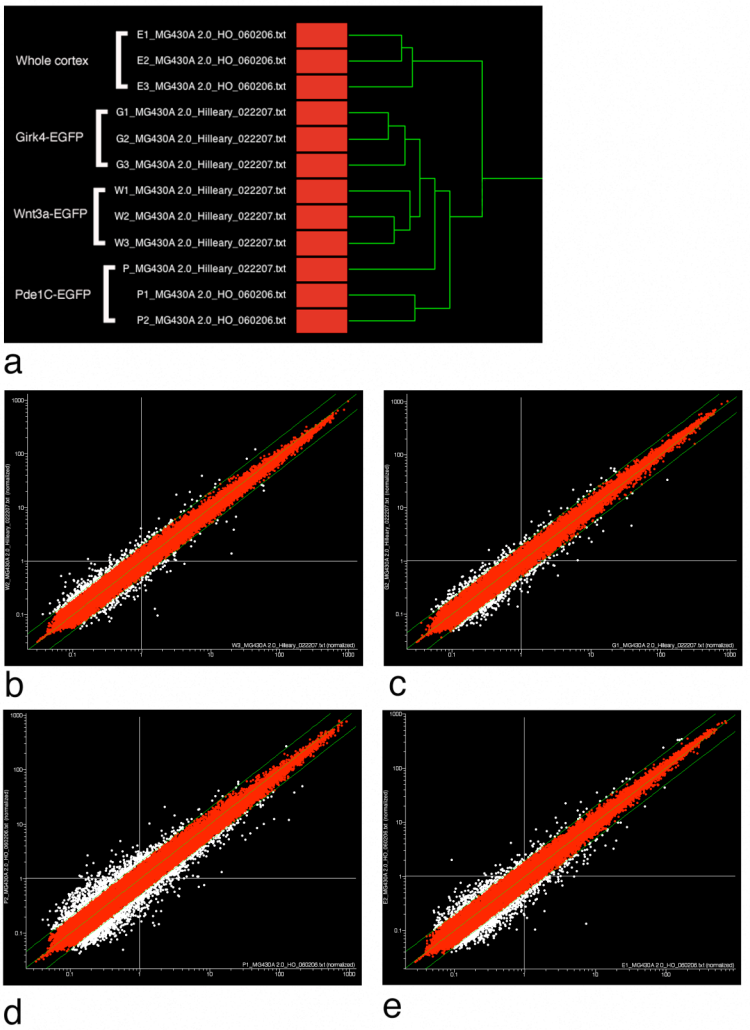

Figure 4.2. Reproducibility of gene array data from purified preplate populations. Box plot (a) showing the distribution of expression values for all samples used in the analysis. In (a), whole cortex replicates are in red, Girk4-EGFP replicates in yellow, Pde1C-EGFP replicates in aqua, and Wnt3a-EGFP replicates in dark blue. Scatter plots (b-e) of normalized expression values comparing replicate samples of each line. Axes are in log scale. Probe sets with greater than 2-fold difference in expression value between sample replicates are colored white, probe sets with less than 2-fold difference between replicates are colored red. Wnt3a-EGFP (b) and Girk4-EGFP (c) replicates have a tighter distribution than Pde1C-EGFP (c) or whole cortex (e) replicates.

correlation coefficients for pairwise comparisons of replicates were calculated. The average correlation coefficient for pairwise comparisons in each line was between 0.99 and 0.97, indicating a high degree of reproducibility between replicates. Finally, expression of individual probe sets in replicate samples were compared in scatter plots, and the number of probe sets increased or decreased 2-fold between replicates for each pairwise comparison was calculated (Fig 4.2b-e). Girk4-EGFP, Wnt3a-EGFP, and whole cortex samples had respectively, an average of 2.3%, 2.1%, and 4.7% probe sets with greater than 2-fold differences in expression between pairwise replicates. Replicates for Pde1C-EGFP had an average of 10% probe sets with greater than 2-fold differences in expression. As Pde1C-EGFP labels a mixed population population of neurons, this line may be more sensitive to slight differences in the age of embryos or the quality of the dissection, yielding slightly less reproducible results than the other lines.

Prior to further analysis, probe sets with low or unreliable expression values were identified for exclusion from the analysis. For each line, genes were included in the analysis only if they were flagged as present in two out of three replicates by the Affymetrix GeneChip Operating Software (GCOS), and if pooled normalized signal intensity was above an arbitrary cutoff of 1. These gene lists were considered to comprise lists of total genes expressed in each subpopulation.

Molecular characterization of Cajal-Retzius cell subpopulations by gene array expression analysis. Probe sets were identified that were greater than 2-fold enriched in each Cajal-Retzius cell transgenic line, as compared to unpurified cortical cells (Fig 4.3a,b). 2305 probe sets were upregulated in Girk4-EGFP cells compared to whole cortex (Fig 4.3b), and 2115 probe sets were upregulated in Wnt3a-EGFP cells compared to whole cortex (Fig 4.3a). I verified that these lists contained genes enriched in the preplate/marginal zone by examining their expression patterns in the Genepaint database of *in situ* hybridizations in E14.5 embryos (www.genepaint.org). 40 genes from each list were randomly selected and scored blind for expression in preplate/marginal zone at E14.5 alongside a random selection of genes from the total list of features present on the array. From the Girk4-EGFP list, 86% of a random selection of genes were found to be present in the preplate or marginal zone. Similarly, 83% of genes selected from the Wnt3a-EGFP list were present in preplate or marginal zone. Both were significantly different from the 38% of random genes from the full array displaying a similar expression pattern. This indicated that array data from each line largely picked up genes expressed in preplate/marginal zone, and that the array data were valid and verifiable.

To determine whether the Cajal-Retzius cell subpopulations represented by the Girk4-EGFP and Wnt3a-EGFP BAC lines were heterogenous with respect to gene expression, fold-change analysis was carried out to find probe sets upregulated in one population of Cajal-Retzius neurons versus the other.

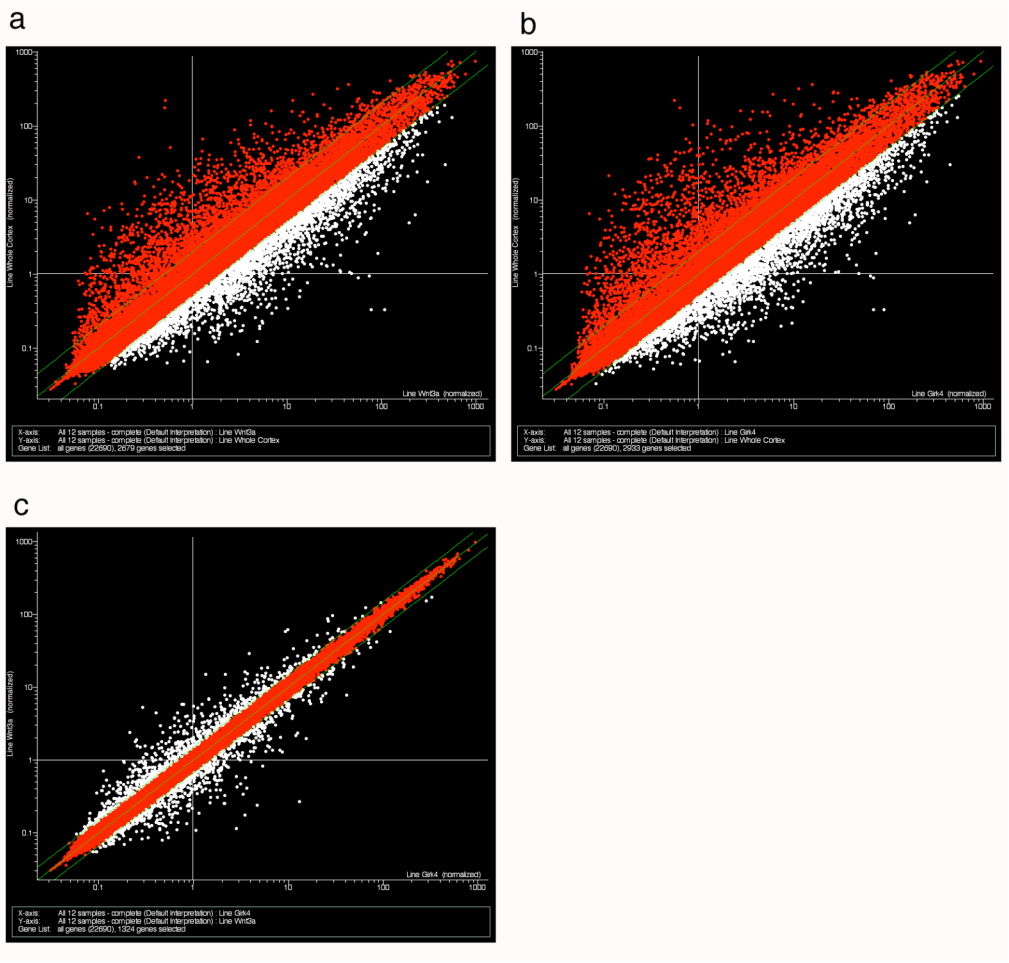

Figure 4.3. Genes upregulated in specific subpopulations of Cajal-Retzius cells. (a,b) Scatter plot of normalized expression values comparing the average expression levels of probe sets in Wnt3a-EGFP-positive cells (a, x axis) and Girk4-EGFP-positive cells (b, x axis) compared to unpurified cortical cells (y axis). Probe sets upregulated more than 2-fold in purified cells compared to unpurified cells are colored white; all other probe sets are colored red. (c) Scatter plot of normalized expression values comparing average expression of probe sets in Girk4-EGFP-positive cells (x axis) compared to Wnt3a-EGFP-positive cells (y axis). Probe sets upregulated more than 1.5-fold in either line are colored white; all other probe sets are colored red. All axes are in log scale, and all probe sets present on the array are represented in scatter plots.

Expression levels were compared between Girk4-EGFP-positive cells and Wnt3a-EGFP-positive cells, and probe sets that were 1.5-fold upregulated in one line versus the other were selected (Fig 4.3c). Probe sets that were not significantly different between lines by t-test ($p>0.05$) were excluded. To identify probe sets upregulated in Girk4-EGFP cells, only probe sets considered expressed in Girk4-EGFP cells as described above were used in the analysis, and likewise for probe sets upregulated in Wnt3a-EGFP cells. For the final step, expression was compared to the control whole cortex samples, in order to identify only probe sets that were specific to Cajal-Retzius neurons – only probe sets expressed greater than 2-fold higher in purified cells compared to unpurified cortex were included. By these criteria, 96 features were specifically upregulated in Girk4-EGFP-positive cells compared to both Wnt3a-EGFP-positive cells and unsorted whole cortex (Appendix, Table 1), and 24 genes were specifically upregulated in Wnt3a-EGFP-positive cells compared to both Girk4-EGFP-positive cells and whole cortex (Appendix, Table 2).

The list of 24 Wnt3a-EGFP-specific genes contained genes known to be expressed in the cortical hem (Dkk3, Wnt3a) but not in the preplate (Grove, Tole et al. 1998; Diep, Hoen et al. 2004). This raised the possibility that the Wnt3a-EGFP samples were contaminated with cortical hem cells due to imperfect dissection, and that the differences between subpopulations were attributable to this contamination. To address this possibility, a list of features upregulated in Wnt3a-EGFP cells versus Girk4-EGFP cells but not versus whole cortex (400

features) was analyzed by functional clustering using the DAVID tool. Genes involved in cell cycle control and cell division and genes upregulated during mitosis were found to be overrepresented ($p=5.6x10^{-29}$). These genes are characteristic of a proliferative zone, and not of post-mitotic neurons. To examine the expression pattern of these genes, a random selection of 40 genes from this list was checked in the Genepaint database for expression at E14.5. Unsurprisingly, 79% of genes from this list present in the database were found to be expressed in the ventricular zone or cortical hem. These data probably indicate contamination of the Wnt3a-EGFP purified cells with Wnt3a-EGFP-positive cortical hem cells, which was due to imperfect dissection. Because the datasets were largely similar, with relatively few genes differentially regulated, this contamination was probably not large but seems to account for the majority of the differences seen between the two populations.

However, based on the expression analysis of genes upregulated in each line compared to whole cortex, it seems likely that the data are valid, and the low number of subpopulation-specific genes identified and the lack of enrichment in preplate of the Wnt3a-EGFP-specific genes are due to an overwhelming similarity between samples, with relatively few genes differentially regulated.

***In situ* hybridization validation of subpopulation-specific gene lists.** A selection of genes from the final subpopulation-specific lists were subjected to *in situ* hybridization to determine the validity of the lists. Based on the expression

patterns of the EGFP transgenes in each line (see Fig 2.10), I expected that genes upregulated in Girk4-EGFP-positive cells should be expressed specifically in the preplate of lateral cortex at E11-12, while genes upregulated in Wnt3a-EGFP-positive preplate cells should be expressed in the dorsomedial preplate, adjacent to the hem. For the genes from the Wnt3a-EGFP list, known hem-specific genes were excluded from the *in situ* analysis, and 8 genes were selected for *in situ* hybridization.

Of the 8 genes tested, 3 were specifically expressed in the cortical hem at E11-12: Sulf2, Rspo2, and Cacna1g (Fig 4.4a-c). The remaining genes showed either no signal in the CNS or were expressed throughout neural tissues, with no specific localization. Although expression in the cortical hem of all three genes was robust, no expression was detected in postmitotic neurons in the hem-adjacent preplate. Thus, the Wnt3a-EGFP-specific list is biased towards genes enriched in cortical hem cells, and either did not identify genes expressed in post-mitotic dorsal preplate neurons, or these genes are expressed in post-mitotic cells at levels too low to detect by *in situ* hybridization.

11 genes were selected for in situ hybridization analysis from the 96 found to be specifically upregulated in Girk4-EGFP-positive cells. Of the 12 genes tested, three were expressed in the lateral preplate at E11-12, but were not expressed in the more dorsal preplate: Rabgap1l, alpha-synuclein, and synaptotagmin 4. The Girk4-specific list, therefore, does seem to be biased towards genes specifically expressed in a subset of Cajal-Retzius neurons

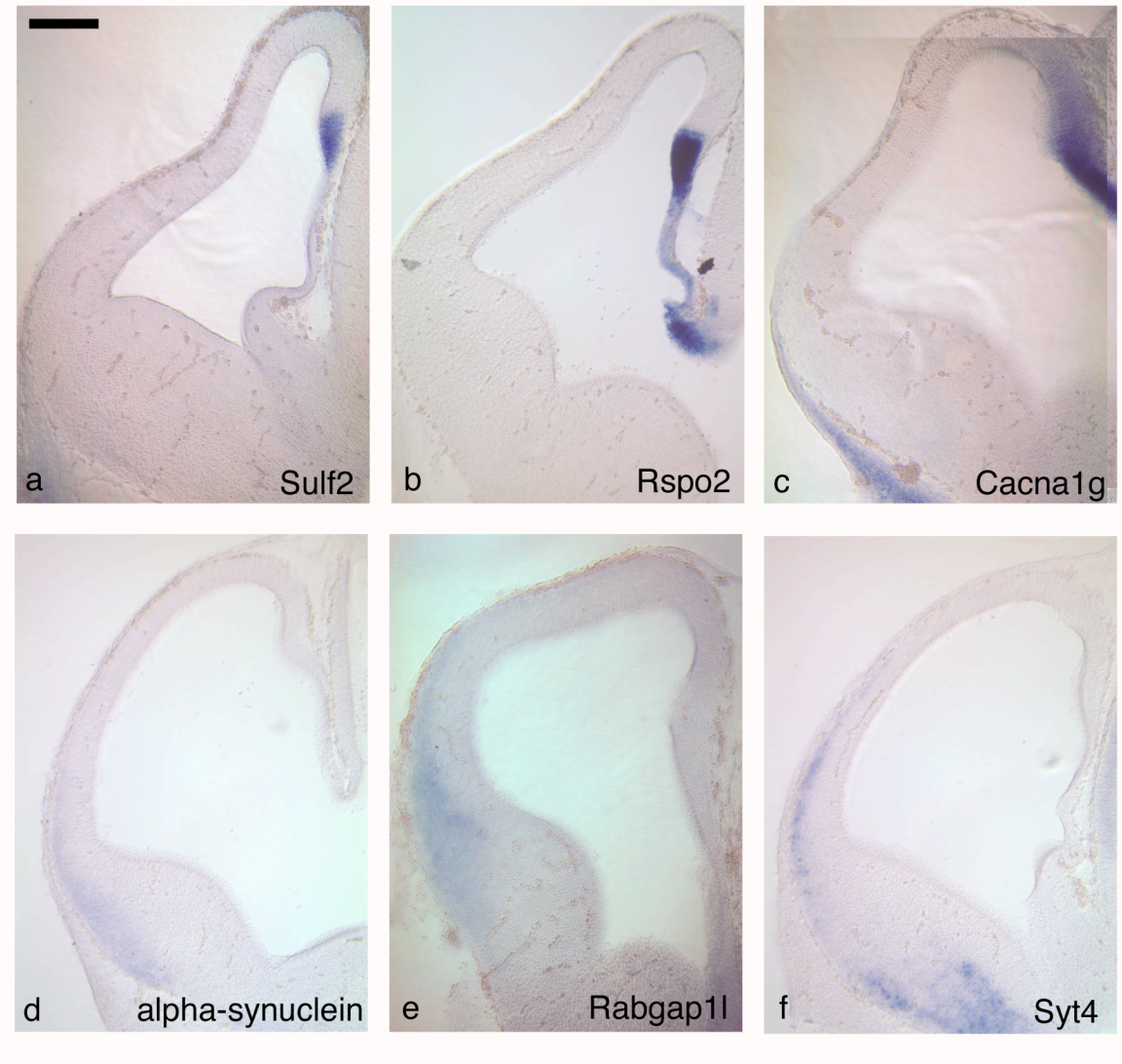

Figure 4.4. Expression in the cortical hem and lateral preplate of genes identified as upregulated in subpopulations of Cajal-Retzius neurons. *In situ* hybridization in E12 coronal sections for genes identified as Wnt3a-EGFP-subpopulation specific (a, Sulf2; b, Rspo2; c, Cacna1g) or Girk4-EGFP-subpopulation specific (d, alpha-synuclein; e, Rabgap1l; f, Syt4). Wnt3a-EGFP-specific genes were expressed in the cortical hem (lateral expression in (c) is localized to skin), while Girk4-EGFP-specific genes were expressed in the lateral preplate. Scale bar = 200 μm.

distinct from the hem-derived population. Functional analysis of this list using the DAVID tool revealed enrichment in protein kinases ($p=1.7x^{10-}11$) including several receptor tyrosine kinases (EphA3, EphA7) and CAM kinases (Camk1, Camk2b, Dcamkl1), and in ion transporters ($p=1.1x10^{-6}$).

Genes enriched in future subplate neurons To generate a list of genes specifically expressed in future subplate neurons, I compared purified Pde1C-EGFP-positive E12 cortical neurons, representing a mixture of both types of preplate neurons, Cajal-Retzius cells and future subplate neurons, to purified Girk4-EGFP-positive E12 neurons, which represent only Cajal-Retzius cells. Genes upregulated in the Pde1C-EGFP-positive population compared to the Girk4-EGFP-positive population have a high likelihood of being expressed in future subplate cells. Because of the possibility of contamination of the Wnt3a-EGFP-positive sample with proliferating cortical hem progenitors, these samples were excluded from this analysis.

The analysis was performed using the complete dataset of all three lines plus whole cortex controls, normalized as described above. Only probe sets considered reliably expressed in Pde1C-EGFP-positive cells as described above were included in the analysis. Probe sets were identified that were enriched by 1.5-fold in Pde1C-EGFP cells versus Girk4-EGFP-positive Cajal-Retzius neurons, and only probe sets with p-values below 0.05 by t-test between samples were included. 229 probe sets met these criteria (Appendix, Table 3).

To validate the subplate-specific list, two approaches were taken. First, a random selection of 40 genes from the subplate-specific list were checked in the Genepaint in situ database for expression in preplate/subplate at E14.5. Genes from the future subplate list were scored blind alongside an equal number of genes randomly selected from the complete array. 59% of genes from the future subplate list were present in preplate/subplate at E14.5, which was significantly different from the random list (28% present in preplate/subplate) by chi-square test ($p<0.05$). The resolution of the in situ images at this early stage, however, did not allow me to determine whether candidate genes were specific for subplate, or were also expressed in Cajal-Retzius marginal zone neurons. To address this issue, I carried out immunohistochemistry for a selection of genes from the subplate list, co-staining with reelin, the Cajal-Retzius cell marker. I also examined several BAC transgenics from GENSAT for genes on the subplate list, co-staining for reelin and EGFP.

Double immunofluorescence antibody staining in wildtype cortex for the candidate marker proteins hippocalcin (Hpca), EAAC1, and Ryr1 along with reelin showed that all three genes were expressed in reelin-negative preplate neurons at E12 (Fig 4.5a,c,e). The reelin-negative cells are located directly beneath the reelin-positive layer, with little intermingling. Reelin-negative cells positive for these markersdo not consistently display the horizontal orientation of reelin-expressing cells. Hpca and EAAC1 were localized in the cytoplasm of reelin-negative cells, while Ryr1 seemed to localize to membranous structures

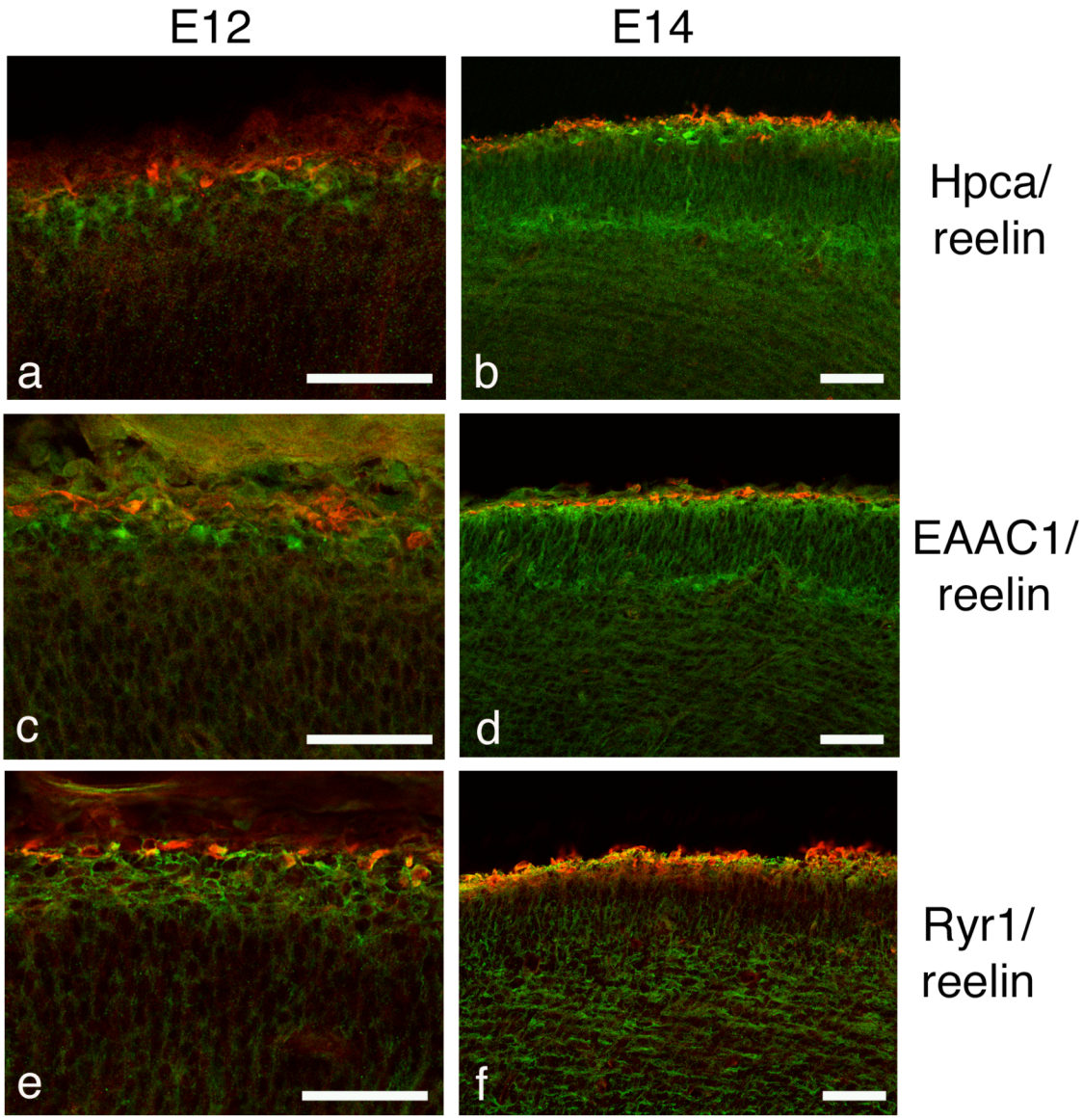

Figure 4.5. Future subplate genes are expressed in reelin-negative preplate and subplate. Double immunofluorescent staining for reelin (red) and future subplate candidate genes (green) in cryostat sections of wildtype E12 (a,c,e) and E14 (b,d,f) brains. Hpca (a,b, green), EAAC1 (c,d, green), and Ryr1 (e,f, green) are all expressed in reelin-negative preplate cells (a,c,e) and in subplate cell bodies (b,d) or subplate fibers (f). Scale bars = 50 μm.

and neurites. At E12, some reelin-positive neurons co-expressed Ryr1. At E14, after preplate splitting, expression of all three proteins was maintained in subplate neurons (Fig 4.5b, d, f). Hpca (FigIb) and EAAC1 (FigId) were expressed in subplate cell bodies, while Ryr1 (Fig 4.5f) localized in projections below subplate cell body layer. The expression of these markers at E14 also reveals the localization of future subplate cells during preplate splitting – some reelin-negative preplate cells remain adjacent to the Cajal-Retzius cell layer at this early stage of cortical plate formation, while others descend into the subplate layer. This suggests that the descent of subplate cells to their destination beneath the cortical plate does not occur all at once, but rather occurs progressively during cortical plate formation. Examination of BAC-EGFP transgenic lines for candidate genes selected from the future subplate list also showed expression in reelin-negative preplate and subplate (Fig 4.6). Sez6-EGFP is expressed in reelin-negative preplate at E12 (Fig 4.6a), as well as subplate and cortical plate at E14 (Fig 4.6b). At E14, strong expression is seen in axonal projections in the intermediate zone. While some colocalization with reelin was seen at E12, by E14 EGFP expression was completely absent from reelin-positive cells.

Taken together, these data show that candidate genes from the future subplate list generated from a screen carried out at E12 are indeed expressed in the future subplate subpopulation of preplate, as well as the subplate layer after preplate splitting. While the list is likely biased towards subplate-specific genes,

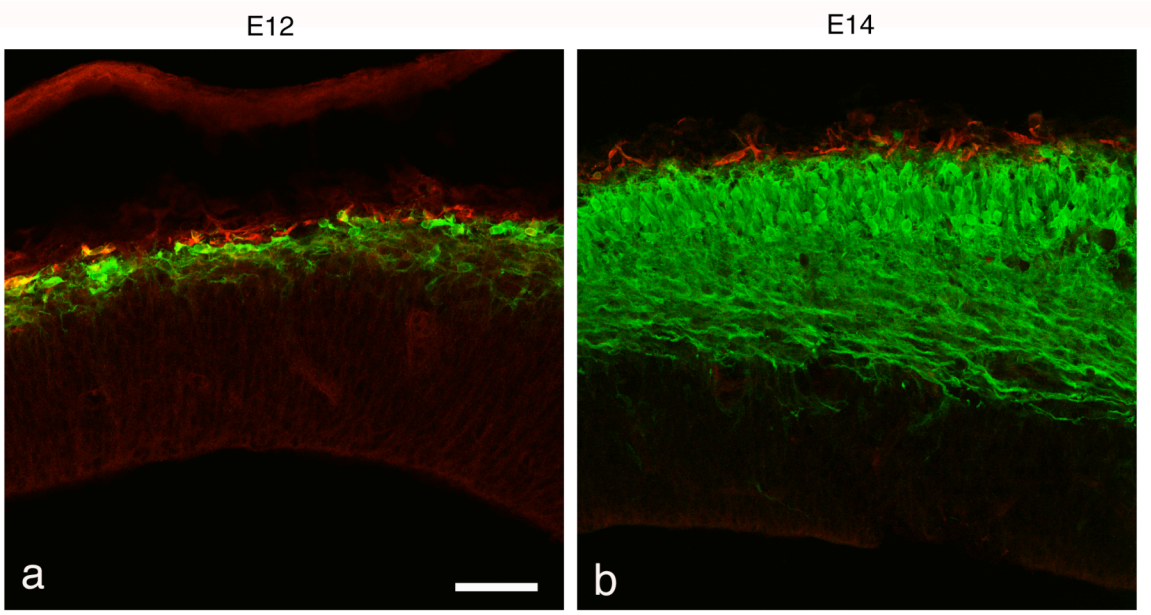

Figure 4.6. Sez6-EGFP is expressed in reelin-negative preplate, subplate, and cortical plate. Double immunofluorescent staining for reelin (red) and EGFP (green) in Sez6-EGFP transgenic E12 (a) and E14 (b) cortex. Sez6-EGFP expression at E12 is largely excluded from reelin-positive cells, and EGFP-positive cells are localized in the preplate. By E14, Sez6-EGFP is entirely excluded from the reelin-poisitive cells and is highly expressed in neurons of the cortical plate, as well as early cortical projections in the intermediate zone. Scale bar = 50 μm.

some genes on the list (like Ryr1) are also expressed in reelin-positive cells, and thus are pan-preplate genes. Some genes on this list, like Sez6-EGFP, are likely to also be expressed in cortical plate neurons, which are probably derived from common progenitors to subplate cells.

To identify functionally related groups of genes overrepresented in the future subplate gene list, I analyzed the list using the DAVID tool for functional classifications (Hosack, Dennis et al. 2003). The four most highly enriched categories were for genes involved in cell adhesion and axonogenesis (8 genes, $p=9.3x10^{-8}$), genes involved in exocytosis and the formation of coated vesicles (5 genes, $p=1.8x10^{-8}$), transcription factors (32 genes, $p=3.1x10^{-24}$), and genes involved in steroid biosynthesis, metabolism, and signaling (4 genes, $p=1.1x10^{-4}$). Additionally, analysis of the list with the Ingenuity Pathways Analysis software (Ingenuity Systems) revealed a network of subplate-specific genes regulated by beta-estradiol (estrogen) signaling (Fig 4.7). Together with the enrichment of genes related in steroid biosynthesis and signaling, this implies a role for estrogen signaling in the development of subplate neurons.

In summary, I attempted to identify genes specifically expressed by subpopulations of Cajal-Retzius neurons by comparing expression levels between Girk4-EGFP-positive neurons and Wnt3a-EGFP neurons. Relatively few genes were found to be differentially regulated between these populations, and

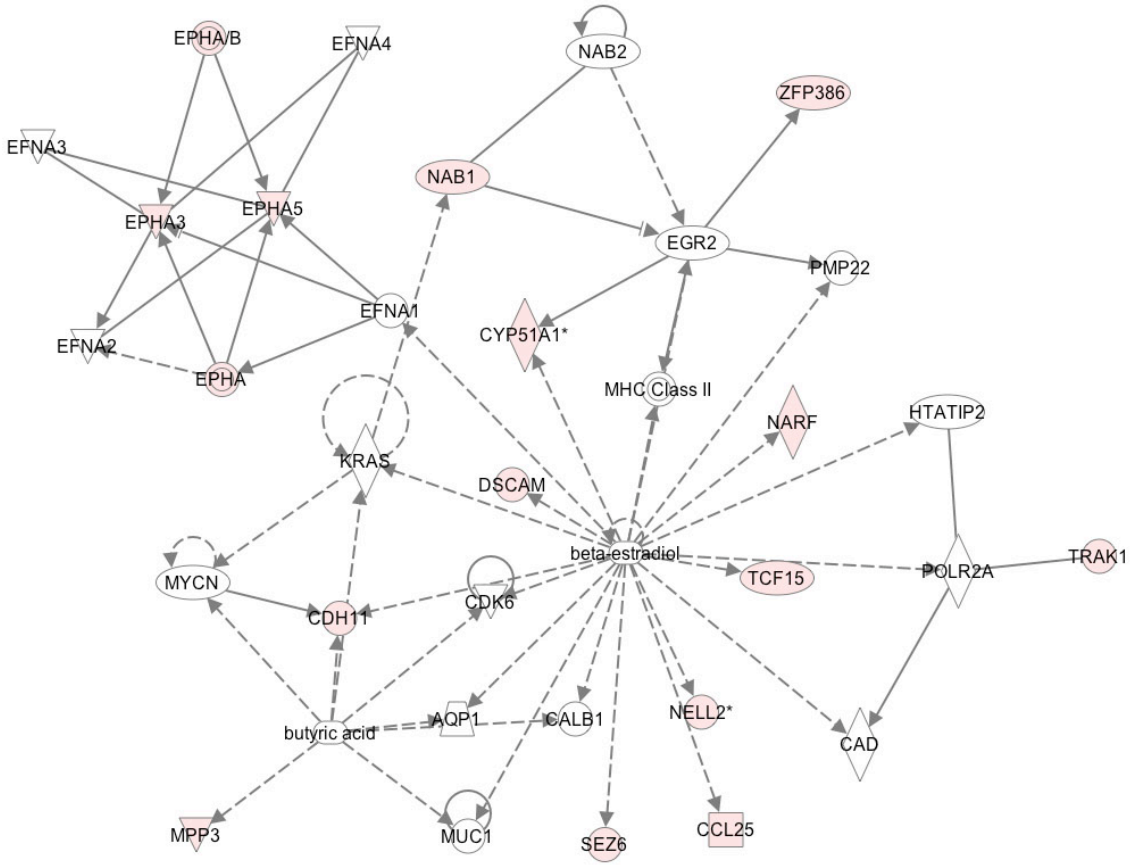

Figure 4.7. Pathway analysis of subplate-specific gene list reveals a network of genes regulated by beta-estradiol (estrogen) signaling. Gene network produced by Ingenuity Pathways Analysis shows multiple genes involved in axonogenesis are regulated by beta-estradiol. Genes colored pink were present on the subplate-specific list; other genes in the network are not specific to subplate.

the Wnt3a-EGFP sample was likely contaminated by proliferating hem cells. Several genes from the list of 96 found to be upregulated in Girk4-EGFP neurons were expressed in lateral but not dorsal preplate by *in situ* hybridization, suggesting that they do represent subpopulation-specific expression. As well, I identified 229 genes specifically expressed in the future subplate preplate population. This gene list was verified by both database searches, immunostaining, and BAC transgenic lines to be expressed in reelin-negative preplate and, after preplate splitting, in subplate.

Chapter 5

Candidate transcription factors in subplate specification

The gene list generated for subplate-specific genes included a number of transcription factors, which are candidate genes for involvement in subplate neuron specification and differentiation. As discussed in the previous chapter, several of these transcription factors have previously been shown to be involved in subplate specification or function. I selected two transcription factors from this list, Fog2 and Id2, for further study of their roles in preplate and subplate development. As knockout lines were available for both of these mice, I examined preplate differentiation, preplate splitting, and the formation of corticofugal projections in mice null for both transcription factors.

Fog2. Fog2 is generally thought to act as a transcriptional corepressor to function in the regulation of cell differentiation and organ morphogenesis. Although much is understood concerning the role of Fog2 in the development of the heart (Tevosian, Deconinck et al. 2000), lung, and diaphragm (Ackerman, Herron et al. 2005), and its biochemical partners and effects upon transcription in these tissues are becoming more well understood, its role in the nervous system has not been studied.

Fog2 acts as a transcriptional corepressor with proteins in the Gata family of transcription factors (Tevosian, Deconinck et al. 1999), and this interaction is required for many of the effects reported in Fog2-null animals (Crispino, Lodish et al. 2001). Fog2 has also been shown to interact with members of the COUP-TF family of nuclear receptors/transcription factors (Huggins, Bacani et al. 2001). COUP-TFI and COUP-TFII have been implicated in the differentiation and specification of preplate neurons (Zhou, Qiu et al. 1999; Studer, Filosa et al. 2005). Analyses of COUP-TFI null brains have shown that COUP-TFI has broad-ranging effects on cell cycle exit, telencephalic patterning, neuronal subtype specification (Faedo, Tomassy et al. 2007), and, importantly, is required for the proper formation of corticothalamic and commissural projections in forebrain(Zhou, Qiu et al. 1999; Armentano, Filosa et al. 2006). Because of its interactions with these important transcriptional regulators in early forebrain, I selected Fog2 as a candidate for involvement in subplate neuron specification and differentiation.

Fog2 is expressed in Pde1C-EGFP-positive neurons and is specific to the subplate. To confirm the results of the gene array data, I first performed qPCR for Fog2 mRNA on RNA from purified Pde1C-EGFP+ cells from E12 cortex. RNA was extracted and amplified as described in Chapter 1, and relative levels of Fog2 mRNA were compared between purified cells and whole, unpurified cortex.

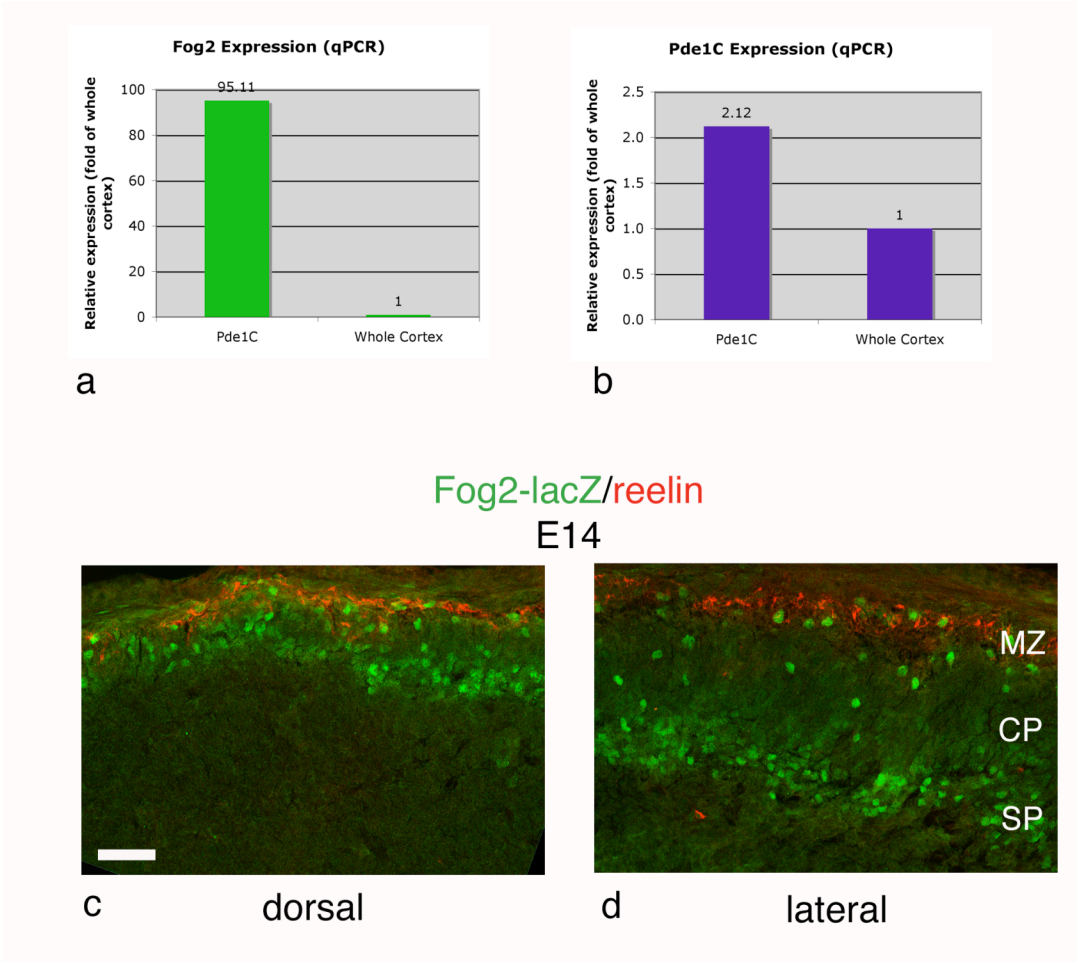

Figure 5.1. Fog2 is enriched in Pde1C-EGFP+ cortical cells, and is expressed in subplate. (a) Realtime quantitative PCR for Fog2 mRNA in FACS-purified E12 Pde1C-EGFP+ cells compared to whole cortex. Relative expression was calculated based on GAPDH expression as an internal control, and standardized to expression levels in unpurified, age-matched cortex. (b) Realtime quantitative PCR for Pde1C mRNA in FACS-purified E12 Pde1C-EGFP+ cells compared to whole cortex, standardized to whole cortex. As expected, Pde1C mRNA is expressed at relatively higher levels in purified cells. (c,d) Immunostaining for beta-galactosidase (green) and reelin (red) in cryostat sections of E14 Fog2-lacZ transgenic dorsal (c) and lateral (d) cortex. Fog2-lacZ is not expressed in reelin-positive Cajal-Retzius neurons, but is expressed in preplate/subplate, as identified by cell position during cortical plate formation. Scale bar = 50 μm

Pde1C-EGFP+ cells expressed nearly 100-fold more Fog2 mRNA than whole cortex (Fig 5.1a). As a control, I also performed qPCR on the same samples for Pde1C mRNA, which, as expected, was also upregulated in purified cells compared to whole cortex (Fig 5.1b).

The expression of a Fog2-lacZ transgene in E14 brains (embryos gift of S. Tevosian, Dartmouth) was examined by fluorescent immunostaining for beta-galactosidase and reelin (Fig 5.1c-d). No colocalization of Fog2-lacZ and reelin was seen in either dorsal (Fig 5.1c) or lateral (Fig 5.1d) cortex. The distribution of Fog2-lacZ-positive cells matched that of subplate neurons: in dorsal cortex, Fog2-lacZ-positive cells were intermingled with and just deep to the superficial layer of reelin-positive cells (Fig 5.1c), whereas in lateral cortex, Fog2-lacZ-positive cells have detached from the preplate layer and occupy a deeper layer, separated from the reelin-positive marginal zone neurons by the developing cortical plate (Fig 5.1d). Taken together, these data show that Fog2 is expressed in Pde1C-EGFP-positive neurons at E12, which are most likely destined for the subplate, and that Fog2 is specifically expressed in subplate neurons during cortical plate development.

Early preplate differentiation occurs normally in Fog2-null embryos. To test the hypothesis that Fog2 is involved in the differentiation and specification of preplate neurons, I examined the expression of preplate markers in the brains of Fog2-null E13 embryos. Knocking out Fog2 results in embryonic lethality

between E12 and E15 (Tevosian, Deconinck et al. 2000), and therefore subplate-relevant processes which occur later in development, such as thalamocortical axon targeting, could not be examined in these animals. However, aspects of subplate neuron development such as marker gene expression and early axon extension could be examined in E13 embryos.

To examine initial differentiation of preplate neurons, I carried out double immunofluorescent staining for the preplate markers reelin and hippocalcin (Hpca). Reelin is the Cajal-Retzius neuron marker, and Hpca specifically marks future subplate neurons at E12-14 (Fig 4.5a,b). In the wildtype brain, there is little colocalization between these markers (Fig 4.5a,b; Fig 5.2a,c), and cells expressing these markers segregate into distinct layers of the preplate, with reelin-positive cells located in a thin subpial layer and Hpca-positive cells in a thicker layer just beneath the reelin-positive cells. These expression patterns are maintained in the Fog2-null brain (Fig 5.2b,d), indicating that preplate neurons are generated and differentiate properly, and the organization of the preplate is maintained in the absence of Fog2. Both dorsal cortex (Fig 5.2a,c) and more lateral cortex (Fig 5.2b,d) were examined. Following the neurogenic gradient (Takahashi, Goto et al. 1999), the wildtype Hpca-positive future subplate layer is thicker in lateral cortex than in dorsal cortex, and this pattern was maintained in the Fog2-null brain.

I quantified the number of total differentiated neurons and the proportions of Cajal-Retzius and subplate neurons present in Fog2-null cortex. To determine

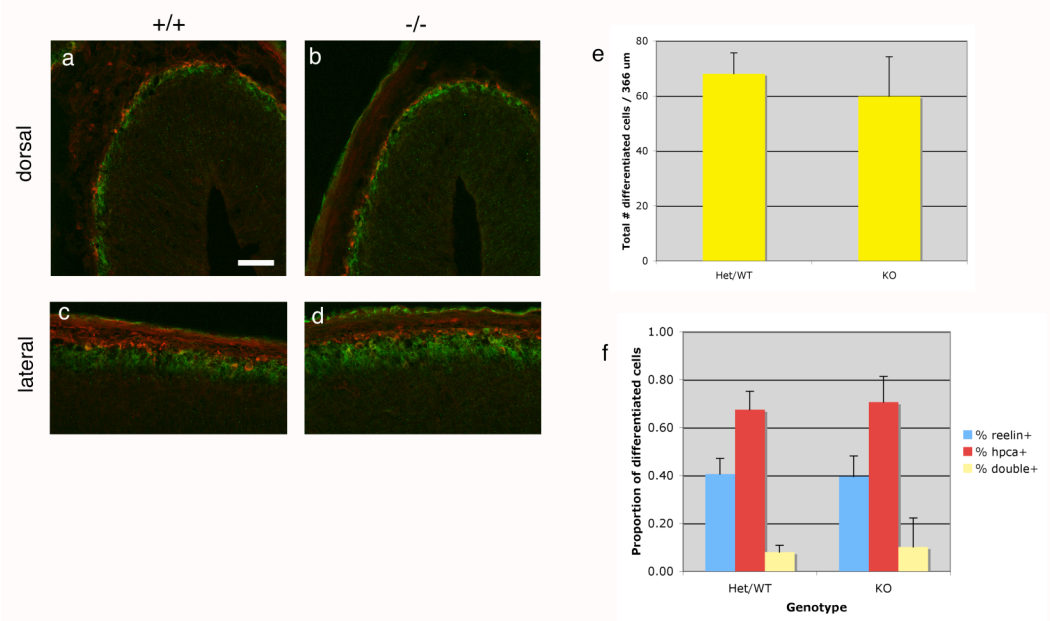

Figure 5.2. Early differentiation of preplate neurons proceeds normally in Fog2-null cortex. a-d) Immunostaining for reelin (red) and hippocalcin (Hpca, green) in E13 Fog2-null cortex (b,d) and wildtype littermate control (a,c). Both Cajal-Retzius neurons (reelin-expressing) and future subplate neurons (Hpca-expressing) are present in null brain, and cells are positioned normally in both dorsal (a,b) and lateral (c,d) cortex. (e) Quantitation of total numbers of differentiated cells in Fog2 null and wildtype brains. Numbers of reelin-positive, Hpca-positive, and double-positive cells were counted in 366 μm fields, and the total number of cells present was considered the number of differentiated neurons per field. Total numbers of differentiated neurons were not significantly different between wildtype/heterozygote and null brains ($p=0.26$ by t-test). (f) Quantitation of the proportion of reelin-, hpca-, and double-positive cells of total differentiated cells. No significant difference in the percentages of reelin ($p=0.82$), Hpca ($p=0.56$), and double-positive ($p=0.70$) cells were seen between genotypes.

the numbers of total differentiated neurons, I counted reelin-positive, Hpca-positive, and double-positive neurons in fields of 366 μm^2 from two sections per embryo (two embryos per genotype per two litters, for 8 total embryos). The total number of cells expressing either marker was considered the total number of differentiated cells. No significant difference was seen in numbers of differentiated cells between Fog2-null and wildtype embryos ($p= 0.26$ by t-test, Fig 5.2e). As well, the proportions of specific preplate subpopulations of total differentiated neurons were not significantly different between genotypes (Fig 5.2f). Of total differentiated neurons, approximately 10% coexpressed both markers in both lines ($p=0.70$ by t-test), 40% expressed reelin ($p=0.82$), and 70% expressed Hpca ($p=0.56$). Based on these data, I conclude that loss of Fog2 does not affect the early expression of preplate differentiation markers, nor does it affect the organization of the preplate before cortical plate formation.

Preplate splitting initiates normally in Fog2-null embryos. To determine whether loss of Fog2 affects the preplate splitting, cortical plate formation was visualized by immunostaining for the subplate marker Hpca and the axonal marker TAG1 in the lateralmost cortex, where preplate splitting initiates at E13. Hpca stains subplate cell bodies both in the preplate and in subplate neurons detached from the preplate. In both wildtype and Fog2-null lateral cortex Hpca-positive subplate neurons were seen coalescing in the subplate layer (Fig

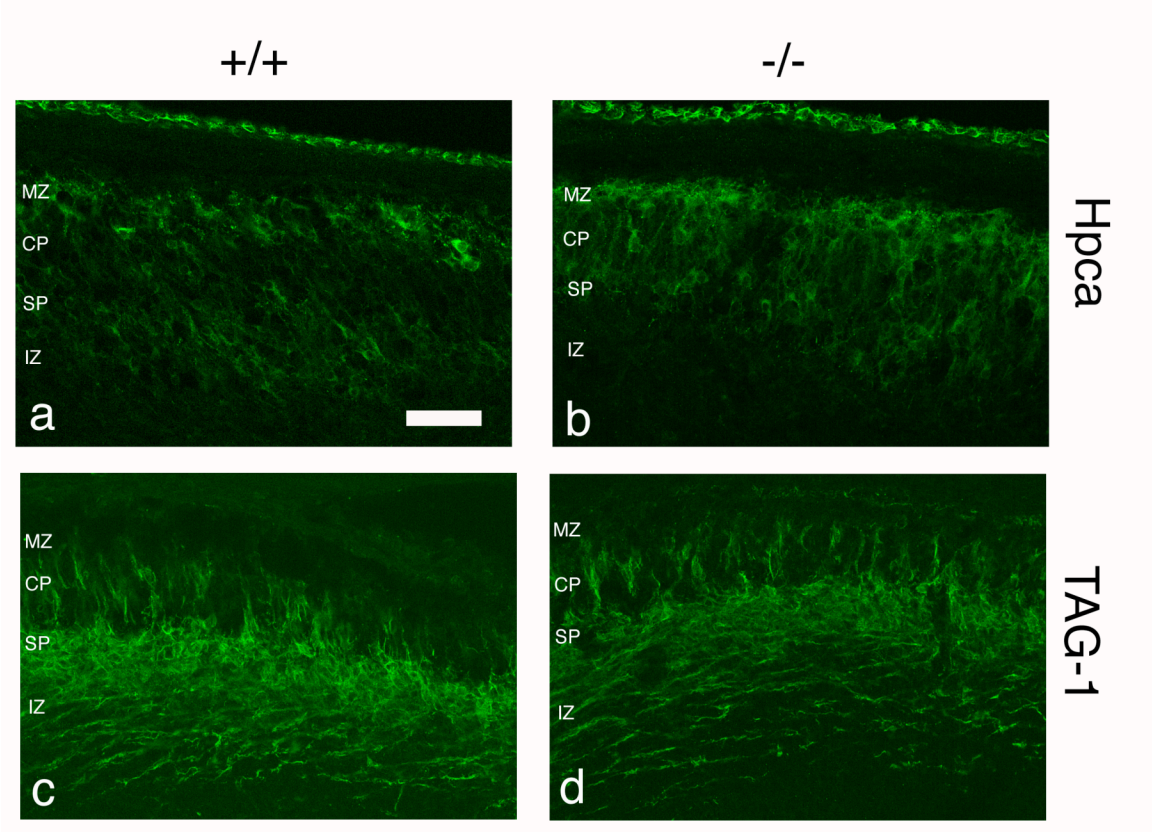

Figure 5.3. Preplate splitting intiates in the lateral cortex in the absence of Fog2. Immunostaining for subplate markers Hpca (a,b) and TAG-1 (c,d) in the lateral cortex of E13 wildtype (a,c) and Fog2-null (b,d) brain. Hpca-positive cells separate from the preplate/marginal zone layer and descend into subplate in null brain (b). TAG-1 positive cells in the subplate form projections in the intermediate zone, and TAG-1 positive radially oriented cells intercalate in the cortical plate similarly in both genotypes(c,d). Abbreviations: marginal zone (MZ), cortical plate (CP), subplate (SP), intermediate zone (IZ). Scale bar = 50 μm.

5.3a,b), while some Hpca-positive were intercalated into the Hpca-negative cortical plate, presumably en route to the subplate.

TAG-1 strongly stained the first corticothalamic projections from subplate neurons in both wildtype and null lateral cortex (Fig 5.3c,d). Radially oriented TAG-1 positive cells within the cortical plate clearly indicate the development and radial organization of the developing cortical plate, which was unaffected in the Fog2-null brain. Fog2-null subplate projections formed normally in the intermediate zone below the subplate layer, and the density and fasciculation of these fibers was unaffected (Fig 5.3d). Taken together, these staining data indicate that the earliest stages of preplate splitting, when the cortical plate and subplate layer initially form, proceed normally in Fog2-null embryonic brain. Subplate cells are able to detach from the preplate layer and descend through the developing cortical plate, and cortical plate neurons are able to migrate past subplate neurons to stop beneath the reelin-positive marginal zone. The radial, columnar organization of the cortical plate is normal in the null brain, and initial TAG-1-positive projections form in the proper location.

Commissural and corticothalamic projections initiate normally in Fog2-null embryos. I examined the initial stages of subplate projection formation by immunostaining for the projection markers L1 and TAG-1. The anti-L1 antibody stains all early corticofugal projections from the subplate (Jones, Lopez-Bendito et al. 2002), and was used to examine the formation of the anterior commissure

in Fog2-null embryos. At E13, cortical axons of the anterior commissure reach the ventral midline of the forebrain, but have not yet crossed to the contralateral hemisphere (Fig 5.4a). Examination of multiple embryos revealed that the anterior commissure was similarly formed in wildtype and null embryos (Fig 5.4b,c). In both genotypes, the tract was thin and poorly fasciculated, with multiple axons straying dorsal to the tract. Considerable variability was seen in both genotypes in the thickness of the anterior commisure and in the number of straying axons observed; the images shown in Fig 5.4 are representative examples of the phenotype most often observed. The early lethality of Fog2-null embryos precluded examination of the behavior of post-midline crossing anterior commissure axons. Morphology of the anterior commissure is highly sensitive to and dependent upon genetic background (Wahlsten, Ozaki et al. 1992); thus, the defasciculation observed in wildtype embryos is probably not unusual.

Corticothalamic projections initiate normally in the absence of Fog2. I examined the formation of subplate projections destined for the thalamus by TAG-1 immunostaining. In early cortex, TAG-1 is specific for corticothalamic axons, and does not label corticocortical axons (Denaxa, Chan et al. 2001). At E13 in wildtype cortex, TAG-1 positive projections have exited the neocortex and reached but not crossed the internal capsule (Fig 5.5a), a cell-free region which

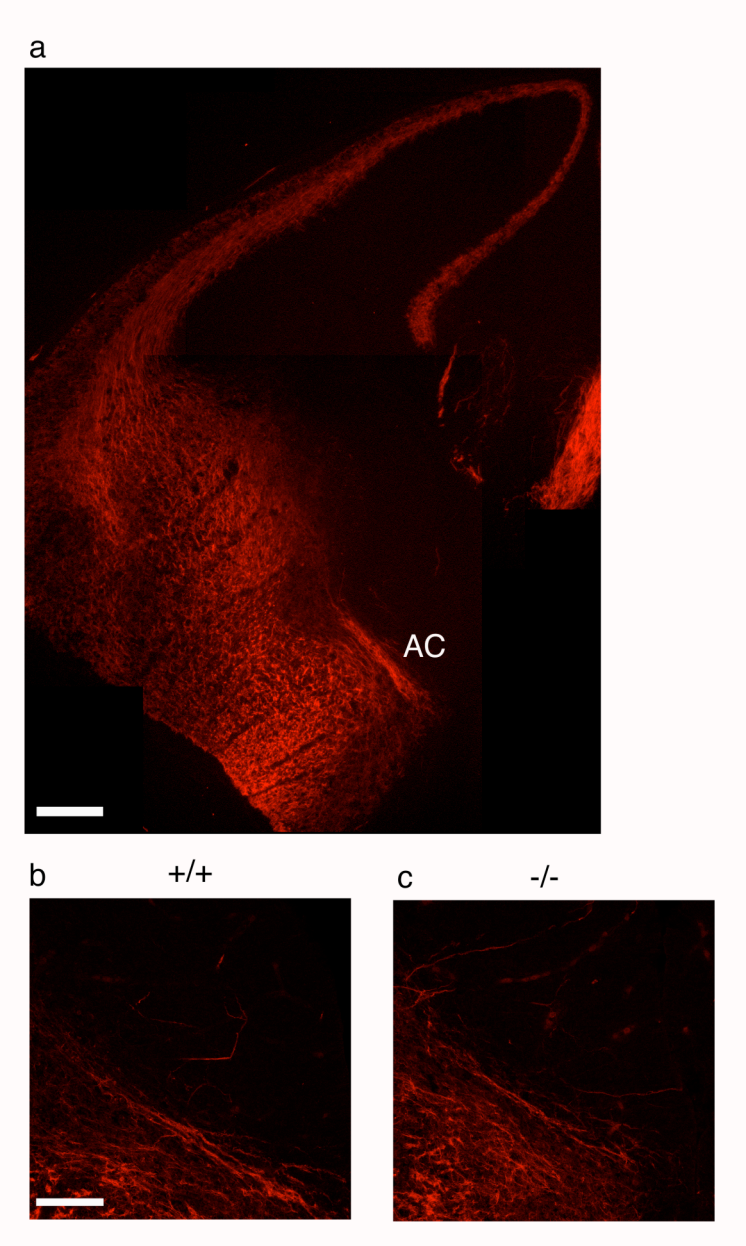

Figure 5.4. Anterior commissure projections initiate normally in the absence of Fog2. Immunostaining for the broad projection marker L1 in WT (a, b) and Fog2-null (c) E13 cortex. L1 stains all early corticofugal fibers, including the anterior commissure (AC), indicated in (a). Magnified views of the anterior commissure in b,c show defasciculation in both wildtype and Fog2-null brains. Scale bar in a = 200 μm; in b,c = 50 μm.

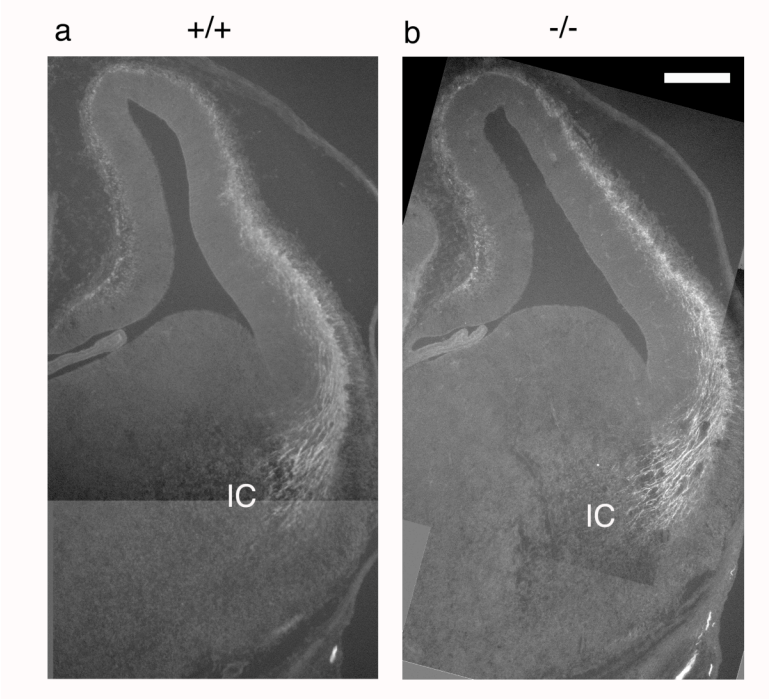

Figure 5.5. Corticothalamic projections initiate normally in the absence of Fog2. Immunostaining for the projection marker TAG-1 in WT (a) and Fog2-null (b) E13 cortex. In early cortex, TAG-1 stains projections destined for the thalamus. At E13, corticothalamic projections have reached but not entered the internal capsule (IC). Scale bar = 200 μm.

at this stage contains the termini of extending thalamocortical projections. The Fog2-null corticothalamic projections are indistinguishable from wildtype at E13 (Fig 5.5b) – Fog2-null TAG-1 projections are confined to the intermediate zone in neocortex, and reach but do not cross the internal capsule, and thus are neither shortened, elongated, or misdirected.

Id2. Id2 (also known as Idb2) was identified as a gene upregulated in Pde1C-EGFP versus Cajal-Retzius neurons and whole cortex. Id2 is one of four Id protein family members, all thought to act as broad inhibitors of the basic helix-loop-helix (bHLH) transcription factors which are major regulators of neurogenesis and neural specification (Ross, Greenberg et al. 2003). Id proteins lack a DNA binding domain, and act by binding and sequestering ubiquitous E proteins necessary for bHLH transcriptional activity (Norton, Deed et al. 1998). Id proteins are generally thought to be act as positive regulators of cell cycle progression and inhibitors of differentiation. Decreased proliferation of neural progenitors and decreased brain size is observed mice null for Id4 and Id1/3, and it is hypothesized that these effects are due to premature activation of proneural bHLH factors, leading to cell cycle exit (Lyden, Young et al. 1999; Yun, Mantani et al. 2004).

Somewhat contrary to these views of Id protein functions, Id2 is expressed in postmitotic cortical plate neurons and not in proliferating progenitors during the cortical plate formation (A. Iavarone, unpublished data). It has been suggested

based on *in vitro* data that Id2 specifically is involved in controlling the timing of differentiation of neural progenitors, and participates in coupling cell cycle exit with changes in morphology associated with differentiation, such as neurite extension (Lasorella, Stegmuller et al. 2006).

By qPCR, expression of Id2 mRNA was upregulated in Pde1C-EGFP-positive cells compared to both unpurified cortex and Girk4-EGFP-positive cells (Fig 5.6). Girk4-EGFP-positive Cajal-Retzius neurons expressed higher levels of Id2 mRNA than did whole cortex (Fig 5.6), suggesting that Id2 is transiently expressed by all cortical neurons. I hypothesized that Id2 might be involved in the timing of differentiation of future subplate neurons, in subplate neuron specification, or in controlling the initial phases of axon outgrowth from subplate cells. I tested these hypotheses by examining embryonic brains for expression of preplate differentiation markers, formation and morphology of early subplate projections, and cortical layer formation in late embryonic brain.

Preplate neurons differentiate normally in Id2-null embryos. In the wildtype forebrain, preplate neurons are born and differentiate between E10 and E12. Cajal-Retzius neurons are generated largely on E10, and significant numbers of reelin-positive cells first appear on E11 (Fig 5.7a). Future subplate neurons are generated a day later than Cajal-Retzius neurons, and at E11 very little expression of the future subplate marker Hpca is seen (Fig 5.7c). Hpca-positive neurons first appear beginning at E12 (Fig 4.5a). To test the hypothesis that Id2

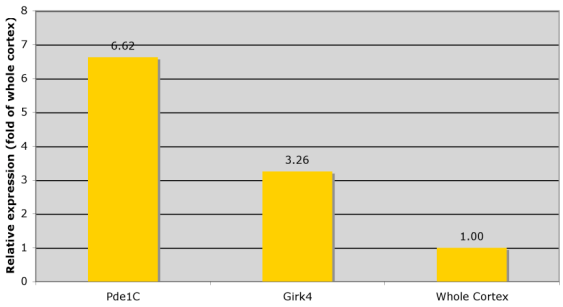

Figure 5.6. Id2 is enriched in Pde1C-EGFP+ and Girk4-EGFP+ cortical cells. Realtime quantitative PCR for Id2 mRNA in FACS-purified E12 Pde1C-EGFP+ and Girk4-EGFP+ cells compared to whole cortex. Relative expression was calculated based on GAPDH expression as an internal control, and standardized to expression levels in unpurified, age-matched cortex. Id2 expression is increased in both Pde1C-EGFP and Girk4-EGFP-expressing cells compared to unpurified cortex, with higher expression seen in the Pde1C-EGFP+ population.

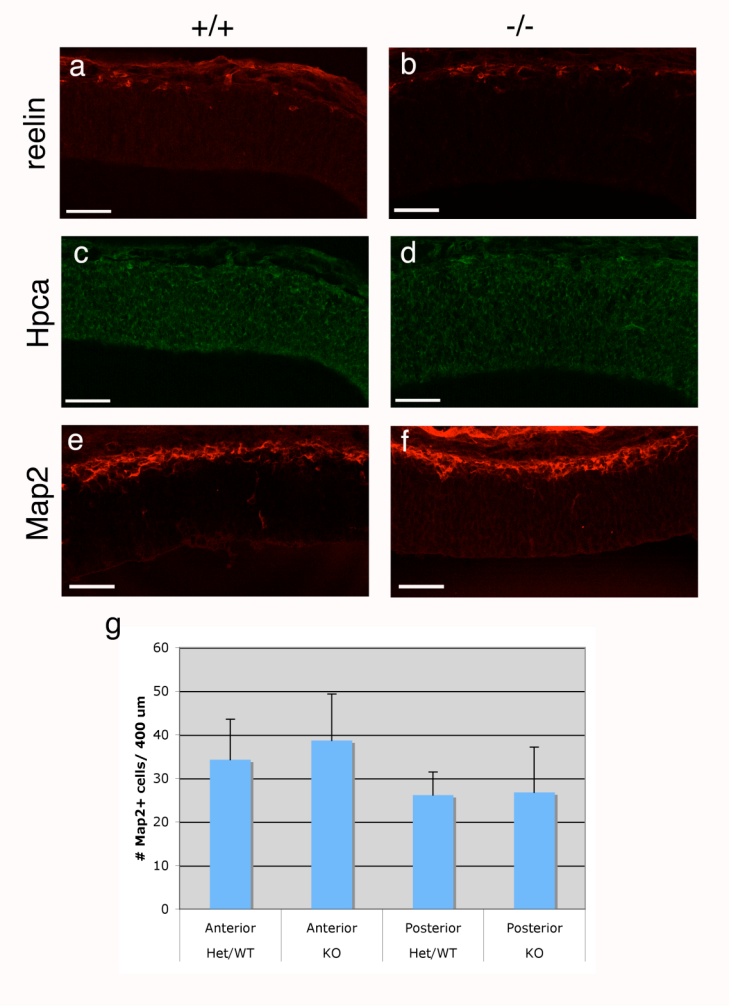

Figure 5.7. Normal numbers of differentiated early preplate neurons in the absence of Id2. Cryostat sections of E11 wildtype (a,c,e) and Id2-null (b,d,f) brains were stained for markers of preplate differentiation: reelin (a,b), Hpca (c,d), and Map2 (e,f). Similar numbers of reelin-positive cells were present in wildtype and null brains (a,b). No Hpca-positive cells were present in either genotype at E11 (c,d), indicating no premature differentiation of future subplate neurons. Map2 marks all differentiated cortical neurons at this stage; similar numbers of Map2-positive neurons were present in null (f) compared to wildtype (e). (g) No significant difference in numbers of Map2-positive differentiated cells was found between wildtype and null in either anterior or posterior cortex ($p=0.52$, 0.90 by t-test, respectively). Scale bars = 50 μm.

might be required for the proper timing of differentiation of preplate neurons, I examined the expression of reelin and Hpca in Id2-null brains at E11. In Id2-null E11 brains, reelin-positive Cajal-Retzius neurons were present in normal numbers (Fig 5.7a,b), and thus were not differentiating early or late. The E11 wildtype preplate was largely lacking in Hpca-positive subplate neurons (Fig 5.7c), and no overexpression of Hpca was seen in the mutant preplate (Fig 5.7d).

Although expression of specific markers of preplate subpopulations is not strong at E11, the pan-neuronal differentiation marker Map2 is strongly expressed in preplate at this stage (Fig 5.7e,f), suggesting that it is an earlier marker of differentiation than reelin or Hpca. I quantitated the number of Map2-positive cells in wildtype and Id2-null cortex at E11, and found no significant difference in the density of Map2-positive differentiated neurons in the Id2-null preplate compared to wildtype (Fig 5.7g). Map2-positive neurons were counted in both anterior and posterior cortex. Consistent with the lateral-to-dorsal and anterior-to-posterior gradient of neurogenesis previously described, more differentiated neurons were seen in the anterior cortex, and similar numbers were found in both genotypes ($p=0.52$ by t-test). Fewer differentiated neurons were found in posterior cortex in both genotypes ($p=0.90$).

At E13, preplate organization and the number of preplate neurons was unchanged in Id2-null cortex (Fig 5.8). Immunostaining for reelin and Hpca revealed that the total number of differentiated neurons (Fig 5.6Bc) and the relative numbers of each subpopulation (Fig 5.8d) were not significantly different

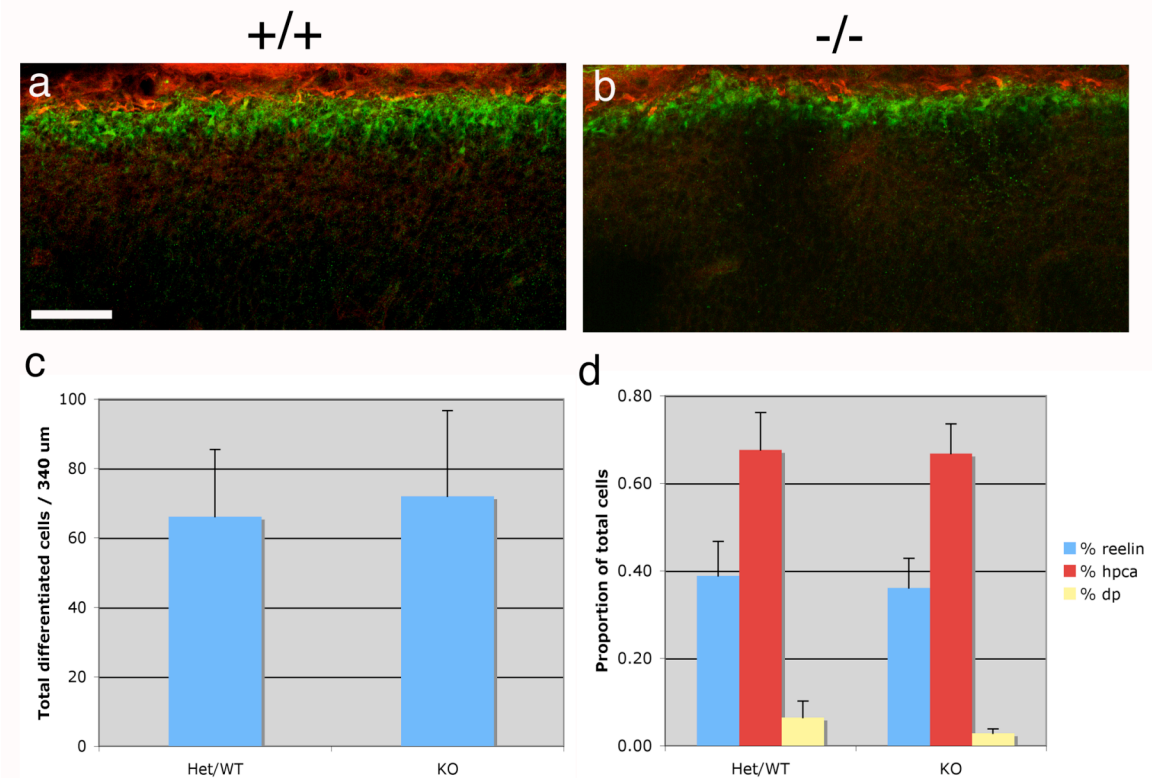

Figure 5.8. Early preplate differentiation occurs normally in the absence of Id2. Cryostat sections of wildtype (a) and Id2-null (b) E13 brain were stained for reelin (red) and Hpca (green). Cajal-Retzius and future subplate neurons are present in the Id2-null preplate, and organization of the preplate is normal. (c) Quantitation of total numbers of differentiated cells in Id2-null and wildtype brains. Numbers of reelin-positive, Hpca-positive, and reelin/Hpca-double positive cells were counted in 340 μm fields, and the total number of cells present was considered the number of differentiated neurons per field. Total numbers of differentiated neurons were not significantly different between wildtype/heterozygote and null brains (p=0.67 by t-test). (d) Quantitation of the proportion of reelin-, hpca-, and double-positive cells of total differentiated cells. No significant difference in the percentages of reelin (p=0.57), Hpca (p=0.86), and double-positive (p=0.09) cells were seen between genotypes.

in the Id2 mutant compared to wildtype. The laminar organization of the preplate was also unchanged in the mutant (Fig 5.8a,b). From these data, I conclude that loss of Id2 does not affect the numbers of preplate neurons produced, the timing of production of preplate neurons, or the organization of the preplate.

Preplate splitting initiates normally in the absence of Id2. The initial formation of the cortical plate in Id2-null embryos was examined by immunostaining for subplate markers in E13 lateral cortex (Fig 5.9). Hpca staining clearly revealed separation of the preplate into marginal zone and subplate in both wildtype and Id2-null lateral cortex (Fig 5.9a,b). Radially oriented Hpca-positive cells were visible in the developing cortical plate as well as the subplate, and many remained in the marginal zone at this early stage of preplate splitting. TAG-1 also stained radially oriented cells in the cortical plate (Fig 5.9c,d), and TAG-1-labeled corticothalamic projections formed in the intermediate zone of both Id2-null and wildtype cortex (Fig 5.9c,d).

Early corticofugal projections form normally in the absence of Id2. Because of the demonstrated effect of Id2 on the control of neurite outgrowth, I hypothesized that loss of Id2 might cause misregulation of the formation of early projections from subplate neurons, leading to shortened, lengthened, or misguided axons. I stained E13 Id2-null and wildtype littermates for the projection

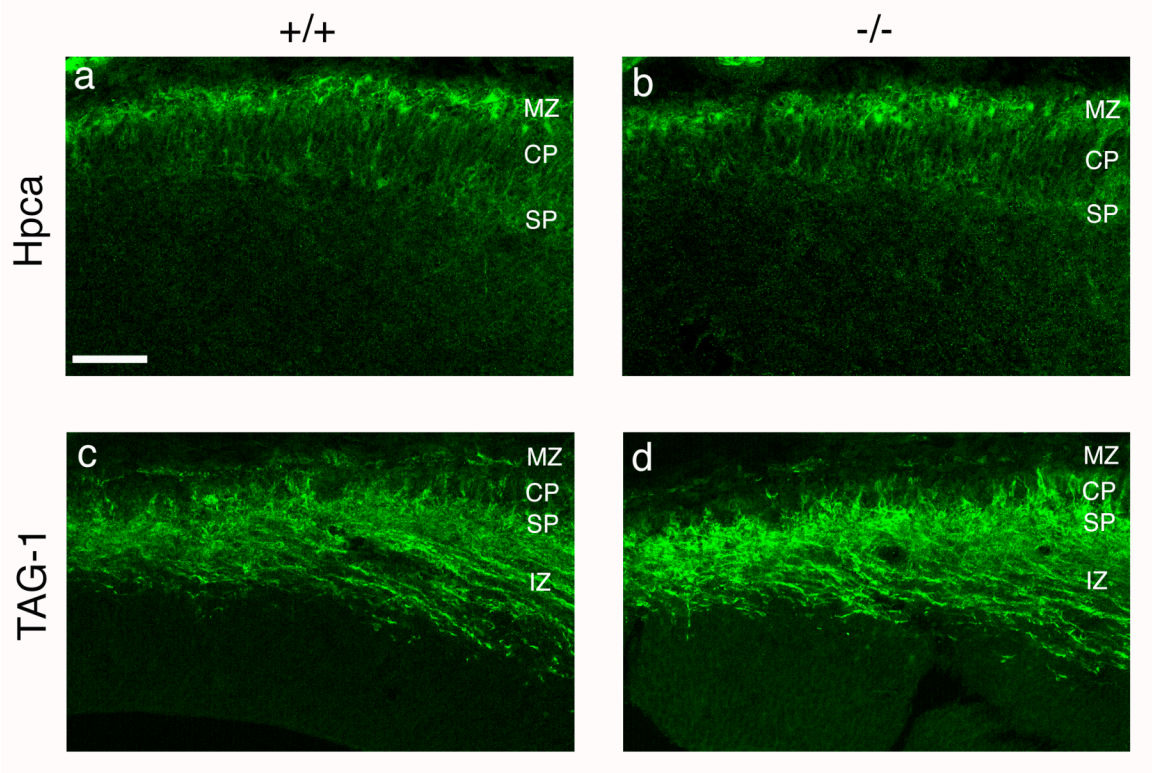

Figure 5.9. Preplate splitting intiates in the lateral cortex in the absence of Id2. Immunostaining for subplate markers Hpca (a,b) and TAG-1 (c,d) in the lateral cortex of E13 wildtype (a,c) and Id2-null (b,d) brain. Hpca-positive cells separate from the preplate/marginal zone layer and descend into subplate in null brain (b). TAG-1 positive cells in the subplate form projections in the intermediate zone, and TAG-1 positive radially oriented cells intercalate in the cortical plate similarly in both genotypes(c,d). Abbreviations: marginal zone (MZ), cortical plate (CP), subplate (SP), intermediate zone (IZ). Scale bar = 50 μm.

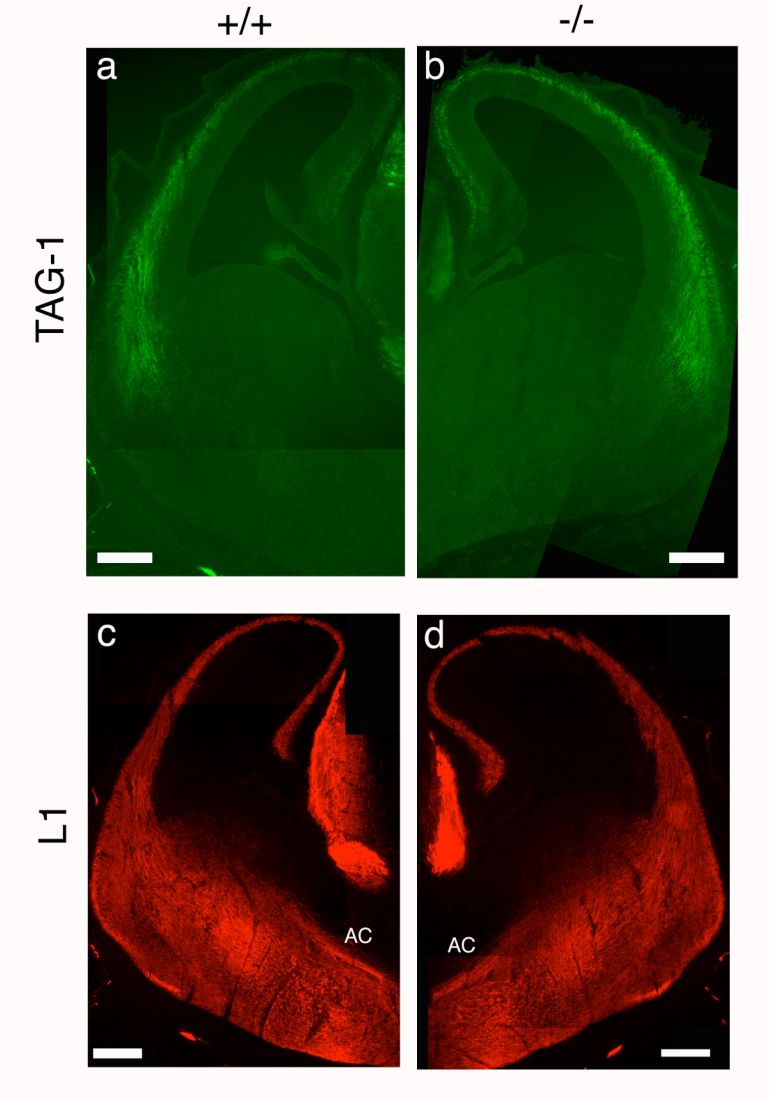

Figure 5.10. Early corticofugal subplate projections are normal in the absence of Id2. Cryostat sections of E13 wildtype (a,c) and Id2-null (b,d) brains were stained for the projection markers TAG-1 (a,b) and L1 (c,d). TAG-1 stains corticothalamic projections, which reached but did not cross the internal capsule in both wildtype (a) and Id2-null (b) brains. L1 stains all corticofugal projections including commissural axons. The L1-positive anterior commissure was present in both wildtype (c) and Id2-null (d) brains. Scale bars = 200 μm.

markers TAG-1 and L1 to determine whether corticothalamic or corticocortical subplate projections were disturbed in the absence of Id2.

Corticothalamic TAG-1-positive neurite outgrowth appeared normal in the Id2-null brain (Fig 5.10a,b). In both wildtype and null E13 brains, TAG-1 fibers reach but do not enter the internal capsule, suggesting that there is no over- or under-growth of the corticothalamic axons. No straying of TAG-1-positive fibers outside of the intermediate zone in cortex, or into the internal capsule in striatum, was seen in the Id2-null cortex. As well, the L1-positive anterior commissure formed normally, reaching but not crossing the midline in both null and wildtype brains (Fig 5.10c,d). No straying L1-positive axons within the cortex were observed.

While no defects in early projection formation were observed in Id2-null embryos, it remains possible that axon growth or guidance defects in subplate neurons might be apparent in later stages of axon targeting (i.e., in post-midline crossing anterior commissure, or targeting to specific thalamic nuclei) not detectable by staining for projection markers at these early stages.

Subplate cells survive but the thickness of the cortical plate is reduced in Id2-null E16 cortex. Analyzing the expression of Cajal-Retzius and subplate markers in later embryonic (E16) cortex revealed that subplate neurons survive in normal numbers in the absence of Id2 (Fig 5.11a-c). At E16, anti-Hpca antibody strongly stains the cell bodies of neurons in the subplate layer, and Hpca is

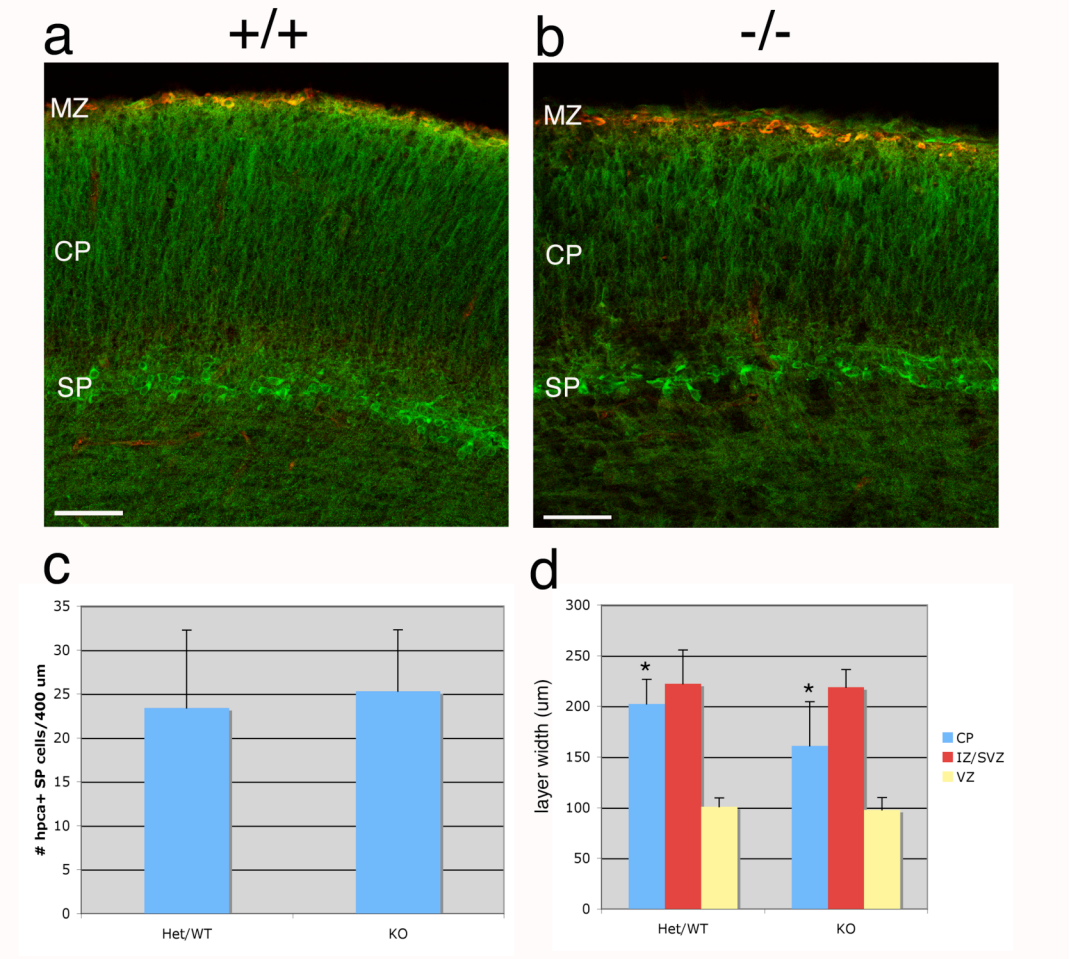

Figure 5.11. Id2-null brain has normal subplate but thin cortical plate at E16. (a,b) Cryostat sections of wildtype (a) and Id2-null (b) E16 brains were stained for marginal zone and subplate markers reelin (red) and Hpca (green). (c) Hpca-positive subplate cells were counted, and no significant difference was seen between genotypes in number of subplate neurons per field ($p=0.56$ by t-test). (d) Cortical plate (CP) thickness is reduced in Id2-null brain ($p=0.003$ by t-test). The thickness of the CP was measured as the distance between reelin-positive cells and Hpca-positive subplate. The thickness of the intermediate zone/subventricular zone (IZ/SVZ) was measured as the thickness of the L1-positive plexiform layer (not shown), and the thickness of the ventricular zone

(VZ) was measured as the distance between the ventricle and the IZ. No difference was seen in the thickness of the IZ/SVZ ($p=0.77$) or the VZ ($p=0.49$). Abbreviations: marginal zone (MZ), subplate (SP). Scale bars = 50 μm.

weakly expressed by radial neurons in the upper cortical plate (Fig 5.11a,b). I compared the number of Hpca-expressing cells in the subplate layer in the presence and absence of Id2, and found no differences in the number of Hpca-positive subplate cells between genotype (Fig 5.11c, p=0.56 by t-test), indicating that subplate neurons can survive in normal numbers in the absence of Id2.

While no changes in the Id2-null subplate were observed, subtle changes in the thickness of the cortical plate was found. The thickness of the cortical plate was measured as the distance between the reelin-positive marginal zone and the Hpca-positive subplate layer. On average, the cortical plate of Id2-null brains was 20% thinner than the wildtype (Fig 5.11d, p=0.003 by t-test). This size decrease did not represent an overall thinning of all cortical layers and was specific to the cortical plate, as no significant difference was found in the thickness of the intermediate zone/subventricular zone (measured as the width of the L1-positive plexiform layer, p=0.77, data not shown) and the ventricular zone (measured as the distance between the ventricular surface and the L1-positive plexiform layer, p=0.49, data not shown).

In summary, no early subplate-specific phenotype was found in mice null for either Fog2 or Id2. However, the Id2 knockout displays a thinner cortical plate than the wildtype, a phenotype which could be due to defects in either subplate neurons or in neurons of the cortical plate. Further analysis of the Id2 knockout will be necessary to determine the cause of the thin cortical plate.

Chapter 6

Discussion

In this work, I have identified BAC transgenic mice expressing EGFP in subpopulations of the cortical preplate. These mice were used to investigate migration and gene expression in specific subpopulations of Cajal-Retzius neurons and subplate neurons. Novel genes with potential roles in preplate development and function were identified, and the roles of two transcription factors in subplate neuron specification and axon extension were examined.

Identification and characterization of BAC-EGFP transgenic mouse lines labeling specific populations of Cajal-Retzius neurons. Over the last decade, it has been demonstrated that Cajal-Retzius neurons, defined as reelin-expressing neurons of the embryonic cortex, are derived from multiple birthplaces and thus represent a heterogeneously derived population (Meyer, Soria et al. 1998; Meyer, Cabrera Socorro et al. 2004; Takiguchi-Hayashi, Sekiguchi et al. 2004; Bielle, Griveau et al. 2005; Hanashima, Fernandes et al. 2007). In order to generate tools to investigate the development of and molecular differences between subpopulations of Cajal-Retzius neurons, I identified two BAC transgenic mouse lines which express EGFP transgenes in specific subpopulations of Cajal-Retzius neurons. These markers are expressed in overlapping populations which likely are comprised of cells previously described

to derive from discrete regions of the dorsal cortex (Bielle, Griveau et al. 2005; Yoshida, Assimacopoulos et al. 2006). Using these transgenic lines in time-lapse imaging experiments, I provided the first direct visualization of tangential migration of Cajal-Retzius neurons through the preplate layer (Fig 3.1, Fig 3.2), and traced different migratory routes of different subpopulations. These studies underscore the utility of live imaging in whole-mounted tissue in the study of the dynamics of neuronal migration in the development of the preplate layer. Using this technique in combination with RNAi or other genetic manipulations could provide the means to investigate novel genes with potential roles in controlling the migration of preplate neurons.

Expression of Wnt3a-EGFP marked a subpopulation of reelin-expressing Cajal-Retzius neurons which first appeared in the medial preplate at E11 (Fig 2.9a,c). By E12, Wnt3a-EGFP-positive cells formed a thin subpial layer reaching from medial cortex to lateral cortex (Fig 2.9e). This expression pattern suggested that Wnt3a-EGFP-positive neurons were derived from the cortical hem, and I confirmed this by both birthdating analyses (Fig 3.5) and live imaging of tangentially migrating Wnt3a-EGFP neurons (Fig 3.1). These hem-derived cells were a subset of a broader population of Cajal-Retzius neurons marked by the expression of Girk4-EGFP. Girk4-EGFP was expressed in the majority of reelin-positive cells, and was not specific to a single subpopulation. Girk4-EGFP-positive cells appeared at E11 simultaneously across the entire cortical surface

(Fig 2.9b,d), suggesting that they were derived from multiple sites of origin and intermingled to form a single layer. Because hem-derived cells expressing Wnt3a-EGFP also coexpressed Girk4 mRNA (Fig 2.10), these cells are probably a subset of the Girk4-EGFP-labeled cells.

Results from both live imaging and birthdating experiments supported the hypothesis that Girk4-EGFP-positive neurons represent a heterogeneous population of Cajal-Retzius neurons derived from multiple sources. Live imaging of Girk4-EGFP-positive cells in whole-mounted cortex revealed diverse migratory pathways through the preplate – unlike Wnt3a-EGFP-positive cells, which migrated exclusively from dorsal to ventral, Girk4-EGFP-positive cells migrated towards both dorsal and ventral regions (Fig 3.2). These migrations would be consistent with at least two sites of origin: one at the cortical hem, from which cells migrated ventrally, as well as a more lateral origin, from which cells migrated dorsally. BrdU birthdating experiments, in which the distribution of cells labeled with BrdU at E10.5 was examined at E11.5, revealed no gradient of newly-born Girk4-EGFP neurons in the dorsoventral axis (Fig 3.6a,b). This distribution was also consistent with cells derived from two focal sites of origin, dorsally-derived and ventrally-derived cells quickly intermingling. In the rostrocaudal axis, an accumulation of newly-born neurons was observed towards the caudal region of the neocortex (Fig 3.6c,d). Conceivably, this accumulation of cells could be derived from dorsally migrating PSB-derived cells, as a larger number of Dbx1-positive PSB cells is seen in the caudal PSB compared to rostral

(Bielle, Griveau et al. 2005). The rostrocaudal level of the PSB corresponds more or less to the rostrocaudal level where newly-born Girk4-EGFP neurons accumulated.

None of these data supporting multiple sites of origin of Girk4-EGFP-positive Cajal-Retzius neurons exclude the possibility of an additional, as-yet unidentified source. For example, it is possible that a small subset of Cajal-Retzius neurons derives from the local cortical ventricular zone, and rather than migrating tangentially into the preplate, translocates radially from the ventricular zone.

Molecular heterogeneity between Cajal-Retzius subpopulations.

Subpopulation-specific ablation experiments have suggested potential roles for Cajal-Retzius neurons in areal patterning (Bielle, Griveau et al. 2005; Yoshida, Assimacopoulos et al. 2006). Although ablation of subpopulations of Cajal-Retzius neurons does not result in gross disruption of the laminar organization of the cortex, subtle region-specific defects in cortical patterning are observed with the loss of either cortical hem-derived neurons (Meyer, Cabrera Socorro et al. 2004; Yoshida, Assimacopoulos et al. 2006) or Dbx1+ progenitors from the PSB and septum (Bielle, Griveau et al. 2005). These ablation studies did not carry out detailed analyses of the region-specific defects, choosing to focus on the laminar patterning of the cortex, so the extent of the phenotypes is not clear. Region-

specific phenotypes could simply be attributable to local changes in reelin signaling levels due to local changes in the numbers of Cajal-Retzius neurons. In this model, high levels of reelin would be permissive for areal patterning, while low levels are sufficient for laminar patterning. Conversely, these defects could be attributable to reelin-independent roles for Cajal-Retzius subpopulations in cortical patterning.

If Cajal-Retzius subtypes indeed have specific functions, what differences in gene expression could mediate these functions? The degree of molecular heterogeneity between subpopulations is unknown. A handful of data indicate that Cajal-Retzius neuron subtypes do have distinct patterns of expression of certain marker genes (calretinin, p73, Ebf2) (Yamazaki, Sekiguchi et al. 2004; Bielle, Griveau et al. 2005; Hanashima, Fernandes et al. 2007). Genes differentially expressed between Cajal-Retzius subpopulations could be involved in both the functions of these subpopulations in cortical development and in the differential developmental histories of these cells – specification, differentiation and control of migration through the preplate from different sites of origin.

Gene array analysis of Cajal-Retzius neuron subpopulations. To address this issue directly, I used the BAC-EGFP transgenic lines identified to represent different Cajal-Retzius subpopulations to carry out a comparative gene expression array analysis, identifying catalogs of genes differentially expressed between subpopulations. Genes comparatively enriched in Wnt3a-EGFP-positive

Cajal-Retzius cells should theoretically be specific to hem-derived cells, while genes comparatively enriched in Girk4-EGFP-positive cells should be specific to populations derived from other sources (PSB, septum).

Only 24 genes out of the 22,626 present on the array were found to be upregulated in hem-derived cells expressing Wnt3a-EGFP, as compared to the population expressing Girk4-EGFP and to unpurified cortical cells. *In situ* hybridization to examine the expression patterns of these genes in early cortex showed that this list identified genes expressed within the cortical hem itself, and not in postmitotic preplate cells: Rspo2, Sulf2, and Cacna1g were all expressed specifically in the hem at E11/12 (Fig 4.4a-c). Because previous work identified two Cajal-Retzius genes specifically expressed in hem-adjacent preplate – p21 and Gdn (Yamazaki, Sekiguchi et al. 2004) – I attribute my results to technical difficulties in dissection, and not to the nonexistence of genes specific to hem-derived neurons. Alternative explanations are that the assay was not sensitive enough to detect differences between largely overlapping populations of cells, or that the *in situ* hybridization was not sensitive enough to detect low levels of expression in postmitotic preplate cells.

Despite the difficulty identifying genes specific to hem-derived neurons, the list of 96 genes shown to be enriched in Girk4-EGFP-positive neurons did appear to represent specific expression in a non-hem-derived subpopulation of Cajal-Retzius cells. Of 11 genes from this list, three were expressed in lateral but not dorsal cortex at E11-12 by *in situ* hybridization: Rabgap1l, Syt4, and alpha-

synuclein (Fig 4.4c-e). The expression pattern of these genes was similar to the expression reported for Ebf2, which was identified in a gene array analysis of total Cajal-Retzius neurons and found to be localized to lateral preplate (Yamazaki, Sekiguchi et al. 2004). Thus, although I did not identify a list of hem-derived subpopulations-specific genes, I succeeded in identifying a set of genes likely to be enriched in lateral preplate, expressed by the derivatives of the identified lateral source of Cajal-Retzius neurons, the Dbx1+ PSB.

The Girk4-EGFP-enriched list includes multiple genes encoding receptors for guidance molecules that might be involved in directing the migration of these cells from their birthplace in the lateral cortex dorsally into the neocortical preplate. Eph receptors EphA3 and EphA7 as well as their associated downstream protein tyrosin kinase Tec, Netrin G1, and Unc5c were included on this list, and are therefore candidates for directing the migration of this subpopulation of Cajal-Retzius neurons. Chemokine signaling through the G-protein coupled receptor CXCR4 is the only pathway known to be involved in the tangential migration of Cajal-Retzius neurons through the preplate layer (Borrell and Marin 2006). At least one intracellular regulator of G-protein signaling that could potentially modulate this pathway was present on the Girk4-EGFP-enriched gene list: Abr is a Rho GTPase activating protein (GAP) which has GAP activity associated with Racs and Cdc42 (Chuang, Xu et al. 1995). Rgs18, a regulator of G protein signaling (Nagata, Oda et al. 2001), was also present on the list but

was not found to be expressed in brain by *in situ* hybridization (data not shown), though this could be due to the sensitivity of this technique.

Several protocadherins (Pcdh8, Pcdh20, Pcdh21) were found to be enriched in Girk4-EGFP-positive Cajal-Retzius neurons. The protocadherin family is implicated in synaptic development in the spinal cord (Weiner, Wang et al. 2005), and the restricted expression patterns of protocadherins in the developing cortex suggests a role for these proteins in the establishment of cortical connectivity (Kim, Chung et al. 2007). Expression of specific protocadherins in subpopulations of Cajal-Retzius neurons might be involved in establishing region-specific synaptic connections in layer I.

In general, the number of genes found to be differentially regulated between Cajal-Retzius subpopulations was relatively small, and few subpopulation-specific genes were identified with potential roles in cortical patterning. It is possible that the array assay was not sensitive enough to cope with the degree of overlap between the subpopulations studied, and a comparison of non-overlapping populations would yield clearer data. It seems likely, however, that, subpopulations of Cajal-Retzius neurons are largely similar with respect to gene expression.

Pde1C-EGFP marks a heterogenous population of Cajal-Retzius neurons and future subplate neurons in the preplate. I identified Pde1C-EGFP as a marker for the two major subtypes of preplate neurons: Pde1C-EGFP was

expressed in all Cajal-Retzius neurons both pre- and post-natally (Fig 2.1), and was also transiently expressed in preplate cells destined for the subplate layer (Figs 2.4, 2.6). Upon preplate splitting, Pde1C-EGFP-positive subplate neurons downregulated expression of EGFP, so it could not be effectively used as a marker for subplate neurons and their projections later than E13.

Fate-mapping of Pde1C-expressing cells with a Pde1C-Cre BAC transgenic showed that Pde1C was transiently expressed by cells in the marginal zone, subplate, and lower cortical plate (Fig 2.6). At E12, however, Pde1C-EGFP expression was restricted to Cajal-Retzius and future subplate neurons, and was a useful tool in identifying genes enriched in future subplate.

Heterogeneity of subplate neurons. Subplate neurons pioneer axonal projections to multiple targets in the thalamus and contralateral hemisphere (McConnell, Ghosh et al. 1989; De Carlos and O'Leary 1992; Jacobs, Campagnoni et al. 2007), and therefore are a functionally heterogeneous population. As well, subplate neurons are known to have molecular heterogeneity, with subsets expressing a variety of neurotransmitters, neuropeptides, and calcium binding proteins (Del Rio, Martinez et al. 2000). Work in the cat has shown that subplate neurons expressing neuropeptides and calbindin are probably local circuit interneurons, while long-range projection neurons in the subplate express excitatory neurotransmitters (Antonini and Shatz 1990). However, no molecular distinctions have been made between subplate

neurons sending long-range projections to different cortical or subcortical targets. My results did not provide a tool to address this issue, as Pde1C-EGFP appeared to be expressed by a heterogeneous population of subplate neurons: weak expression of the EGFP transgene was seen in both TAG-1-positive fibers destined for the thalamus, and TAG-1-negative fibers, which do not project to the thalamus (Fig 2.7). Parallel work in our lab has identified a BAC transgenic line, Lrp12-EGFP, in which transgene expression is restricted to only those subplate neurons projecting to the anterior commissure, and not in those neurons projecting to the corpus callosum or thalamus (S. Schneider & M.E. Hatten, unpublished data). Comparative analyses of BAC transgenic lines marking various populations of subplate neurons will be an invaluable tool in correlating molecular phenotypes with functional phenotypes in the subplate layer.

Migration and birthdating of Pde1C-EGFP preplate neurons. The birthplace of subplate neurons, generally assumed to be the local neocortical ventricular zone, has never been firmly established. There is evidence from imaging studies that the local VZ gives rise to at least some preplate neurons which translocate radially into the preplate layer (O'Leary and Borngasser 2006), and subplate neurons express transcription factors common to VZ-derived layer V and VI neurons such as Sox5 and Tbr1 (Lai, Jabaudon et al. 2008). While I attempted to address this issue using live imaging and birthdating of Pde1C-EGFP-positive preplate cells, the nonspecific expression of Pde1C-EGFP in both Cajal-Retzius

neurons and future subplate neurons made these data difficult to interpret. Time-lapse imaging of Pde1C-EGFP-positive neurons in whole-mounted E12 cortex revealed large numbers of cells migrating tangentially within the preplate (Fig 3.3). It is probable that the majority, if not all, of migrating Pde1C-EGFP cells were Cajal-Retzius neurons, but the possibility that a subset of future subplate neurons also undergo tangential migration cannot be excluded. To determine unambiguously whether subplate neurons migrate tangentially, it will be necessary to repeat these experiments with a subplate-specific BAC-EGFP transgenic line.

Short-term birthdating of Pde1C-EGFP cells was similarly confounded by the heterogeneity of the labeled population. However, comparing the results from the birthdating analyses of Pde1C-EGFP-positive cells to that of Girk4-EGFP-positive cells, which labels only Cajal-Retzius neurons, may be useful. As both lines express EGFP in Cajal-Retzius neurons, the differences between the results from Girk4-EGFP and Pde1C-EGFP may be attributable to the presence of future subplate neurons in the latter line. In the dorsoventral axis, newly-born Pde1C-EGFP neurons were concentrated in the lateral cortex, with more BrdU/EGFP+ cells observed laterally than dorsally (Fig 3.7a). This gradient was not seen in the Girk4-EGFP cortex (Fig 3.6b), and thus likely represents newly-born subplate neurons. The simplest explanations for the lateral-to-dorsal gradient in newly-born Pde1C-EGFP neurons are either a) subplate neurons are generated at a focal point in lateral cortex, and migrate tangentially towards

dorsal cortex, or b) subplate neurons are generated in the cortical ventricular zone, and the gradient is due to the lateral-to-dorsal gradient of neurogenesis observed for cortical projection neurons. Subplate neurons might also be derived from heterogenous sources as in the case of Cajal-Retzius neurons, with a mixed population of radially translocating and tangentially migrating neurons making up this layer.

In the rostrocaudal axis, the short-term birthdating analysis of the Pde1C-EGFP line resulted in a very similar distribution of newly-born neurons as that seen in the Girk4-EGFP cortex (Fig 3.7b, Fig3.6d). The sagittal sections used for this analysis did not include the lateralmost regions of the cortex. As the lateral regions of early embryonic cortex contain the majority of reelin-negative, future subplate neurons (Fig 2.4), the sagittal sections likely did not contain significant numbers of future subplate neurons. Together, these data suggest that the distribution of newly-born cells observed in rostrocaudal axis of Pde1C-EGFP cortex represents largely Cajal-Retzius neurons, and not subplate neurons. Again, repeating this analysis with more specific subplate markers will be necessary to extract clearer information about the sources of subplate neurons and their migratory properties.

Gene array analysis identifies novel markers of future subplate neurons.

A more complete picture of gene expression in the subplate is necessary to further our understanding of the development and function of subplate neurons,

as well to provide markers that can be used to specifically identify subplate neurons in the developing cortex. Current markers for subplate neurons are co-expressed by either Cajal-Retzius neurons or by neurons of the cortical plate (e.g. Map2, CSPG, Tbr1), and thus are nonspecific. The exceptions are the golli promoter-driven proteins and transgenes (Landry, Pribyl et al. 1998; Jacobs, Campagnoni et al. 2007), the latter of which have the disadvantages of requiring crossbreeding for visualization in various genetic backgrounds, and transient early expression in Cajal-Retzius neurons, making the golli promoter an inappropriate driver for subplate-specific ablations and genetic manipulations at early embryonic time points (Xie, Skinner et al. 2002). I carried out a screen for genes enriched in future subplate neurons at the preplate stage, and identified both specific markers of future subplate and candidate genes for involvement in subplate neuron specification, subplate axon extension, and guidance of thalamocortical afferent projections.

To identify genes expressed in subplate neurons, I compared gene expression array data from purified Pde1C-EGFP-positive preplate cells to array data from Girk4-EGFP-positive Cajal-Retzius cells. 229 probe sets were upregulated in Pde1C-EGFP cells as compared to Girk4-EGFP cells and to unpurified cortex, and these genes were enriched in the future subplate neurons. Candidates from this list were selected for expression analysis by immunostaining, and all were found to be expressed in future subplate at E12, and in the developing subplate layer at E14 (Figs 4.5, 4.6). Not all were specific

to the reelin-negative cells – some overlapped in expression with the reelin-positive population, as in the case of RyR1 (Fig 4.5e,f). Future subplate genes co-expressed by reelin-positive cells may be more highly expressed by subplate neurons than Cajal-Retzius neurons, or they may be expressed in only a subset of Cajal-Retzius neurons.

As well, some were excluded from the reelin-positive population but were expressed in both the subplate and in cortical plate neurons at E14, as in the case of the Sez6-EGFP transgenic line (Fig 2.6). However, Hpca and EAAC1 expression specifically marked reelin-negative preplate neurons at E12, as well as labeling only the subplate layer at E14 (Fig 4.5a-d).

Subplate genes involved in axon guidance and axonogenesis. A major function of subplate neurons is being instructive in cortical development: signaling molecules expressed by subplate neurons are thought to guide thalamocortical axons within the cortex (Li, Oohira et al. 2005; Maruyama, Matsuura et al. 2008), and subplate neurons might have as yet uncovered roles in regulating the radial migration of cortical plate neurons from the ventricular zone. Identification of genes that are candidates for involvement in these processes was one of the rationales for this screen. Functional classification of the subplate-enriched gene list using the DAVID tool identified a cluster of 8 genes coding for proteins likely to be involved in neural development and neuritogenesis (Cck, Cckra, Slitrk1, Sema4d, Dscam, Ncam2, Nrcam,

9030425E11Rik). These genes may be involved in subplate axon outgrowth and targeting, and a subset of these genes may participate in cell-to-cell signaling. Manual inspection of the list uncovered further candidates for regulating axon targeting and migration in the cortex, due to their functions as secreted or membrane-bound ligands (PACAP, Sema7d, Ccl25, Insl6, Cdh11, and Pcdh8). Of these genes, only one, Sema7d, has been previously shown to be involved in the guidance of thalamocortical axons (Maruyama, Matsuura et al. 2008). However, many have been shown to play roles in neuritogenesis, like Dscam (Fuerst, Koizumi et al. 2008), or in the control of migration of some neuronal subtypes, like PACAP (Cameron, Galas et al. 2007). Finally, Eph receptors A3 and A5 were found to be upregulated in future subplate, and are therefore candidates for involvement in the guidance of subplate axons.

Estrogen signaling networks. Functional analysis with the DAVID tool identified an enriched cluster of four genes involved in cholesterol metabolism or estrogen signaling (Cy51, Cyp7b1, Tm7sf2, mevalonate (diphospho) decarboxylase). Additionally, network analysis using Ingenuity Pathway Analysis (Ingenuity Systems) revealed that a number of the genes upregulated in the subplate list can be regulated by beta-estradiol (estrogen) signaling (Fig 4.7). Estrogen, synthesized de novo in brain, has been shown to have effects on dendritogenesis in multiple neuronal types including cerebellar Purkinje neurons(Sasahara, Shikimi et al. 2007) and hippocampal neurons (Prange-Kiel and Rune 2006), and

estrogen receptor beta is required for normal migration and survival of some cortical plate neurons (Wang, Andersson et al. 2003). Among the genes regulated by beta-estradiol are some of the candidate axon extension and signaling molecules described above (Dscam, Cdh11, Ccl25), and other genes known to be involved in neuritogenesis (Sez6, Nell2). Taken together, these data suggest that steroid hormone signaling may be involved in the development and maturation of subplate neurons. As well, they imply a potential role for the preplate in the sex-specific differentiation of the brain.

Subplate-specific transcription factors: candidates for subplate neuron specification. There were 32 transcription factors on the subplate-specific gene list, which included several genes previously known to be involved in subplate specification or function. Included on the list was Lmo4, a calcium-activated transcription factor which, when conditionally deleted in forebrain, results in errors in thalamocortical pathfinding (Kashani, Qiu et al. 2006), which may be attributable to defects in subplate gene expression, as subplate neurons have been shown to have an instructional role in the guidance of thalamocortical axons (Ghosh, Antonini et al. 1990). A similar phenotype of mistargeted thalamocortical axons has been observed in the cortex of mice lacking the bHLH transcription factor NeuroD2 (Ince-Dunn, Hall et al. 2006), which was also found to be enriched in future subplate. Finally, the transcription factor Sox5 was found to be required for the proper specification of subplate neurons and early-born

projection neurons (Lai, Jabaudon et al. 2008). The other transcription factors identified to be enriched in future subplate neurons could potentially be involved in the specification of subplate neuron identity, and in the regulation of expression of subplate-specific signaling molecules which are instructive in the patterning of the cortex.

Transcription factors in subplate specification: analysis of two candidate genes

I chose to analyze the phenotypes of mice with loss-of-function of two transcriptional regulators that were found to be upregulated in Pde1C-EGFP neurons: Fog2 and Id2.

Fog2. Fog2, also known as Zfpm2, was shown to be highly expressed in Pde1C-EGFP cells at E12 by qPCR (Fig 5.1a), and a Fog2-lacZ transgenic mouse expressed beta-gal in the reelin-negative preplate and subplate (Fig 5.1c,d), indicating that Fog2 is specifically expressed in future subplate neurons. In other cell types, Fog2 negatively regulates two families of transcription factors: the GATA factors 1-4 and the COUP-TFs (Tevosian, Deconinck et al. 1999; Crispino, Lodish et al. 2001; Huggins, Bacani et al. 2001). As two COUP-TF family members have been shown to be involved in preplate and subplate specification and in the formation of subcortical projections (Zhou, Qiu et al. 1999; Studer, Filosa et al. 2005; Armentano, Filosa et al. 2006; Faedo, Tomassy et al. 2007), I

hypothesized that Fog2 might be involved in regulating cell fate in preplate neurons, and might be necessary for proper subplate neuron specification. The nervous system of the Fog2 knockout had not been previously characterized, as the mutation is embryonic lethal after E13 due to failures of organ morphogenesis (Tevosian, Deconinck et al. 2000).

Preplate neurons differentiated normally in Fog2-null E13 embryos, and no differences were found in the numbers of each type of preplate neuron or in their distribution within the cortex (Fig 5.2). The Fog2-null preplate was properly organized, and preplate splitting initiated in the lateral cortex, with subplate neurons assuming normal positions deep to the preplate layer (Fig 5.3). I also examined the positioning of early cortical efferents from subplate neurons to subcortical targets by immunostaining for TAG-1 and L1, markers of corticothalamic and all corticofugal projections, respectively. TAG-1 positive projections initiated normally in the Fog2-null brain, reaching but not crossing the internal capsule at E13 (Fig 5.5), and the L1-positive projection to the anterior commissure also formed normally, reaching but not crossing the ventral midline (Fig 5.4). In summary, no defects in early preplate specification, preplate organization, axon projection, or preplate splitting were detected in the absence of Fog2.

Because Fog2 embryos could only be examined at early stages of cortical development, it remains possible that loss of Fog2 could have subplate-specific effects later in development – Fog2 could control the expression of genes

involved in the final targeting of the corticothalamic, thalamocortical, or corticocortical projections, or regulate subplate cell survival. Conditional deletion of Fog2 in the nervous system will be necessary to determine whether loss of Fog2 function has any later developmental effects.

Id2. The second candidate transcriptional regulator I selected was one of broader function, Id2. Id2 is one of four Id family members which act as repressors of bHLH transcription factors. Ids 1, 3, and 4 have all been shown to regulate proliferation of neural progenitors, and are generally thought of as necessary for cell cycle progression. It has been hypothesized that Ids repress neural differentiation by inhibiting the action of proneural bHLH factors. The cortical phenotype of the Id1/3 knockout seems to support this hypothesis, as it displayed decreased proliferation coupled with premature neuronal differentiation (Lyden, Young et al. 1999). Id2 has not been described to have a role in neurogenesis *in vivo*, and its expression pattern is distinct from that of Id1 and Id3. Id1/3 are expressed in the proliferative ventricular zone, whereas Id2 and Id4 are expressed in differentiated cortical neurons (Jen, Manova et al. 1997) (A. Iavarone, unpublished data). *In vitro*, Id2 overexpression causes deregulation of axon outgrowth, possibly by repressing bHLH factors controlling terminal differentiation of neurons (Lasorella, Stegmuller et al. 2006). As Id2 stability is regulated by its interaction with the anaphase promoting complex (APC), it is hypothesized that Id2 expression and stability provides a molecular link coupling

cell cycle exit to neuronal differentiation (Lasorella, Stegmuller et al. 2006). Id2 is thought to be expressed in the majority of developing neurons, and its expression is maintained in specific layers of the mature cortex (Neuman, Keen et al. 1993). Based on these data, I hypothesized that Id2 expression in the preplate might regulate the timing of preplate neuron differentiation. Because of its demonstrated *in vitro* role in regulating axon outgrowth, I also hypothesized that loss of Id2 might cause defects in early subplate projections. I examined preplate neuron differentiation, cortical plate formation, and formation of corticothalamic and anterior commissure projections in Id2-null embryos at E11, E13, and E16.

No changes were observed in early neuronal differentiation in the E11 cortex. Similar numbers of reelin-positive and Map2-positive differentiated neurons were seen in Id2-null embryos compared to wildtype, and no premature differentiation of future subplate neurons was observed (Fig 5.7). As well, the preplate at E13 contained normal numbers of reelin-positive and Hpca-positive Cajal-Retzius and subplate neurons, and the preplate was properly laminated (Fig 5.8). Cortical plate formation initiated normally in lateral cortex at E13 (Fig 5.9), and a complete cortical plate, marginal zone, and subplate were present by E16 (Fig 5.11). Subplate neurons were examined at E16 by Hpca staining, and the later subplate was found to contain similar numbers of Hpca-positive neurons in both the presence and absence of Id2 (Fig 5.11c). Axonal projections from subplate neurons initiated normally, as tested by examining the distribution of TAG-1 and L1-positive fibers at E13 – corticothalamic fibers were not misguided,

overgrown, or undergrown, and the anterior commissure formed properly pre-midline crossing (Fig 5.10).

Although no differences were observed in subplate cell number or projection formation in the Id2-null brain, the size of the cortical plate was reduced in the absence of Id2 (Fig 5.11). The cortical plate of Id2-null brain at E16 was approximately 20% thinner than the wildtype. This phenotype was specific to the cortical plate and not an overall reduction in cortical thickness, as the sizes of the ventricular zone and intermediate zone/subventricular zone were unchanged. Whether this phenotype is attributable to a cell-autonomous effect on cortical plate neurons expressing Id2 or to a cell-non-autonomous effect, perhaps mediated by subplate neurons, is not clear. Further studies of neuronal differentiation, proliferation, migration, and apoptosis in the Id2-null brain are currently being carried out to pinpoint the cause of the defect observed. Because Id2 is transiently expressed in many cortical neurons, it is possible that its loss affects the formation of specific cortical layers, and the expression of layer-specific markers will also be examined in the Id2-null brain.

Further directions. The BAC transgenic mice identified, while not perfectly specific to subpopulations of preplate neurons, may still be useful in the study of preplate specification and development. Crossing mice transgenic for the EGFP markers with knockout mice with impaired preplate development will allow us to distinguish whether subpopulations are specifically affected. For example,

crossing the Wnt3a-EGFP line onto knockout backgrounds with increased or decreased Cajal-Retzius neuron specification will easily clarify whether specific sources of Cajal-Retzius neurons are affected in these knockouts.

This work identified genes specifically expressed in subpopulations of Cajal-Retzius neurons and subplate neurons. Many of these genes are candidates for involvement in the specification and function of preplate subpopulations. Novel transcription factors were identified as being expressed in future subplate neurons, and analysis of mice null for these genes or manipulation of expression of these genes in early embryonic brain should shed light on the mechanisms of subplate neuron specification, as well as genetic pathways controlling subplate axon guidance and targeting.

In addition to the identification of candidate genes in subplate development, this work also yielded the more immediate benefit of identifying novel antibody markers for future subplate neurons. These markers will facilitate the study of the development of the subplate layer, providing a useful tool for examining the specification, morphology, and cell movements of subplate neurons during corticogenesis. The genes identified also suggest novel candidates for the construction of BAC transgenic mice that could be used to screen for subpopulations of subplate neurons with specific patterns of axonal projection, which could be used in the gene expression array experiments I developed to understand the molecular basis of subplate projection heterogeneity.

Chapter 7

Materials and Methods

Preparation of cryostat sections for immunohistochemistry and in situ hybridization. For embryos, the dam was killed by cervical dislocation and embryos dissected in ice-cold PBS. Embryos E13.5 and younger were immediately immersed in fixative (4% paraformaldehyde/PBS). For embryos E14.5 and older, brains were dissected out, then immersion fixed. For postnatal brains, animals were perfused with 4% paraformaldehyde/PBS, brains were removed, and then immersed in fixative. Embryonic brains or whole embryos were fixed for several hours and postnatal brains were fixed overnight at 4°C on a rotator. Brains/embryos were then transferred to 30% sucrose/PBS for cryoprotection overnight at 4°C. Brains/embryos were embedded in Neg-50 embedding medium (Richard-Allen Scientific), frozen on dry ice, and stored at -80°C until sectioning. Sections were cut on a Microm HM500 cryostat, mounted on Permafrost slides (Fisher), and dried for several hours at room temperature before storage at -20°C. For immunohistochemistry, 20 micron sections were cut, and for in situ hybridization, 60 micron sections were cut.

Immunohistochemistry. For fluorescent staining, cryostat sections were rinsed in PBS to remove mounting medium and blocked for one hour at room temperature in 5% normal donkey or goat serum/0.02% Triton X-100/PBS. For

mouse IgG primary antibodies, slides were then rinsed again in PBS and an additional blocking step with donkey anti-mouse IgG Fab fragments (Jackson ImmunoResearch) in PBS for one hour was carried out. Slides were rinsed again in PBS before adding diluted primary antibodies. Primary antibodies were diluted in blocking buffer with serum and incubated overnight at 4°C. Slides were rinsed in PBS 3 x 10 minutes, and incubated with fluorescent-conjugated secondary antibodies diluted in blocking buffer for one hour at room temperature, then rinsed again in PBS and mounted in Gelmount mounting medium (Biomeda). As controls for secondary antibody background and autofluorescence, slides were subjected to this protocol omitting the primary antibody. Images were acquired with a Radiance 2000 confocal laser-scanning microscope.

Primary antibodies used were: mouse anti-reelin (1:1000, MAB5364, Chemicon), rabbit anti-GFP (1:2000, Molecular Probes), sheep anti-EGFP (1:200, AbD Serotec), rabbit anti-calbindin (1:5000, Swant), rabbit anti-calretinin (1:2000, Swant), rabbit anti-hippocalcin (1:2000, Abcam), goat anti-EAAC1 (1:2000, Chemicon), rabbit anti-Ryr1 (1:1000, Chemicon), mouse anti-phospho-histone H3 (1:150, Upstate Biotechnology), rat anti-L1 (1:20, a gift from Dr. J. Trotter), mouse IgM anti-TAG-1 (1:2, a gift from Dr. Jane Dodd, Columbia University, NY), rabbit anti-betagalactosidase (1:2000, Chemicon), rabbit anti-Id2 (1:500, Zymed). Secondary antibodies used were: donkey anti-rabbit, anti-mouse IgM, anti-goat, and anti-rat Alexas 488, 555, 594, and 647 (1:500, Molecular Probes), donkey

anti-sheep FITC (1:250, Jackson ImmunoResearch), donkey anti-mouse IgG Cy3 (1:700, Jackson ImmunoResearch).

Animals. BAC-EGFP and BAC-Cre recombinase transgenic lines were maintained on the Swiss-Webster background in the Rockefeller University animal facility. Experiments were carried out in accordance with the Principles of Laboratory Animal Care, conforming to NIH guidelines under approved protocols. For timed pregnancies, the day of vaginal plug discovery was considered embryonic day 0.5 (E0.5). BAC-EGFP transgenic mice and embryos were genotyped by PCR for the EGFP transgene using the following primers: 5'-CGGCGAGCTGCACGCTGCGTCCTC-3', 5'-CCTACGGCGTGCAGTGCTTCAGC-3'. BAC-Cre mice and embryos were genotyped by PCR for the Cre transgene using the following primers: 5'-CCGGTGAACGTGCAAAACAGGCTCTA-3', 5'-CTTCCAGGGCGCGAGTTGATAGC-3'.

Fog2 knockout embryos were kindly provided by Sergei Tevosian (Dartmouth). Id2 knockout embryos were kindly provided by Antonio Iavarone and Anna Lasorella (Columbia University).

Bromodeoxyuridine (BrdU) labeling. Pregnant dams were given a single intraperitoneal injection of 50 mg BrdU (Sigma) in PBS. Embryos were collected,

fixed and sectioned by cryostat as described above. For BrdU staining in conjunction with another antibody such as anti-EGFP, staining for EGFP was carried out as described above, including incubation with fluorescent-conjugated secondary. After post-secondary washes in PBS, slides were fixed for 15 minutes in 4% paraformaldehyde/PBS, rinsed twice in PBS, and incubated in 2N HCl for 20 minutes at 37°C to denature DNA and expose the BrdU epitope. Slides were then rinsed twice in PBS and neutralized in 0.1 M boric acid (pH 8.5) for 10 minutes. Slides were rinsed three times in PBS, blocked in 5% donkey serum/0.2% TX-100/PBS for 1 hour, and incubated overnight at 4°C with mouse anti-BrdU antibody (Becton Dickson) diluted 1:100 in blocking solution. Slides were rinsed in PBS and Cy3-conjugated donkey anti-mouse IgG (Jackson Immunochemistry) was applied, diluted 1:700 in blocking solution, for 1 hour. Slides were rinsed in PBS and mounted in Gelmount (Biomeda).

X-gal staining. Paraformaldehyde-fixed cryostat sections were rinsed several times in PBS and permeabilized in a detergent solution (0.01% deoxycholate, 0.02% NP-40, 2 mM $MgCl_2$ in PBS) for 10 minutes at 4°C. Sections were developed in staining solution (detergent solution plus 5 mM $K_3Fe(CN)_6$, 5 mM $K_4Fe(CN)_6$, 5 mM EGTA, 1 mg/ml X-gal (5-bromo-4-chloro-3-indolyl-β-D-galactoside, Invitrogen) at 37°C for several hours or overnight. After staining, sections were rinsed in PBS and mounted in Crystal/Mount (Biomeda).

Dissociation and purification of EGFP+ cortical neurons by FACS. Pregnant dams were killed by cervical dislocation, and E12 embryos collected in ice-cold EBSS (Sigma) with 0.2% glucose. Embryos were genotyped by EGFP fluorescence under a Leica M2FL111 dissection microscope equipped with fluorescence. Brains were removed and cortices dissected away from basal forebrain. In the case of Wnt3a-EGFP+ embryos, the cortical hem was removed under the fluorescent dissection microscope. During dissection, cortices were kept at 37°C in EBSS. Cortices were pooled by genotype, the EBSS removed, and activated papain (Worthington Biochemical) in EBSS, passed through a 20 μm filter, was added. Cortices were incubated in papain solution at 37°C for approximately 30 minutes. The tube was inverted several times during this incubation. Digested tissue was pelleted by centrifugation at low speed (500g for 5 minutes). The papain solution was removed and the pellet tritutated gently with a 5 ml pipet in trituration solution preheated to 37°C (1 mg/ml ovomucoid trypsin inhibitor/BSA (Worthington Biochemical), 0.1% DNAse (Worthington Biochemical) in EBSS/0.2% glucose). Two mls of ovomucoid/BSA (10 mg/ml) was added to the bottom of the tube to form two aqueous layers, and the tube was centrifuged at 500g for 5 minutes. The pellet was washed and resuspended in ACSF (125 mM NaCl, 2.5 mM KCl, 1 mM NaH_2PO_4, 25 mM $NaHCO_3$, 11 mM glucose, 1.25 mM $MgCl_2$, 2.5 mM $CaCl_2$). Immediately prior to sorting, the cell suspension was filtered through a cell-strainer cap (Falcon).

Debris and clusters of cells were removed by gating for forward and side scatter. EGFP-negative cells were used to set the gates for EGFP fluorescence, and EGFP+ cells were collected by sorting for EGFP fluorescence.

Preparation of total RNA from FACS purified cells. Total RNA was extracted from EGFP+ purified cells with the RNAqueous Micro kit (Ambion), with modifications to the given protocol. All buffers were RNAse free. Cells were pelleted by centrifugation at 3000 g, and lysed by trituration in 200 μl Lysis Buffer. 50 μl EtOH was added, and the resulting suspension was applied to Micro Filter Columns. Next, an on-column DNAse digestion was carried out (RNAse-free DNAse kit, Qiagen) for 15 minutes at room temperature. The column was washed once in Wash Solution 1, twice in Wash Solution 2/3, and centrifuged at high speed to dry the membrane prior to eluting twice with 5 μl of Elution Solution preheated to 75°C, yielding 10 μl total eluate. RNA samples were stored at -80°C. An Agilent 2100 Bioanalyzer was used to check for total RNA integrity and genomic DNA contamination, and RNA concentration was measured on a NanoDrop-1000 Spectrophotometer.

Affymetrix GeneChip probe preparation and hybridization. Amplified biotinylated cRNA was produced from total RNA using the Two-Cycle Labeling Kit with spike-in controls (Affymetrix, Inc). Briefly, double-stranded cDNA was produced from total RNA using a T7-oligo dT primer for the first strand, and

amplified antisense cRNA was produced from the resulting cDNA template by in vitro transcription. A second round of cDNA synthesis from amplified cRNA was performed, and another round of in vitro transcription was used to produce biotinylated cRNA. Labeled cRNA was fragmented before hybridization, and an Agilent 2100 Bioanalyzer was used to ensure proper fragment size.

Hybridization to Mouse Genome 430A 2.0 Microarrays (Affymetrix, Inc.) and scanning was performed by the Rockefeller University Genomics Facility. Raw data files were processed with Affymetrix GCOS software to generate CEL files, which were imported into Genespring for further analysis (described in Results).

Quantitative real-time PCR. Real-time PCR was performed on amplified cDNA made from RNA extracted from FAC sorted cells. RNA was reverse transcribed and amplified using the Ovation RNA Amplification System (NuGEN Technologies, Inc.) without modifications to the protocol. Briefly, this method involves one round of first strand cDNA synthesis, one round of second strand cDNA synthesis, and amplification with a RNA-DNA primer, DNA polymerase, and RNAse H, resulting in linear amplification of input RNA. Total RNA input was 10 ng per reaction. Unpurified, amplified cDNA was diluted 1:10, and 1 μl of the dilution was used in qPCRs. For each experiment, three biological replicates for each cell type were used.

Real-time qPCR was performed in an iCycler iQ (Biorad). Each 25 μl reaction was performed in triplicate, using 12.5 μl 2x iQ SYBR Green Supermix (Biorad), 1 μl each primer (10 μM stocks), and 1 μl diluted template cDNA. Reactions were run in 96-well plates with 40 cycles of 95°C (30 seconds), 55°C (30 seconds), 72°C (30 seconds). GAPDH was amplified for an internal standard with the following primers: 5'-AGTGGAGATTGTTGCCATCA-3', 5'-TCCACCACCCTGTTGCTGTA-3'. Girk4 was amplified with the following primers: 5'GATGTCTCGTGCTCAACTGG-3', 5'-GAACTGGTGTGAATCGGTGAC-3'. Id2 was amplified with the following primers: 5' GGACATCAGCATCCTGTCCT-3', 5' CTCCTGGTGAAATGGCTGAT-3'. Fog2 was amplified by the following primers: 5'-TTTCTGTCCATTTTCTCAAACA-3', 5'-GCATCGGCGAAAGAAAATAC-3'. Pde1C was amplified with the following primers: 5'-TTGATCTCCTCTGCCCTGTC-3', 5'-CATGGTTGCTCAGTCACAAG-3'. Relative Girk4, Fog2, Pde1C, and Id2 levels were calculated based on GAPDH levels.

***In situ* hybridization.** All aqueous solutions used for *in situ* hybridization were made from DEPC-treated H_2O. Embryos for in situ hybridization were fixed overnight in 4% paraformaldehyde, cryoprotected in 30% sucrose/PBS, and embedded in Neg-50. Sixty μm thick cryostat sections were cut and mounted on Probe-on Plus slides (Fisher) and air-dried overnight at room temperature before storage at -80°C.

Probe templates were TOPO-cloned into pCR4, and digoxygenin-labeled RNA probes were transcribed from linearized template plasmid. 20 μl transcription reactions included: 1 μg template plasmid, 2 μl 10X DIG-labeled dNTP mix (Roche), 1 μl RNAsin RNAse inhibitor (Promega), and 1 μl T3 or T7 polymerase (Promega). The reaction was incubated at 37°C for 2 hours and then purified on a Mini Quick Spin RNA column (Roche). RNA concentration was checked by spectrophotometer.

For *in situ* hybridization, sections were washed twice in PBS to rehydrate, prefixed in 4% paraformaldehyde/PBS for 15 min, and washed again in PBS/1% Tween (PBST). Sections were permeabilized with three 30 minute washes in detergent mix (1% Nonidet P-40, 1% SDS, 0.5% Deoxycholate, 50 mM Tris (pH 8), 1 mM EDTA (pH 8), 150 mM NaCl), and then postfixed in 4% paraformaldehyde/PBST for 15 min. Slides were rinsed twice in PBST, then prehybridized at 70°C for one to two hours in hybridization solution (50% formamide, 5X SSC (pH 4.5), 2% SDS, 500 μg/ml yeast RNA (Sigma), 2% nucleic acid blocking reagent (Roche), 50 μg/ml heparin). Hybridization was carried out overnight at 70°C in hybridization solution, with a probe concentration of approximately 0.5 μg/ml. Posthybridization washes to remove unbound probe were carried out at 70°C four times for 20 minutes each in posthyb solution (50% formamide, 2X SSC (pH 4.5), 1% SDS). Sections were rehydrated in TBS/1% Tween (TBST), blocked in 10% normal goat serum/TBST for two hours, and

incubated overnight at 4 °C with anti-DIG AP Fab fragments (Roche) diluted 1:5000 in 1% NGS/TBST. Postantibody washes were carried out at room temperature in TBST/5 mM levamisole (3 washes of 5 minutes, 4 washes of 30 minutes). For colorization, sections were equilibrated in NTMT (100 mM NaCl, 100 mM Tris (pH 9.5), 50 mM $MgCl_2$, 1% Tween) and the colorization reaction was carried out with 5-bromo-4-chloro-3-indolyl-phosphate (50 μg/ml, Roche) and 4-Nitro Blue tetrazolium chloride (100 μg/ml, Roche) for up to several days. The reaction was stopped in TE buffer and slides were mounted in 80% glycerol/PBS.

	Forward primer	Reverse Primer	Probe size
Rabgap1l	AAAGCCACATAGGCCACAAC	TATTGAATGTGACCCCAGCA	1011 bp
Rspo2	CAAGCATGGACTCAGCGTTA	CTGGATCAGCCAGGGAAATA	1198 bp
Snca	CAGCACACAAGACCCTGCTA	GGGGAAAACAGGAAGAATCG	714 bp
Sulf2	GACAGGGACGTCCTTAACCA	GGGGCAGGAACACTGTAAGA	1036 bp
Syt4	AGCATGTGCCACTTAGCAA	AGAAGCGAGACCTCAATGG	976 bp

Live imaging of EGFP neurons in whole-mounted embryonic cortex.

Embryonic brains were dissected from E12 embryos in ice-cold PBS, keeping the pial membrane intact. Cortices were hemisected and embedded on movie dishes (Mattek) in Matrigel (BD Biosciences). Cortices were flattened pial side down on the coverslip, and Matrigel was carefully added around and on top of the tissue to

fully cover. The Matrigel was allowed to polymerize in a 37°C 5% CO_2 incubator for approximately 20 minutes before adding preheated imaging medium (50% Neurobasal (Invitrogen), 50% Leibovitz's L-15 supplemented with 0.5% glucose, 1X ITS (Sigma), 60 μg/ml N-acetyl cysteine, 2 mM L-glutamine, 10 mM HEPES, 50 U/ml penicillin/streptomycin).

EGFP-positive neurons in the preplate were imaged with a Carl Zeiss Axiovert 200M equipped with a 40x, 1.3-NA, Plan Neofluar objective. A PerkinElmer Wallace UltraView confocal head with 488-nm excitation filter and Orca ER cooled CCD camera (Hamamatsu) were used to collect z-stacks (5-10 μm slices, 8-15 images per stack) every 5 minutes for 2-6 hours. Images were processed and analyzed using MetaMorph (Universal Imaging Corp.).

Appendix

Table 1. Girk4-EGFP subpopulation-specific genes

Common	Genbank	Description
1110065A22Rik	BB768838	phosphotriesterase related
2900026H06Rik	BB560759	RIKEN cDNA 2900026H06 gene
3110038O15Rik	BB768064	RIKEN full-length enriched library, clone:B930029M01 product:calcium channel, voltage-dependent, beta 4 subunit, full insert sequence
6330442E10Rik	AV328515	RIKEN cDNA 6330442E10 gene
8430421H08Rik	AV226672	RIKEN cDNA 9630005B12 gene
9030407H20Rik	BC019416	RIKEN cDNA 9030407H20 gene
9030425E11Rik	BG072972	RIKEN cDNA 9030425E11 gene
A230052E19Rik	AV338343	RIKEN cDNA A230052E19 gene
A830037N07Rik	BB752393	RIKEN cDNA A830037N07 gene
A830037N07Rik	BB752393	RIKEN cDNA A830037N07 gene
Abr	AV325116	active BCR-related gene
Aldh1a7	NM_013467	aldehyde dehydrogenase family 1, subfamily A1
Atp1b1	AV152334	AV152334 Mus musculus hippocampus C57BL/6J adult Mus musculus cDNA clone 2900036A18, mRNA sequence.
C76213	C76213	valosin containing protein
Cacnb4	AW106929	calcium channel, voltage-dependent, beta 4 subunit
Camk1	NM_133926	calcium/calmodulin-dependent protein kinase I
Camk2b	NM_007595	calcium/calmodulin-dependent protein kinase II, beta
Catnd2	NM_008729	catenin delta 2
Cbln1	AA016422	cerebellin 1 precursor protein
Cd59a	AK005507	CD59a antigen
Chl1	NM_007697	cell adhesion molecule with homology to L1CAM
Clec2	NM_019985	C-type lectin-like receptor 2
Cntn1	NM_007727	contactin 1
Cntn1	AK004399	contactin 1
Copg2as2	BE653037	0 day neonate lung cDNA, RIKEN full-length enriched library, clone:E030030K01 product:coatomer protein complex, subunit gamma 2, antisense 2, full insert sequence
Copg2as2	BE653037	0 day neonate lung cDNA, RIKEN full-length enriched library, clone:E030030K01 product:coatomer protein complex, subunit gamma 2, antisense 2, full insert sequence
Cpeb3	BB770826	cytoplasmic polyadenylation element binding protein 3
Cpeb4	NM_026252	cytoplasmic polyadenylation element binding protein 4
Cplx1	BC014803	complexin 1
Ctla2b	NM_007796	trophoblast specific protein beta
Ctla2b	NM_007796	trophoblast specific protein beta
Ctla2b	BG064656	trophoblast specific protein beta
D6Ertd365e	BG071922	zinc finger/RING finger 2
Dbccr1	AB060589	deleted in bladder cancer chromosome region candidate 1 (human)
Dcamkl1	BQ174703	double cortin and calcium/calmodulin-dependent protein kinase-like 1
Dncic1	NM_010063	dynein, cytoplasmic, intermediate chain 1

Table 1, continued

Common	Genbank	Description
Dnm	L31397	dynamin
Dtna	BM117918	dystrobrevin alpha
E430021N18Rik	BC021842	RIKEN cDNA E430021N18 gene
Ebf1	BB125261	early B-cell factor 1
Epha3	M68513	Eph receptor A3
Epha7	BB075797	Eph receptor A7
Epha7	BC026153	Eph receptor A7
Fgf14	AV141013	fibroblast growth factor 14
Fst	NM_008046	follistatin
Galnt2	BG064057	UDP-N-acetyl-alpha-D-galactosamine:polypeptide N-acetylgalactosaminyltransferase 2
Gata1	NM_008089	GATA binding protein 1
Gata2	NM_008090	GATA binding protein 2
Grb14	NM_016719	growth factor receptor bound protein 14
Grik1	X66118	glutamate receptor, ionotropic, kainate 1
Gt(ROSA)26Sor	U83174	4 days neonate thymus cDNA, RIKEN full-length enriched library, clone:B630013J18 product:gene trap ROSA 26, Philippe Soriano, full insert sequence
Hist1h1c	BB533903	histone 1, H1c
Hist1h1c	NM_015786	histone 1, H1c
Itga2b	NM_010575	integrin alpha 2b
Lor	AI036317	loricrin
Mapk10	BB313689	expressed sequence AV344025
Mapk10	L35236	mitogen activated protein kinase 10
Mapk10	BB453775	BB453775 RIKEN full-length enriched, 12 days embryo spinal ganglion Mus musculus cDNA clone D130026N06 3' similar to L35236 Mus musculus (clone m3F12) mitogen activated protein (MAP) kinase stress activated protein B mRNA, mRNA sequence.
Mapt	BC014748	microtubule-associated protein tau
Masp1	BB477214	mannan-binding lectin serine protease 1
Myl9	AK007972	myosin, light polypeptide 9, regulatory
Nap1l5	NM_021432	nucleosome assembly protein 1-like 5
Ndph	NM_010883	Norrie disease homolog
Ntng1	NM_030699	netrin G1
Olfm3	AF442824	secreted protein; related to olfactomedin; alternatively spliced; Mus musculus optimedin form B mRNA, complete cds; alternatively spliced.
Pcdh20	BB528056	RIKEN cDNA C630015B17 gene
Pcdh21	NM_130878	protocadherin 21
Pcdh8	NM_021543	protocadherin 8
Plat	NM_008872	plasminogen activator, tissue
Plek	AF181829	pleckstrin
Ppargc1a	BB745167	peroxisome proliferative activated receptor, gamma, coactivator 1 alpha
Prg	NM_011157	proteoglycan, secretory granule
Prkar1b	NM_008923	protein kinase, cAMP dependent regulatory, type I beta

Table 1, continued

Common	Genbank	Description
Ptgs1	AA833146	prostaglandin-endoperoxide synthase 1
Rab3b	NM_023537	RAB3B, member RAS oncogene family
Rap1b	BM246972	RAS related protein 1b
Rgs18	BB139986	regulator of G-protein signaling 18
Rgs18	BB139986	regulator of G-protein signaling 18
Scn1a	AV336781	RIKEN cDNA 2410066K11 gene
Sdc3	BB528350	syndecan 3
Slc1a1	NM_009199	solute carrier family 1 (neuronal/epithelial high affinity glutamate transporter, system Xag), member 1
Snca	NM_009221	synuclein, alpha
Snca	AI324124	mh26h04.x1 Soares mouse placenta 4NbMP13.5 14.5 Mus musculus cDNA clone IMAGE:443671 3' similar to gb:L08850 SYNUCLEIN (HUMAN);, mRNA sequence.
Syt4	AV336547	synaptotagmin 4
Tec	NM_013689	cytoplasmic tyrosine kinase, Dscr28C related (Drosophila)
Thbs1	AI385532	thrombospondin 1
Tm6sf1	AV378394	transmembrane 6 superfamily member 1
Tmsb10	NM_025284	thymosin, beta 10
Treml1	AK017256	triggering receptor expressed on myeloid cells-like 1
Unc5c	NM_009472	unc-5 homolog C (C. elegans)
Usp29	NM_021323	ubiquitin specific protease 29
Zfp179	BB546771	BB546771 RIKEN full-length enriched, 0 day neonate eyeball Mus musculus cDNA clone E130314D07 3' similar to AF054586 Rattus norvegicus brain finger protein (BFP) mRNA, mRNA sequence.
Zfpm2	NM_011766	zinc finger protein, multitype 2
Zfpm2	NM_011766	zinc finger protein, multitype 2
	BB316578	0 day neonate lung cDNA, RIKEN full-length enriched library, clone:E030030K01 product:coatomer protein complex, subunit gamma 2, antisense 2, full insert sequence
	BB336256	Transcribed sequence with moderate similarity to protein sp:P00722 (E. coli) BGAL_ECOLI Beta-galactosidase

Table 2. Wnt3a-EGFP-specific genes.

Common	Genbank	Description
2610028F08Rik	BG067392	RIKEN cDNA 2610028F08 gene
4832415H08Rik	BC025654	RIKEN cDNA 4832415H08 gene
4933402K10Rik	NM_134112	
A2bp1	NM_021477	ataxin 2 binding protein 1
A930019K20Rik	BB435342	RIKEN cDNA A930019K20 gene
BC022960	BC022960	cDNA sequence BC022960
Bcl2l2	BB485989	Bcl2-like 2
		Transcribed sequence with weak similarity to protein ref:NP_081764.1 (M.musculus) RIKEN cDNA
C81521	BG067055	5730493B19 [Mus musculus]
Cacna1g	AW494038	calcium channel, voltage-dependent, T type, alpha 1G subunit
Clybl	BC023398	citrate lyase beta like
Dkk3	AK004853	dickkopf homolog 3 (Xenopus laevis)
Eya2	BC003755	eyes absent 2 homolog (Drosophila)
Ggtla1	NM_011820	gamma-glutamyltransferase-like activity 1
Nope	NM_020043	neighbor of Punc E11
Plxdc2	BB559706	BB559706 RIKEN full-length enriched, 2 days pregnant adult female ovary Mus musculus cDNA clone E330040D03 3', mRNA sequence.
Pnpt1	BB777815	BB777815 RIKEN full-length enriched, Nullipotent stem cell CRL-2070 NE cDNA Mus musculus cDNA clone G430042F07 3', mRNA sequence.
Rnasel	BF714880	Transcribed sequence with moderate similarity to protein ref:NP_081764.1 (M.musculus) RIKEN cDNA 5730493B19 [Mus musculus]
Serpine2	NM_009255	serine (or cysteine) proteinase inhibitor, clade E, member 2
Sulf2	AK008108	sulfatase 2
Wnt3a	NM_009522	wingless-related MMTV integration site 3A
Zfp288	BB751546	zinc finger protein 288
Zfp288	AY028963	zinc finger protein 288
		Transcribed sequence with weak similarity to protein prf:2018199A (E. coli) 2018199A beta lactamase IRT-4
	BM055476	[Escherichia coli]
	BI664122	Transcribed sequences

Table 3. Subplate-specific genes

Transcriptional regulators

Common	Genbank	Description
2310001H13Rik	BB010301	RIKEN cDNA 2310001H13 gene
4933416E05Rik	AV226931	RIKEN cDNA 4933416E05 gene
Atf7	BE225843	Activating transcription factor 7 (Atf7), mRNA
Basp1	AK011545	10 days neonate medulla oblongata cDNA, RIKEN full-length enriched library, clone:B830039F09 product:BRAIN ACID SOLUBLE PROTEIN 1 (BASP1 PROTEIN) (NEURONAL AXONAL MEMBRANE PROTEIN NAP-22) homolog [Rattus norvegicus], full insert sequence
Bcl11b	NM_021399	B-cell leukemia/lymphoma 11B
Cbfa2t1h	BG072085	CBFA2T1 identified gene homolog (human)
Copeb	AV025472	core promoter element binding protein
Dr1	NM_026106	down-regulator of transcription 1
Idb2	BF019883	inhibitor of DNA binding 2
Lmo4	NM_010723	LIM domain only 4
Lyl1	BI249259	602995539F1 NCI_CGAP_Mam5 Mus musculus cDNA clone IMAGE:5151536 5', mRNA sequence.
Mtf2	BG066919	Transcribed sequences
Myc	BC006728	myelocytomatosis oncogene
Myt1	NM_008665	myelin transcription factor 1
Nab1	NM_008667	Ngfi-A binding protein 1
Neurod2	NM_010895	neurogenic differentiation 2
Neurod6	NM_009717	neurogenic differentiation 6
Polr3d	BC016102	polymerase (RNA) III (DNA directed) polypeptide D
Pou3f1	BG065255	POU domain, class 3, transcription factor 1
Sitpec	NM_012029	signaling intermediate in Toll pathway-evolutionarily conserved
Snapc3	AW537061	small nuclear RNA activating complex, polypeptide 3
Sod2	NM_013671	superoxide dismutase 2, mitochondrial
Sox5	AK015212	Mus musculus adult male testis cDNA, RIKEN full-length enriched library, clone:4930427H18 product:SRY-box containing gene 5, full insert sequence.
Srf	BI662291	serum response factor
Tcf15	NM_009328	transcription factor 15
Tle2	AU067681	transducin-like enhancer of split 2, homolog of Drosophila E(spl)
Zfp386	BC004747	zinc finger protein 386 (Kruppel-like)
Zfp68	NM_013844	Zinc finger protein 68
Zfpm2	NM_011766	zinc finger protein, multitype 2

Exocytosis

Ica1	NM_010492	islet cell autoantigen 1
Sec24d	AK009425	SEC24 related gene family, member D (S. cerevisiae)
Syn2	NM_013681	synapsin II
Syngr1	BB272743	synaptogyrin 1
Syt4	AV336547	synaptotagmin 4

Table 3 continued

Axonogenesis and cell-cell adhesion

Common	Genbank	Description
3200001I04Rik	AK014285	RIKEN cDNA 3200001I04 gene
9030425E11Rik	BG072972	RIKEN cDNA 9030425E11 gene
C130076O07Rik	BB202655	RIKEN cDNA C130076O07 gene
Cck	NM_031161	cholecystokinin
Cckar	BC020534	cholecystokinin A receptor
Dscam	NM_031174	Down syndrome cell adhesion molecule
Ncam2	AF001287	neural cell adhesion molecule 2
Sema4d	AV256403	sema domain, immunoglobulin domain (Ig), transmembrane domain (TM) and short cytoplasmic domain, (semaphorin) 4D

Cholesterol biosynthesis and steroid signaling

Common	Genbank	Description
Aacs	AI987654	acetoacetyl-CoA synthetase
Cyp51	NM_020010	cytochrome P450, 51
Cyp7b1	NM_007825	cytochrome P450, family 7, subfamily b, polypeptide 1
Mvd	NM_138656	mevalonate (diphospho) decarboxylase
Stard3	NM_021547	START domain containing 3
Tm7sf2	BC014769	transmembrane 7 superfamily member 2

Subplate - other genes

Common	Genbank	Description
1110007M04Rik	AV156568	RIKEN cDNA 1110007M04 gene
1110008J03Rik	NM_029096	RIKEN cDNA 1110008J03 gene
1110019C08Rik	AA408371	RIKEN cDNA 1110019C08 gene
1110031M08Rik	BI080136	Bernardinelli-Seip congenital lipodystrophy 2 homolog (human)
1110054H05Rik	BM206907	RIKEN cDNA 1110054H05 gene
1110054H05Rik	BM206907	RIKEN cDNA 1110054H05 gene
1200003M09Rik	BB462079	BB462079 RIKEN full-length enriched, 12 days embryo spinal ganglion Mus musculus cDNA clone D130074O08 3', mRNA sequence.
1300018I05Rik	AK005044	RIKEN cDNA 1300018I05 gene
1500001A10Rik	BC024130	RIKEN cDNA 1500001A10 gene
1810012I05Rik	BI081895	RIKEN cDNA 1810012I05 gene
1810029G24Rik	AK007641	RIKEN cDNA 1810029G24 gene
1810046J19Rik	NM_025559	RIKEN cDNA 1810046J19 gene
1810054D07Rik	BB259628	RIKEN cDNA 1810054D07 gene
2310039E09Rik	NM_026509	RIKEN cDNA 2310039E09 gene
2410012A13Rik	NM_023396	RIKEN cDNA 2410012A13 gene
2410153K17Rik	BB402275	RIKEN cDNA 2410153K17 gene
2810408E11Rik	NM_134105	RIKEN cDNA 2810408E11 gene
2810423E13Rik	AV024565	RIKEN cDNA 2810423E13 gene

Table 3, continued

Subplate - other genes

Common	Genbank	Description
2810460C24Rik	AK013368	unnamed protein product; hypothetical TPR repeat containing protein (InterProIIPR001440, evidence: InterPro) putative; Mus musculus 10, 11 days embryo whole body cDNA, RIKEN full-length enriched library, clone:2810460C24 product:hypothetical TPR repeat containing protein, full insert sequence.
3732412D22Rik	AV024662	Adult male corpora quadrigemina cDNA, RIKEN full-length enriched library, clone:B230216K11 product:unclassifiable, full insert sequence
4430402O11Rik	BI452475	RIKEN cDNA 4430402O11 gene
4631426J05Rik	AK019474	RIKEN cDNA 4631426J05 gene
4930471M23Rik	BB408093	RIKEN cDNA 4930471M23 gene
5430401D19Rik	BB280300	myocyte enhancer factor 2C
5730409F24Rik	BC025865	PRP19/PSO4 homolog (S. cerevisiae)
5830457J20Rik	BC023059	RIKEN cDNA 5830457J20 gene
6330406I15Rik	AK018128	RIKEN cDNA 6330406I15 gene
6330442E10Rik	AV328515	RIKEN cDNA 6330442E10 gene
9130422G05Rik	AK018685	RIKEN cDNA 9130422G05 gene
9130422G05Rik	AK018685	RIKEN cDNA 9130422G05 gene
A030007L17Rik	AA673177	RIKEN cDNA A030007L17 gene
A130073L17Rik	BB246182	RIKEN cDNA A130073L17 gene
A2bp1	NM_021477	ataxin 2 binding protein 1
A530089I17Rik	NM_133999	RIKEN cDNA A530089I17 gene
A730011F23Rik	AK012475	RIKEN cDNA A730011F23 gene
A730034C02	BM937510	microtubule-associated protein 2
Abcc8	BB515948	ATP-binding cassette, sub-family C (CFTR/MRP), member 8
Adamts4	BG064671	a disintegrin-like and metalloprotease (reprolysin type) with thrombospondin type 1 motif, 4
Adamts4	BB443585	a disintegrin-like and metalloprotease (reprolysin type) with thrombospondin type 1 motif, 4
Adcyap1	AI323434	adenylate cyclase activating polypeptide 1
AI413782	NM_134044	expressed sequence AI413782
AI428795	AW492543	expressed sequence AI428795
AI428795	AW492543	expressed sequence AI428795
AI843918	AF220355	expressed sequence AI843918
Aig1	NM_025446	androgen-induced 1
Aldh1b1	BC020001	aldehyde dehydrogenase 1 family, member B1
Angptl6	BC025904	angiopoietin-like 6
Apba2bp	AK013520	amyloid beta (A4) precursor protein-binding, family A, member 1 binding protein
Armcx3	AK004598	RIKEN cDNA 1200004E24 gene
Atcay	BQ042885	ataxia, cerebellar, Cayman type homolog (human)
Atp2b2	AV343478	ATPase, Ca++ transporting, plasma membrane 2
Atp6v1g1	BI154058	ATPase, H+ transporting, V1 subunit G isoform 1
Auh	NM_016709	AU RNA binding protein/enoyl-coenzyme A hydratase
BC005752	BC005752	cDNA sequence BC005752

Table 3, continued

Subplate - other genes

Common	Genbank	Description
Bcat1	X17502	branched chain aminotransferase 1, cytosolic
Bdh	BF322712	3-hydroxybutyrate dehydrogenase (heart, mitochondrial)
Bid	NM_007544	BH3 interacting domain death agonist
Bloc1s3	BC025913	cDNA sequence BC043666
Bzw2	BM932775	basic leucine zipper and W2 domains 2
C79468	BQ086025	Transcribed sequences
Camk1d	BG071931	RIKEN cDNA E030025C11 gene
Casp9	BB815299	caspase 9
Ccl25	NM_009138	chemokine (C-C motif) ligand 25
Ccrn4l	AF199491	CCR4 carbon catabolite repression 4-like (S. cerevisiae)
Cd1d1	NM_007639	CD1d1 antigen
Cdh11	NM_009866	cadherin 11
Cdh13	BB776961	cadherin 13
Cog1	BB210424	component of oligomeric golgi complex 1
Cog1	BB236453	component of oligomeric golgi complex 1
Cplx1	BC014803	complexin 1
Crtac1	BB426194	cartilage acidic protein 1
Cugbp1	AK014492	unnamed protein product; CUG triplet repeat, RNA binding protein 1 (MGDIMGI:1342295) putative; Mus musculus 14 days embryo liver cDNA, RIKEN full-length enriched library, clone:4432412L08 product:CUG triplet repeat, RNA binding protein 1, full insert sequence.
Cyfip2	NM_133769	cytoplasmic FMR1 interacting protein 2
Cygb	BM899392	cytoglobin
Cyp51	NM_020010	cytochrome P450, 51
D10Ertd610e	AK010452	DNA segment, Chr 10, ERATO Doi 610, expressed
D10Ertd610e	AU014694	DNA segment, Chr 10, ERATO Doi 610, expressed
D130012J15Rik	AV340147	RIKEN cDNA D130012J15 gene
D1Ertd622e	NM_133825	DNA segment, Chr 1, ERATO Doi 622, expressed
D6Ertd365e	BG071922	zinc finger/RING finger 2
D7Ertd458e	BB049138	DNA segment, Chr 7, ERATO Doi 458, expressed
E130012P22Rik	BB538661	RIKEN cDNA E130012P22 gene
E330009J07Rik	NM_133929	engulfment and cell motility 1, ced-12 homolog (C. elegans)
Elmo1	BC024727	enolase 2, gamma neuronal
Eno2	NM_013509	Eph receptor A3
Epha3	M68513	Eph receptor A5
Epha5	NM_007937	excision repair cross-complementing rodent repair deficiency, complementation group 4
Ercc4	NM_015769	RIKEN cDNA 0710008C12 gene
Fbxo37	NM_133694	gamma-aminobutyric acid (GABA-A) receptor, subunit alpha 2
Gabra2	NM_008066	golgi coiled coil 1
Gcc1	AV339946	glutamine fructose-6-phosphate transaminase 1
Gfpt1	AF334736	guanine nucleotide binding protein (G protein), gamma 3 subunit
Gng3	NM_010316	histocompatibility 47
H47	NM_024439	

Table 3, continued

Subplate - other genes

Common	Genbank	Description
H47	AK005204	histocompatibility 47
Hip2	AI551201	huntingtin interacting protein 2
Hist2h3c2	BC015270	histone 2, H2aa1
Hpca	AK002992	unnamed protein product; hippocalcin (MGDIMGI:1336200) putative; Mus musculus adult male brain cDNA, RIKEN full-length enriched library, clone:0710005G22 product:hippocalcin, full insert sequence.
Idh3a	NM_029573	isocitrate dehydrogenase 3 (NAD+) alpha
Idh3a	NM_029573	isocitrate dehydrogenase 3 (NAD+) alpha
Igfbpl1	BM935068	insulin-like growth factor binding protein-like 1
Insl6	NM_013754	insulin-like 6
Itpk1	AW552407	inositol 1,3,4-triphosphate 5/6 kinase
Itsn	BM248471	intersectin (SH3 domain protein 1A)
Kctd4	NM_026214	potassium channel tetramerisation domain containing 4
Khdrbs2	NM_133235	KH domain containing, RNA binding, signal transduction associated 2
Khdrbs3	AK014353	Mus musculus 17 days embryo head cDNA, RIKEN full-length enriched library, clone:3300001L07 product:etoile, full insert sequence.
Lnx2	NM_080795	ligand of numb-protein X 2
Lss	C77434	lanosterol synthase
Mab21l2	NM_011839	mab-21-like 2 (C. elegans)
Masp1	BB477214	mannan-binding lectin serine protease 1
Mef2c	BB280300	myocyte enhancer factor 2C
Mfap4	BC022666	RIKEN cDNA 1110007F23 gene
Mmd2	BC025064	monocyte to macrophage differentiation-associated 2
Mpp3	NM_007863	membrane protein, palmitoylated 3 (MAGUK p55 subfamily member 3)
Mtif2	NM_133767	mitochondrial translational initiation factor 2
Mus81	AF425647	MUS81 endonuclease homolog (yeast)
Mvd	NM_138656	mevalonate (diphospho) decarboxylase
Myo5a	AK002362	Mus musculus adult male kidney cDNA, RIKEN full-length enriched library, clone:0610009A05 product:unclassifiable, full insert sequence.
Ndrg3	BE631549	N-myc downstream regulated 3
Nef3	NM_008691	neurofilament 3, medium
Nefl	M20480	neurofilament, light polypeptide
Nelf	NM_020276	nasal embryonic LHRH factor
Nelf	BB266960	BB266960 RIKEN full-length enriched, 10 days neonate cortex Mus musculus cDNA clone A830028B20 3', mRNA sequence.
Nell2	AI838010	nel-like 2 homolog (chicken)
Nell2	AI838010	nel-like 2 homolog (chicken)
Nrip3	NM_020610	nuclear receptor interacting protein 3
Nudt3	BC016534	nudix (nucleotide diphosphate linked moiety X)-type motif 3
Ogfrl1	BE650508	opioid growth factor receptor-like 1
ORF21	AY037804	open reading frame 21

Table 3, continued

Subplate - other genes

Common	Genbank	Description
Pcdh8	NM_021543	protocadherin 8
Pcp4	NM_008791	Purkinje cell protein 4
Pde10a	BQ180352	phosphodiesterase 10A
Pdxp	NM_020271	pyridoxal (pyridoxine, vitamin B6) phosphatase
Pfkfb3	NM_133232	6-phosphofructo-2-kinase/fructose-2,6-biphosphatase 3
Ppp1r14a	NM_026731	protein phosphatase 1, regulatory (inhibitor) subunit 14A
Ppp1r14c	NM_133485	protein phosphatase 1, regulatory (inhibitor) subunit 14c
Rabggta	BC012214	Rab geranylgeranyl transferase, a subunit
Rasl11b	BC008101	RIKEN cDNA 1190017B18 gene
Rnf41	AK015745	ring finger protein 41
Rohn	NM_009708	ras homolog N (RhoN)
Rpel1	AV259240	RPEL repeat containing 1
Ryr1	X83932	ryanodine receptor 1, skeletal muscle
Ryr3	AV238793	apoptosis, caspase activation inhibitor
Sec14l1	BI652727	SEC14-like 1 (S. cerevisiae)
Sema7a	AA144045	sema domain, immunoglobulin domain (Ig), and GPI membrane anchor, (semaphorin) 7A
Sept4	NM_011129	septin 4
Serpinb2	NM_011111	serine (or cysteine) proteinase inhibitor, clade B, member 2
Serpini1	NM_009250	serine (or cysteine) proteinase inhibitor, clade I, member 1
Sez6	D29763	seizure related gene 6
Sh3gl2	AF326561	SH3-domain GRB2-like 2
Sh3gl2	AF326561	SH3-domain GRB2-like 2
Sh3kbp1	AK018032	SH3-domain kinase binding protein 1
Sh3kbp1	BB326929	SH3-domain kinase binding protein 1
Siat8a	NM_011374	sialyltransferase 8 (alpha-2, 8-sialyltransferase) A
Slc1a1	NM_009199	solute carrier family 1 (neuronal/epithelial high affinity glutamate transporter, system Xag), member 1
Slc1a1	U75214	solute carrier family 1 (neuronal/epithelial high affinity glutamate transporter, system Xag), member 1
Slc20a1	NM_015747	solute carrier family 20, member 1
Slc27a4	BC023114	solute carrier family 27 (fatty acid transporter), member 4
Slc39a11	BC019647	solute carrier family 39 (metal ion transporter), member 11
Slco3a1	NM_023908	solute carrier organic anion transporter family, member 3a1
Slco3a1	NM_023908	solute carrier organic anion transporter family, member 3a1
Smarca2	BM230202	SWI/SNF related, matrix associated, actin dependent regulator of chromatin, subfamily a, member 2
Spg4	AK007793	spastic paraplegia 4 homolog (human)
Sstr2	NM_009217	somatostatin receptor 2

Table 3, continued

Subplate - other genes

Common	Genbank	Description
Tiam2	BM228957	T-cell lymphoma invasion and metastasis 2
Tollip	BB400304	toll interacting protein
Ttl	BC018513	tubulin tyrosine ligase
Uap1	NM_133806	UDP-N-acetylglucosamine pyrophosphorylase 1
Ubxd4	AV174556	UBX domain containing 4
Vps52	BF468377	vacuolar protein sorting 52 (yeast)
Ywhaz	AV027921	tyrosine 3-monooxygenase/tryptophan 5-monooxygenase activation protein, zeta polypeptide
Znrf2	AV226579	zinc finger/RING finger 2
Znrf2	AV226579	zinc finger/RING finger 2
	BC019122	MRNA similar to H2B histone family, member J (cDNA clone MGC:29103 IMAGE:5003093), complete cds
	BB125596	0 day neonate cerebellum cDNA, RIKEN full-length enriched library, clone:C230080E09 product:hypothetical protein, full insert sequence
	BB559097	BB559097 RIKEN full-length enriched, 2 days pregnant adult female ovary Mus musculus cDNA clone E330037F09 3', mRNA sequence.
	BB130195	BB130195 RIKEN full-length enriched, 16 days neonate cerebellum Mus musculus cDNA clone 9630044E19 3', mRNA sequence.
	BB307071	RIKEN cDNA 9530020D24 gene

References

Ackerman, K. G., B. J. Herron, et al. (2005). "Fog2 is required for normal diaphragm and lung development in mice and humans." PLoS Genet **1**(1): 58-65.

Alcantara, S., M. Ruiz, et al. (1998). "Regional and cellular patterns of reelin mRNA expression in the forebrain of the developing and adult mouse." J Neurosci **18**(19): 7779-99.

Allendoerfer, K. L. and C. J. Shatz (1994). "The subplate, a transient neocortical structure: its role in the development of connections between thalamus and cortex." Annu Rev Neurosci **17**: 185-218.

Anderson, S. A., D. D. Eisenstat, et al. (1997). "Interneuron migration from basal forebrain to neocortex: dependence on Dlx genes." Science **278**(5337): 474-6.

Angevine, J. B., Jr. and R. L. Sidman (1961). "Autoradiographic study of cell migration during histogenesis of cerebral cortex in the mouse." Nature **192**: 766-8.

Antonini, A. and C. J. Shatz (1990). "Relation Between Putative Transmitter Phenotypes and Connectivity of Subplate Neurons During Cerebral Cortical Development." Eur J Neurosci **2**(9): 744-761.

Armentano, M., A. Filosa, et al. (2006). "COUP-TFI is required for the formation of commissural projections in the forebrain by regulating axonal growth." Development **133**(21): 4151-62.

Bayer, S. A. and J. Altman (1990). "Development of layer I and the subplate in the rat neocortex." Exp Neurol **107**(1): 48-62.

Benhayon, D., S. Magdaleno, et al. (2003). "Binding of purified Reelin to ApoER2 and VLDLR mediates tyrosine phosphorylation of Disabled-1." Brain Res Mol Brain Res **112**(1-2): 33-45.

Bicknese, A. R., A. M. Sheppard, et al. (1994). "Thalamocortical axons extend along a chondroitin sulfate proteoglycan-enriched pathway coincident with the neocortical subplate and distinct from the efferent path." J Neurosci **14**(6): 3500-10.

Bielle, F., A. Griveau, et al. (2005). "Multiple origins of Cajal-Retzius cells at the borders of the developing pallium." Nat Neurosci **8**(8): 1002-12.

Borrell, V. and O. Marin (2006). "Meninges control tangential migration of hem-derived Cajal-Retzius cells via CXCL12/CXCR4 signaling." Nat Neurosci **9**(10): 1284-93.

Cameron, D. B., L. Galas, et al. (2007). "Cerebellar cortical-layer-specific control of neuronal migration by pituitary adenylate cyclase-activating polypeptide." Neuroscience **146**(2): 697-712.

Caviness, V. S., Jr. and D. O. Frost (1983). "Thalamocortical projections in the reeler mutant mouse." J Comp Neurol **219**(2): 182-202.

Caviness, V. S., Jr. and R. L. Sidman (1973). "Time of origin or corresponding cell classes in the cerebral cortex of normal and reeler mutant mice: an autoradiographic analysis." J Comp Neurol **148**(2): 141-51.

Chuang, T. H., X. Xu, et al. (1995). "Abr and Bcr are multifunctional regulators of the Rho GTP-binding protein family." Proc Natl Acad Sci U S A **92**(22): 10282-6.

Chun, J. J. and C. J. Shatz (1989). "Interstitial cells of the adult neocortical white matter are the remnant of the early generated subplate neuron population." J Comp Neurol **282**(4): 555-69.

Costa, M. R., N. Kessaris, et al. (2007). "The marginal zone/layer I as a novel niche for neurogenesis and gliogenesis in developing cerebral cortex." J Neurosci **27**(42): 11376-88.

Crispino, J. D., M. B. Lodish, et al. (2001). "Proper coronary vascular development and heart morphogenesis depend on interaction of GATA-4 with FOG cofactors." Genes Dev **15**(7): 839-44.

D'Arcangelo, G., G. G. Miao, et al. (1995). "A protein related to extracellular matrix proteins deleted in the mouse mutant reeler." Nature **374**(6524): 719-23.

De Carlos, J. A. and D. D. O'Leary (1992). "Growth and targeting of subplate axons and establishment of major cortical pathways." J Neurosci **12**(4): 1194-211.

Del Rio, J. A., A. Martinez, et al. (2000). "Developmental history of the subplate and developing white matter in the murine neocortex. Neuronal organization and relationship with the main afferent systems at embryonic and perinatal stages." Cereb Cortex **10**(8): 784-801.

del Rio, J. A., A. Martinez, et al. (1995). "Glutamate-like immunoreactivity and fate of Cajal-Retzius cells in the murine cortex as identified with calretinin antibody." Cereb Cortex **5**(1): 13-21.

Denaxa, M., C. H. Chan, et al. (2001). "The adhesion molecule TAG-1 mediates the migration of cortical interneurons from the ganglionic eminence along the corticofugal fiber system." Development **128**(22): 4635-44.

Derer, P. and M. Derer (1990). "Cajal-Retzius cell ontogenesis and death in mouse brain visualized with horseradish peroxidase and electron microscopy." Neuroscience **36**(3): 839-56.

Diep, D. B., N. Hoen, et al. (2004). "Characterisation of the Wnt antagonists and their response to conditionally activated Wnt signalling in the developing mouse forebrain." Brain Res Dev Brain Res **153**(2): 261-70.

Dulabon, L., E. C. Olson, et al. (2000). "Reelin binds alpha3beta1 integrin and inhibits neuronal migration." Neuron **27**(1): 33-44.

Faedo, A., G. S. Tomassy, et al. (2007). "COUP-TFI Coordinates Cortical Patterning, Neurogenesis, and Laminar Fate and Modulates MAPK/ERK, AKT, and {beta}-Catenin Signaling." Cereb Cortex.

Fuerst, P. G., A. Koizumi, et al. (2008). "Neurite arborization and mosaic spacing in the mouse retina require DSCAM." Nature **451**(7177): 470-4.

Fukuda, T., H. Kawano, et al. (1997). "Immunohistochemical localization of neurocan and L1 in the formation of thalamocortical pathway of developing rats." J Comp Neurol **382**(2): 141-52.

Ghosh, A., A. Antonini, et al. (1990). "Requirement for subplate neurons in the formation of thalamocortical connections." Nature **347**(6289): 179-81.

Gong, S., M. Doughty, et al. (2007). "Targeting Cre recombinase to specific neuron populations with bacterial artificial chromosome constructs." J Neurosci **27**(37): 9817-23.

Gong, S., C. Zheng, et al. (2003). "A gene expression atlas of the central nervous system based on bacterial artificial chromosomes." Nature **425**(6961): 917-25.

Grove, E. A., S. Tole, et al. (1998). "The hem of the embryonic cerebral cortex is defined by the expression of multiple Wnt genes and is compromised in Gli3-deficient mice." Development **125**(12): 2315-25.

Hack, I., M. Bancila, et al. (2002). "Reelin is a detachment signal in tangential chain-migration during postnatal neurogenesis." Nat Neurosci **5**(10): 939-45.

Hack, I., S. Hellwig, et al. (2007). "Divergent roles of ApoER2 and Vldlr in the migration of cortical neurons." Development **134**(21): 3883-91.

Hanashima, C., M. Fernandes, et al. (2007). "The role of Foxg1 and dorsal midline signaling in the generation of Cajal-Retzius subtypes." J Neurosci **27**(41): 11103-11.

Hartfuss, E., E. Forster, et al. (2003). "Reelin signaling directly affects radial glia morphology and biochemical maturation." Development **130**(19): 4597-609.

Hatten, M. E. (1999). "Central nervous system neuronal migration." Annu Rev Neurosci **22**: 511-39.

Hevner, R. F., R. A. Daza, et al. (2004). "Postnatal shifts of interneuron position in the neocortex of normal and reeler mice: evidence for inward radial migration." Neuroscience **124**(3): 605-18.

Hevner, R. F., R. A. Daza, et al. (2003). "Beyond laminar fate: toward a molecular classification of cortical projection/pyramidal neurons." Dev Neurosci **25**(2-4): 139-51.

Hevner, R. F., T. Neogi, et al. (2003). "Cajal-Retzius cells in the mouse: transcription factors, neurotransmitters, and birthdays suggest a pallial origin." Brain Res Dev Brain Res **141**(1-2): 39-53.

Hevner, R. F., L. Shi, et al. (2001). "Tbr1 regulates differentiation of the preplate and layer 6." Neuron **29**(2): 353-66.

Hiesberger, T., M. Trommsdorff, et al. (1999). "Direct binding of Reelin to VLDL receptor and ApoE receptor 2 induces tyrosine phosphorylation of disabled-1 and modulates tau phosphorylation." Neuron **24**(2): 481-9.

Hosack, D. A., G. Dennis, Jr., et al. (2003). "Identifying biological themes within lists of genes with EASE." Genome Biol **4**(10): R70.

Huggins, G. S., C. J. Bacani, et al. (2001). "Friend of GATA 2 physically interacts with chicken ovalbumin upstream promoter-TF2 (COUP-TF2) and COUP-TF3 and represses COUP-TF2-dependent activation of the atrial natriuretic factor promoter." J Biol Chem **276**(30): 28029-36.

Ince-Dunn, G., B. J. Hall, et al. (2006). "Regulation of thalamocortical patterning and synaptic maturation by NeuroD2." Neuron **49**(5): 683-95.

Jacobs, E. C., C. Campagnoni, et al. (2007). "Visualization of corticofugal projections during early cortical development in a tau-GFP-transgenic mouse." Eur J Neurosci **25**(1): 17-30.

Janusonis, S., V. Gluncic, et al. (2004). "Early serotonergic projections to Cajal-Retzius cells: relevance for cortical development." J Neurosci **24**(7): 1652-9.

Jen, Y., K. Manova, et al. (1997). "Each member of the Id gene family exhibits a unique expression pattern in mouse gastrulation and neurogenesis." Dev Dyn **208**(1): 92-106.

Jimenez, D., R. Rivera, et al. (2003). "Origin of the cortical layer I in rodents." Dev Neurosci **25**(2-4): 105-15.

Jones, L., G. Lopez-Bendito, et al. (2002). "Pax6 is required for the normal development of the forebrain axonal connections." Development **129**(21): 5041-52.

Kashani, A. H., Z. Qiu, et al. (2006). "Calcium activation of the LMO4 transcription complex and its role in the patterning of thalamocortical connections." J Neurosci **26**(32): 8398-408.

Keshvara, L., S. Magdaleno, et al. (2002). "Cyclin-dependent kinase 5 phosphorylates disabled 1 independently of Reelin signaling." J Neurosci **22**(12): 4869-77.

Kim, S. Y., H. S. Chung, et al. (2007). "Spatiotemporal expression pattern of non-clustered protocadherin family members in the developing rat brain." Neuroscience **147**(4): 996-1021.

Kirmse, K., A. Dvorzhak, et al. (2007). "Cajal Retzius cells in the mouse neocortex receive two types of pre- and postsynaptically distinct GABAergic inputs." J Physiol **585**(Pt 3): 881-95.

Kwon, Y. T. and L. H. Tsai (1998). "A novel disruption of cortical development in p35(-/-) mice distinct from reeler." J Comp Neurol **395**(4): 510-22.

Lai, T., D. Jabaudon, et al. (2008). "SOX5 controls the sequential generation of distinct corticofugal neuron subtypes." Neuron **57**(2): 232-47.

Landry, C. F., T. M. Pribyl, et al. (1998). "Embryonic expression of the myelin basic protein gene: identification of a promoter region that targets transgene expression to pioneer neurons." J Neurosci **18**(18): 7315-27.

Lasorella, A., J. Stegmuller, et al. (2006). "Degradation of Id2 by the anaphase-promoting complex couples cell cycle exit and axonal growth." Nature **442**(7101): 471-4.

Li, H. P., A. Oohira, et al. (2005). "Aberrant trajectory of thalamocortical axons associated with abnormal localization of neurocan immunoreactivity in the cerebral neocortex of reeler mutant mice." Eur J Neurosci **22**(11): 2689-96.

Luque, J. M., J. Morante-Oria, et al. (2003). "Localization of ApoER2, VLDLR and Dab1 in radial glia: groundwork for a new model of reelin action during cortical development." Brain Res Dev Brain Res **140**(2): 195-203.

Lyden, D., A. Z. Young, et al. (1999). "Id1 and Id3 are required for neurogenesis, angiogenesis and vascularization of tumour xenografts." Nature **401**(6754): 670-7.

Magdaleno, S., L. Keshvara, et al. (2002). "Rescue of ataxia and preplate splitting by ectopic expression of Reelin in reeler mice." Neuron **33**(4): 573-86.

Maruyama, T., M. Matsuura, et al. (2008). "Cooperative activity of multiple upper layer proteins for thalamocortical axon growth." Dev Neurobiol **68**(3): 317-31.

McConnell, S. K. (1989). "The determination of neuronal fate in the cerebral cortex." Trends Neurosci **12**(9): 342-9.

McConnell, S. K., A. Ghosh, et al. (1989). "Subplate neurons pioneer the first axon pathway from the cerebral cortex." Science **245**(4921): 978-82.

Meyer, G., A. Cabrera Socorro, et al. (2004). "Developmental roles of p73 in Cajal-Retzius cells and cortical patterning." J Neurosci **24**(44): 9878-87.

Meyer, G. and A. M. Goffinet (1998). "Prenatal development of reelin-immunoreactive neurons in the human neocortex." J Comp Neurol **397**(1): 29-40.

Meyer, G., A. M. Goffinet, et al. (1999). "What is a Cajal-Retzius cell? A reassessment of a classical cell type based on recent observations in the developing neocortex." Cereb Cortex **9**(8): 765-75.

Meyer, G., J. M. Soria, et al. (1998). "Different origins and developmental histories of transient neurons in the marginal zone of the fetal and neonatal rat cortex." J Comp Neurol **397**(4): 493-518.

Molnar, Z., R. Adams, et al. (1998). "The role of the first postmitotic cortical cells in the development of thalamocortical innervation in the reeler mouse." J Neurosci **18**(15): 5746-65.

Molnar, Z. and C. Blakemore (1995). "How do thalamic axons find their way to the cortex?" Trends Neurosci **18**(9): 389-97.

Nadarajah, B. and J. G. Parnavelas (2002). "Modes of neuronal migration in the developing cerebral cortex." Nat Rev Neurosci **3**(6): 423-32.

Nagata, Y., M. Oda, et al. (2001). "A novel regulator of G-protein signaling bearing GAP activity for Galphai and Galphaq in megakaryocytes." Blood **97**(10): 3051-60.

Neuman, T., A. Keen, et al. (1993). "Neuronal expression of regulatory helix-loop-helix factor Id2 gene in mouse." Dev Biol **160**(1): 186-95.

Norton, J. D., R. W. Deed, et al. (1998). "Id helix-loop-helix proteins in cell growth and differentiation." Trends Cell Biol **8**(2): 58-65.

O'Leary, D. D. and D. Borngasser (2006). "Cortical ventricular zone progenitors and their progeny maintain spatial relationships and radial patterning during preplate development indicating an early protomap." Cereb Cortex **16 Suppl 1**: i46-56.

Ogawa, M., T. Miyata, et al. (1995). "The reeler gene-associated antigen on Cajal-Retzius neurons is a crucial molecule for laminar organization of cortical neurons." Neuron **14**(5): 899-912.

Prange-Kiel, J. and G. M. Rune (2006). "Direct and indirect effects of estrogen on rat hippocampus." Neuroscience **138**(3): 765-72.

Radnikow, G., D. Feldmeyer, et al. (2002). "Axonal projection, input and output synapses, and synaptic physiology of Cajal-Retzius cells in the developing rat neocortex." J Neurosci **22**(16): 6908-19.

Rakic, S., C. Davis, et al. (2006). "Role of p35/Cdk5 in preplate splitting in the developing cerebral cortex." Cereb Cortex **16 Suppl 1**: i35-45.

Reep, R. L. (2000). "Cortical layer VII and persistent subplate cells in mammalian brains." Brain Behav Evol **56**(4): 212-34.

Ross, S. E., M. E. Greenberg, et al. (2003). "Basic helix-loop-helix factors in cortical development." Neuron **39**(1): 13-25.

Sasahara, K., H. Shikimi, et al. (2007). "Mode of action and functional significance of estrogen-inducing dendritic growth, spinogenesis, and

synaptogenesis in the developing Purkinje cell." J Neurosci **27**(28): 7408-17.

Schiffmann, S. N., B. Bernier, et al. (1997). "Reelin mRNA expression during mouse brain development." Eur J Neurosci **9**(5): 1055-71.

Schmid, R. S., R. Jo, et al. (2005). "Reelin, integrin and DAB1 interactions during embryonic cerebral cortical development." Cereb Cortex **15**(10): 1632-6.

Sheldon, M., D. S. Rice, et al. (1997). "Scrambler and yotari disrupt the disabled gene and produce a reeler-like phenotype in mice." Nature **389**(6652): 730-3.

Sheppard, A. M. and A. L. Pearlman (1997). "Abnormal reorganization of preplate neurons and their associated extracellular matrix: an early manifestation of altered neocortical development in the reeler mutant mouse." J Comp Neurol **378**(2): 173-9.

Shimogori, T., V. Banuchi, et al. (2004). "Embryonic signaling centers expressing BMP, WNT and FGF proteins interact to pattern the cerebral cortex." Development **131**(22): 5639-47.

Shinozaki, K., T. Miyagi, et al. (2002). "Absence of Cajal-Retzius cells and subplate neurons associated with defects of tangential cell migration from ganglionic eminence in Emx1/2 double mutant cerebral cortex." Development **129**(14): 3479-92.

Sidman, R. L. and P. Rakic (1973). "Neuronal migration, with special reference to developing human brain: a review." Brain Res **62**(1): 1-35.

Soriano, E., J. A. Del Rio, et al. (1994). "Organization of the embryonic and early postnatal murine hippocampus. I. Immunocytochemical characterization of neuronal populations in the subplate and marginal zone." J Comp Neurol **342**(4): 571-95.

Studer, M., A. Filosa, et al. (2005). "The nuclear receptor COUP-TFI represses differentiation of Cajal-Retzius cells." Brain Res Bull **66**(4-6): 394-401.

Super, H., J. A. Del Rio, et al. (2000). "Disruption of neuronal migration and radial glia in the developing cerebral cortex following ablation of Cajal-Retzius cells." Cereb Cortex **10**(6): 602-13.

Takahashi, T., T. Goto, et al. (1999). "Sequence of neuron origin and neocortical laminar fate: relation to cell cycle of origin in the developing murine cerebral wall." J Neurosci **19**(23): 10357-71.

Takiguchi-Hayashi, K., M. Sekiguchi, et al. (2004). "Generation of reelin-positive marginal zone cells from the caudomedial wall of telencephalic vesicles." J Neurosci **24**(9): 2286-95.

Tevosian, S. G., A. E. Deconinck, et al. (1999). "FOG-2: A novel GATA-family cofactor related to multitype zinc-finger proteins Friend of GATA-1 and U-shaped." Proc Natl Acad Sci U S A **96**(3): 950-5.

Tevosian, S. G., A. E. Deconinck, et al. (2000). "FOG-2, a cofactor for GATA transcription factors, is essential for heart morphogenesis and development of coronary vessels from epicardium." Cell **101**(7): 729-39.

Torii, M. and P. Levitt (2005). "Dissociation of corticothalamic and thalamocortical axon targeting by an EphA7-mediated mechanism." Neuron **48**(4): 563-75.

Torres-Reveron, J. and M. J. Friedlander (2007). "Properties of persistent postnatal cortical subplate neurons." J Neurosci **27**(37): 9962-74.

Trommsdorff, M., M. Gotthardt, et al. (1999). "Reeler/Disabled-like disruption of neuronal migration in knockout mice lacking the VLDL receptor and ApoE receptor 2." Cell **97**(6): 689-701.

Tueting, P., E. Costa, et al. (1999). "The phenotypic characteristics of heterozygous reeler mouse." Neuroreport **10**(6): 1329-34.

Valverde, F., J. A. De Carlos, et al. (1995). "Time of origin and early fate of preplate cells in the cerebral cortex of the rat." Cereb Cortex **5**(6): 483-93.

Wahlsten, D., H. S. Ozaki, et al. (1992). "Deficient corpus callosum in hybrids between ddN and three other abnormal mouse strains." Neurosci Lett **136**(1): 99-101.

Wang, L., S. Andersson, et al. (2003). "Estrogen receptor (ER)beta knockout mice reveal a role for ERbeta in migration of cortical neurons in the developing brain." Proc Natl Acad Sci U S A **100**(2): 703-8.

Weiner, J. A., X. Wang, et al. (2005). "Gamma protocadherins are required for synaptic development in the spinal cord." Proc Natl Acad Sci U S A **102**(1): 8-14.

Wichterle, H., D. H. Turnbull, et al. (2001). "In utero fate mapping reveals distinct migratory pathways and fates of neurons born in the mammalian basal forebrain." Development **128**(19): 3759-71.

Wood, J. G., S. Martin, et al. (1992). "Evidence that the earliest generated cells of the murine cerebral cortex form a transient population in the subplate and marginal zone." Brain Res Dev Brain Res **66**(1): 137-40.

Xie, Y., E. Skinner, et al. (2002). "Influence of the embryonic preplate on the organization of the cerebral cortex: a targeted ablation model." J Neurosci **22**(20): 8981-91.

Yamazaki, H., M. Sekiguchi, et al. (2004). "Distinct ontogenic and regional expressions of newly identified Cajal-Retzius cell-specific genes during neocorticogenesis." Proc Natl Acad Sci U S A **101**(40): 14509-14.

Yoshida, M., S. Assimacopoulos, et al. (2006). "Massive loss of Cajal-Retzius cells does not disrupt neocortical layer order." Development **133**(3): 537-45.

Yun, K., A. Mantani, et al. (2004). "Id4 regulates neural progenitor proliferation and differentiation in vivo." Development **131**(21): 5441-8.

Zhou, C., Y. Qiu, et al. (1999). "The nuclear orphan receptor COUP-TFI is required for differentiation of subplate neurons and guidance of thalamocortical axons." Neuron **24**(4): 847-59.